

Crystal structure determination of hyaluronidase, a major bee venom allergen, in complex with an IgG Fab fragment and purification and biophysical characterization of bovine testes hyaluronidase

Inauguraldissertation

zur

Erlangung der Würde eines Doktors der Philosophie

vorgelegt der

Philosophisch-Naturwissenschaftlichen Fakultät

der Universität Basel

von

Sivaraman Padavattan

aus

Indien

Basel, 2006

Genehmigt von der Philosophisch-Naturwissenschaftlichen Fakultät

auf Antrag von

Prof. Dr. Tilman Schirmer

Dr. Zora Markovic-Housley

Prof. Dr. Andreas Engel

Basel, den 4.7.2006

Prof. Dr. Hans-Jakob Wirz

Dekan

Declaration

I declare that I wrote this thesis, **Crystal structure determination of hyaluronidase, a major bee venom allergen, in complex with an IgG Fab fragment and purification and biophysical characterization of bovine testes hyaluronidase**, with the help indicated and only handed it into the Faculty of Science of the University of Basel and to no other faculty and no other university.

Acknowledgments

I would like to thank my supervisor, Dr. Zora Markovic-Housely for her guidance, constant encouragement, valuable suggestion and support throughout my thesis. My sincere thanks to Prof Tilman Schirmer, for his excellent supervision through constructive criticism. I was able to receive immediate feedback from him during entire course of my PhD studies. I am grateful to Prof Andreas Engel for accepting to be an examiner and Prof Thomas Kiefhaber for moderating the viva voce.

Thank to Dr Jun-ichi Saito (Guru), the best friend I got in Basel, for his support both scientifically and personally which will remain in my memories forever. It was great pleasure to thank my group members Dr. Dinesh, Dr. Carmen Chan, Dr. Caroline Peneff, Dr. Arnaude Basle, Paul Wassmann, Christophe Wirth for their support and valuable discussion. Special thanks to Dietrich Samoray for his technical help and for translating German letters.

I wish to thank Dr. Joseph, for his support and invaluable technical help during my PhD thesis. Thanks to Dr. Paul Jenoe and Ariel Lustig for mass fingerprinting and analytical ultracentrifugation analyses.

Thanks to Mrs. Ute Gruetter for the administrative work and Roland Buerki and Margrit Jenny for the computer installation.

Many thanks to Senthil, Dinesh, Mathi, Ravi and Rajesh for supporting me all throughout my thesis writing.

Special thanks to Senthil (Seni), Dinesh, Kavitha, naughty Charen. We were like family and they made my Basel stay a memorable one. Thanks to other Basel friends Balasubramanian, Balamurugan, Arundhathi, Satheesh, Rathi, Murali and Rajeshwaren they all made me to feel at home.

My special regards to Stephanie Goulet, a Canadian girl, my neighbor in student home, for her support and help during my stay in Basel. Thanks to Lausanne friends Kannu, Vidya, Gnana, Renuga for their constant support during my PhD studies.

My humble thanks to Prof H.S. Savithri and Prof M.R.N Murthy who are my 'role models' in the scientific profession. They gave me the motivation, encouragement and support for find my PhD position.

Thanks to Isai, who trained me in protein purification and crystallization during my Master's study.

My special thanks to my parents, Ragupathy uncle, Kumarasamy teacher, they gave me the motivation, encouragement throughout my studies and they well deserve the credit of my work.

*.....to my parents, Ragupathy uncle and
Kumarasamy teacher*

Abbreviation

Ab	Antibody
Ag	Antigen
APC	Antigen presenting cells
AU	Analytical ultracentrifugation
CDR	Complementary determining region
CHES	2-(N-cyclohexylamino) ethanesulfonic acid
Da	Dalton
DC	Dendritic cell
DTT	Dithiothreitol
EDTA	Ethylenediaminetetraacetic acid
Fab	Fragment antigen binding
Fc	Fragment crystallizable
FWR	Frame work region
GPI	Glycosyl phosphatidylinositol
HA	Hyaluronic acid or hyaluronan
Hya	Hyaluronidase
Hyal	Hyaluronidase (mammals)
His-tag	Hexahistidine tag
IgG	Immunoglobulin G
IL	Interleukin
kDa	Kilo dalton
LS-MS	Liquid chromatography-Mass spectrometry
mAb	Monoclonal antibody
MALDI-TOF	Matrix assisted laser desorption ionization-Time of flight
min	Minute
MW	Molecular weight
OD	Optical density
PEG	Polyethylene glycol
PDB	Protein data bank
PH20₆₀	60-kDa PH-20 protein purified from commercial bovine testicular extract (Sigma)

PH20₆₉	69-kDa PH-20 protein purified from commercial bovine testicular extract (Sigma)
PH20₈₀	80-kDa PH-20 protein purified from bovine testes
PI-PLC	Phosphatidylinositol-specific phospholipase C
PMSF	Phenylmethanesulphonyl fluoride
R_{factor}	Crystallographic residual for working set of reflections
R_{free}	Crystallographic residual for test set of reflections
RT	Room temperature
rms	Root-mean-squared
rpm	Rotation per minute
SDS-PAGE	Sodium dodecylsulphate-polyacrylamide gel electrophoresis
SPAM1	Sperm adhesion molecule1
TABS	N-tris[Hydroxymethyl]methyl-4-aminobutanesulfonic acid
TCR	T-cell receptor
Th2	T helper cell 2

Table of contents

Declaration	II
Acknowledgments	III
Abbreviation	V
1.0 Hyaluronidases: background and significance	1
Bibliography	9
2.0 Identification of a B-cell epitope of hyaluronidase, a major bee venom allergen, from its crystal structure in complex with a specific Fab (S.Padavattan et al., JMB, v. 368, p. 742-52)	13
2.1 Supplementary information (Hya/Fab complex)	25
2.1.1 Hya/Fab complex formation, crystallization, diffraction and structure solution	26
2.1.1.1 IgG purification	26
2.1.1.2 IgG digestion	27
2.1.1.3 Purification of Fab using cation exchange chromatography (Mono-S)	28
2.1.1.4 Complex formation and purification using gelfiltration column (Superdex S-75 16/60)	28
2.1.1.5 Crystallization and diffraction	31
2.1.1.6 Structure solution: Search for right Fab model for molecular replacement (MR)	34
2.1.1.7 Crystal packing of Hya/Fab -21E11 complex	37
2.1.2 Mechanism of type 1 hypersensitivity reaction	38

2.1.3	Specific immunotherapy	40
	Bibliography	42
3.0	Purification and biophysical characterization of bovine testes hyaluronidase	43
3.1	Abstract	44
3.2	PH-20/Sperm adhesion molecule (SPAM1)	45
3.3	Methods and material	50
3.3.1	Substrate gel assay	50
3.3.2	Protein Electrophoresis and Immunoblotting	50
3.3.3	Cloning and expression of human PH-20	51
3.3.4	Protein purification from crude extract (type IV-S: From bovine testes, Sigma)	51
3.3.5	Protein purification from bovine testes	52
3.3.6	Analytical ultracentrifugation	53
3.3.7	Mass spectral analysis	53
3.3.8	Mass fingerprinting	54
3.3.9	Crystallization attempts	54
3.3	Results	55
3.3.1	Expression of recombinant human PH-20 protein	55
3.3.2	Purification of PH-20 protein from Sigma crude extract	55
3.3.3	Purification of PH-20 from bovine testes	63
3.3.4	Endoproteolytic cleavage of PH-20 protein	66

3.3.5	Mass spectrometry	67
3.3.6	PH-20 aggregation	68
3.4	Discussion	71
3.4.1	PH-20 purification	71
3.4.2	Endoproteolytic cleavage of PH-20	71
3.4.3	PH-20 crystallization and aggregation	72
3.5	Conclusion	74
	Bibliography	75
	Appendix	78
	curriculum vitae	78

1.0 Hyaluronidases: background and significance

1.0 Hyaluronidases: background and significance

The hyaluronidases are the enzymes, which hydrolyze β -1, 4 glycosidic linkage of hyaluronan (Hyaluronic acid, HA) [1], a linear, non-sulfated polysaccharide composed of repeating disaccharide units [D-glucuronic acid (1- β -3) N-acetyl-D-glucosamine (1- β -4)]_n (Figure 1) [1, 2]. HA is ubiquitously distributed in the extracellular matrix of vertebrates, particularly abundant in the soft connective tissues such as cartilage, synovial fluid, umbilical cord etc. The viscoelastic properties of HA, determined by its concentration and molecular weight, enable HA to act as stabilizer, lubricant, and shock absorbent. The level of HA is markedly elevated in many biological processes in which high turnover of HA is required such as embryogenesis, cell migration, wound healing, malignant transformation, and tissue turnover. [3].

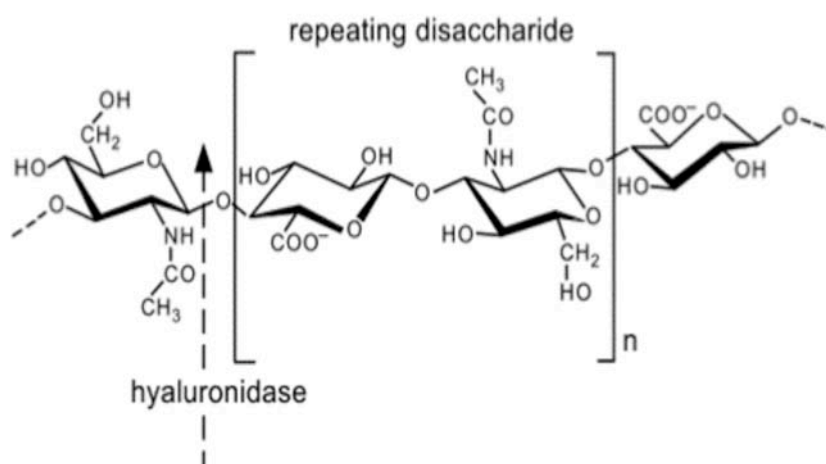


Figure 1. Structure of hyaluronan. The polymer is built of alternating units of glucuronic acid (GlcUA) and N-acetylglucosamine (GlcNAc). All the glycosidic linkages are β type, 1-3 glycosidic bonds between GlcUA and GlcNAc, and 1-4 bonds between GlcNAc and GlcUA. The vertebrate hyaluronidase cleaves the β 1-4 glycosidic bond between GlcUA-GlcNAc as shown.

Hyaluronidases are widely distributed in nature, being found in mammals, insects, leeches and bacteria [1, 2]. Hyaluronidase (Hya) activity was first identified as a 'spreading factor' based on the spreading properties exhibited by the extracts from mammalian testes. Hya from different sources are classified under three distinct classes based on substrate specificity and biochemical analyses of the reaction products as outlined in *Karl Meyer 1971* [1].

- ▶ Group 1 is represented by the mammalian hyaluronidases (E.C. 3.2.1.35) and the enzymes from venom of insects, snakes, scorpions which hydrolyze β -1, 4 glycosidic bond between GlcNac and GlcUA, generating tetra- and hexasaccharides as the predominant end products. They also digest chondroitin sulfate and to small extent dermatan sulfate. Bee venom hyaluronidase and PH-20 protein from mammalian testis are best characterized enzymes.
- ▶ Group 2 is represented by leeches enzymes (E.C. 3.2.1.36) which act as endo- β -glucuronidases. These enzymes generate tetra- and hexasaccharide end products.
- ▶ Group 3 comprises bacterial HA-lyases (E.C. 4.2.99.1) that act as endo-N-acetyl-hexosaminidases by β -elimination, yielding predominantly disaccharides as end products.

Based on the sequence homology, hyaluronidases from insect (honeybees and vespids) venom and mammalian hyaluronidases (EC 3.2.1.35) found in tissues (testis and plasma), snakes and scorpion enzymes have been classified into the glycosidase family 56 [4, 5]. Hya from honey bee venom shares greater than 50% sequence identity with other hymenopterans Hya [6, 7] and 30% sequence identity with the sperm PH-20, involved in fertilization, and the human lysosomal enzymes Hyal-1 and Hyal-2 which regulate HA turnover [8, 9]. The crystal structure of bee venom hyaluronidase, the first representative structure of glycosidase family 56, has been determined at 1.6 Å resolution. The overall fold resembling closely a classical (α/β)₈ TIM barrel with the exception that seven β -strands form the barrel [9]. The structure of Hya in complex with HA-tetramer (2.65 Å) enabled the elucidation of an acid-base catalytic mechanism in which Glu113 acts as the proton donor whereas the N-acetyl group of the substrate is the nucleophile. This unusual substrate-assisted acid-base catalytic mechanism is most probably also used by homologous mammalian enzymes since the active site residues and the residues in the substrate binding cleft are highly conserved. In addition, four cysteine residues forming two disulfide bridges are highly conserved (Figure 2). In comparison to bee venom hyaluronidase (350 residues), vertebrate hyaluronidases have an additional C-terminal domain EGF-like domain in Hyal-1 and a putative cell adhesion domain in PH-20. In addition, C-terminus of PH-20 has a transmembrane glycosyl phosphatidylinositol (GPI) lipid anchor [10, 11] (Figure 3).

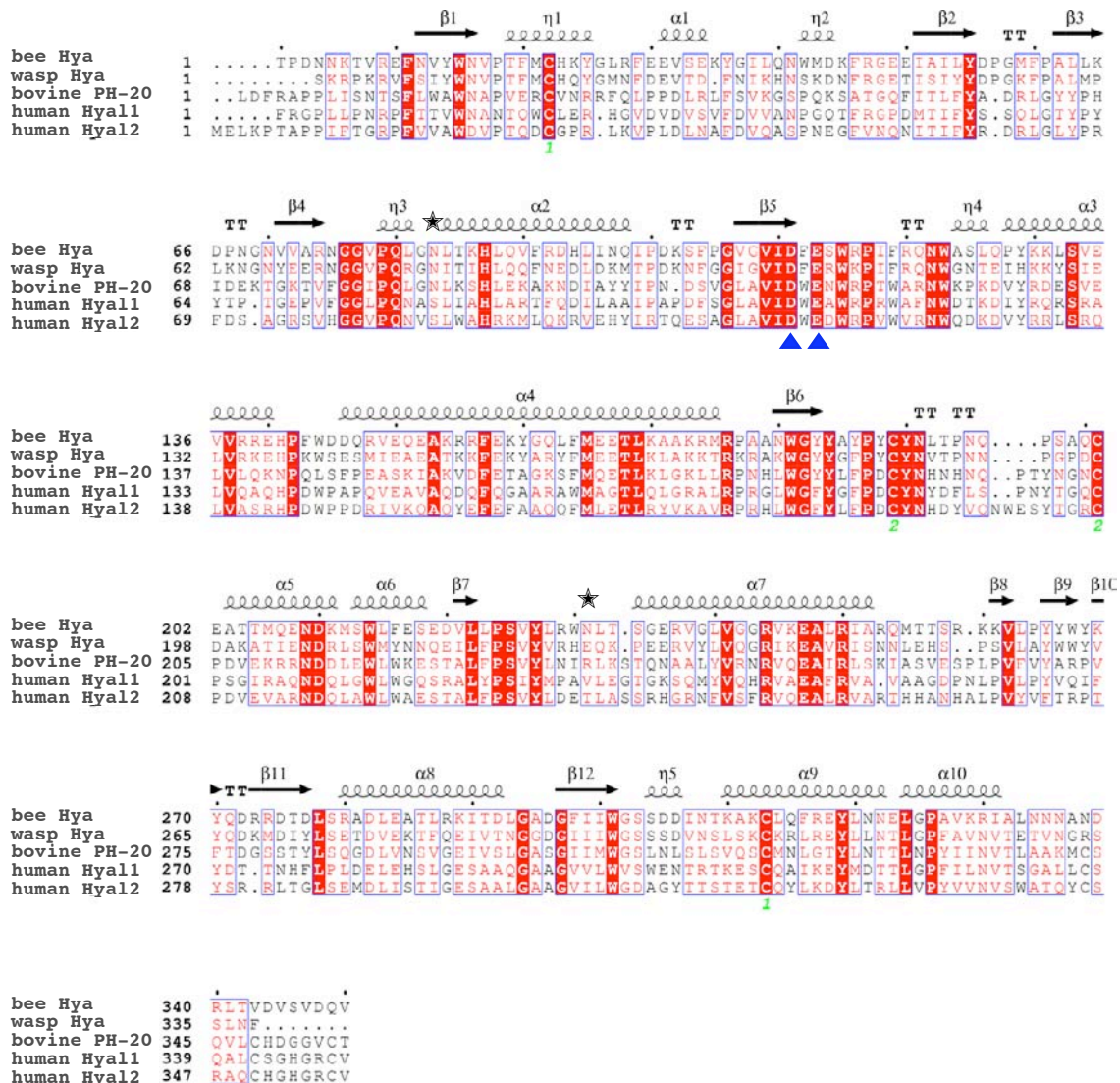


Figure 2. Multiple sequence alignment of hyaluronidases. The proteins listed from top to bottom: bee venom hyaluronidase (residues 1-350, NCBI accession number Q08169), wasp hyaluronidase (1-337, Q9U6V9), bovine PH-20 protein (1-353, Q7YS45), human lysosomal hyaluronidase Hyal-1 (1-349, Q12794) and human Hyal-2 (1-355, Q12891). Fully conserved residues shown in red box with white character and partially conserved residues shown in red character. Secondary structure elements are shown in top of the sequence. Blue arrowheads denote the active site residues Asp111 and Glu113. The four cysteine residues forming two disulfide bridges, Cys22-Cys313 (marked as 1 in green color) and Cys189-Cys201 (marked as 2 in green colour). Two N-glycosylation sites of bee venom hyaluronidase are indicated by (★) on the bottom of the sequence alignment.

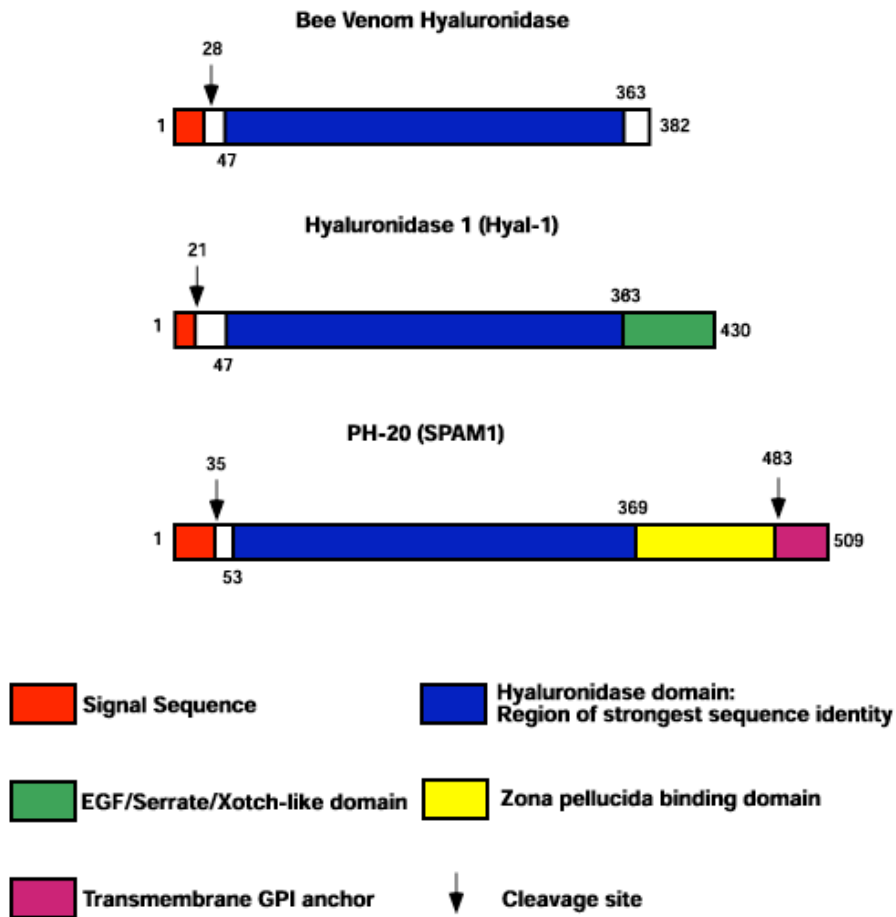


Figure 3. Diagram represents the putative domains in bee venom hyaluronidase, Hyal-1 (plasma hyaluronidase) and PH-20/sperm adhesion molecule 1 (SPAM1). The N-terminal region shows strongest homology between the three enzymes (indicated in blue). The C-terminal domain of the mammalian enzymes shows minimal homology and is absent in the bee venom enzyme. PH-20 has zona pellucida binding domain in the C-terminal region. Similarly Hyal1 has EGF-like domain in the C-terminal region which has sequence homology to serrate protein in the fruit fly, *Drosophila melanogaster*, and to Xotch protein in the frog, *Xenopus laevis*. Relative polypeptide lengths are drawn to scale. The picture adapted from Glycoforum's 'Hyaluronan Today', of Seikagaku Corp (www.glycoforum.gr.jp/today.html).

Bee venom hyaluronidase: It is one of the major allergens present in bee venom which specifically degrades HA in the extracellular matrix of skin thereby facilitating penetration of venom constituents into the body [12]. Native hyaluronidase, isolated from honeybee venom, is a single chain secreted protein composed of 350 amino acids, which is derived from a precursor composed of a signal peptide and a short prosegment. Recombinant His-tagged Hya expressed in eukaryotic (*Baculovirus*) expression system, has enzymatic activity and IgE-binding capacity similar to native Hya [13]. Hya contains four potential N-glycosylation motifs (Asn-X-Thr, where X is any amino acid). The crystal structure of the recombinant (*Baculovirus*) bee venom hyaluronidase shows that the Asn residues at 83 and 231 have weak density extending from

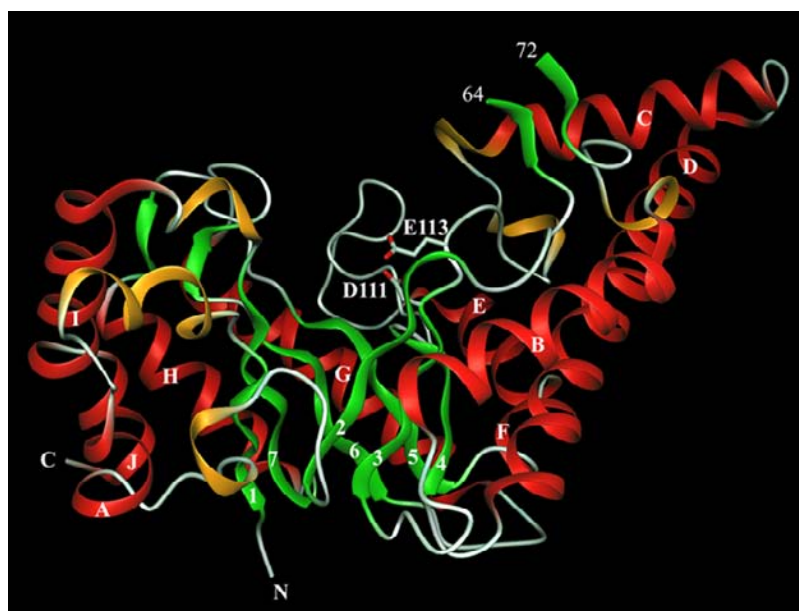


Figure 4. Ribbon representation of the bee venom hyaluronidase. The barrel formed by β strands 1-7 (green arrows), α helices marked A-J (red spirals) on the outside of the barrel and 3_{10} helices in orange. The substrate binding groove is located at the C-terminal end of the β barrel and the active site residues Asp111 and Glu113 are shown as stick models.

these residues, which is indicative of glycosylation. In contrast, Asn191 is buried in the protein interior so that it can be ruled out as glycosylation site and Asn4 in the N-terminus is not defined by electron density. Hya contains two disulfide bridges: Cys189-Cys201 which stabilizes the base of a long loop at the C-terminal end, whereas the Cys22-Cys313 bridge joins the secondary structure elements, a 3_{10} helix near the N-terminus and α -helix near the C-terminus. The prominent feature of Hya structure is the large gap between stands 1 and 2 (7-8Å) and a

long groove formed by the loops at the C-terminal end of β -barrel, suited for substrate binding. Another unusual feature is the presence of two α -helices (helix C and D) resembling a ‘handle’ like structure which extend away from globular domain (Figure 4) [9].

Mammalian hyaluronidases: Mammalian hyaluronidases are presumably responsible for hyaluronan (HA) turnover in diverse tissue but the details of HA catabolism remain obscure. Mammalian genome consists of six hyaluronidase genes, clustered into two groups and shares 40% sequence identity to each other. In the human, three genes (HYAL1, HYAL2 and HYAL3) are found tightly clustered on chromosome 3p21.3 and likewise, another three genes HYAL4, HYALP1 (a pseudogene), and PH-20/SPAM1 are clustered on chromosome 7q31.3 (Figure 5) [11]. The extensive homology between the different hyaluronidase genes suggests ancient gene duplication. Correspondingly, mouse genome also contains six hyaluronidase genes, except HYALP1 ortholog does not contain any mutation, and may encode for an active enzyme.

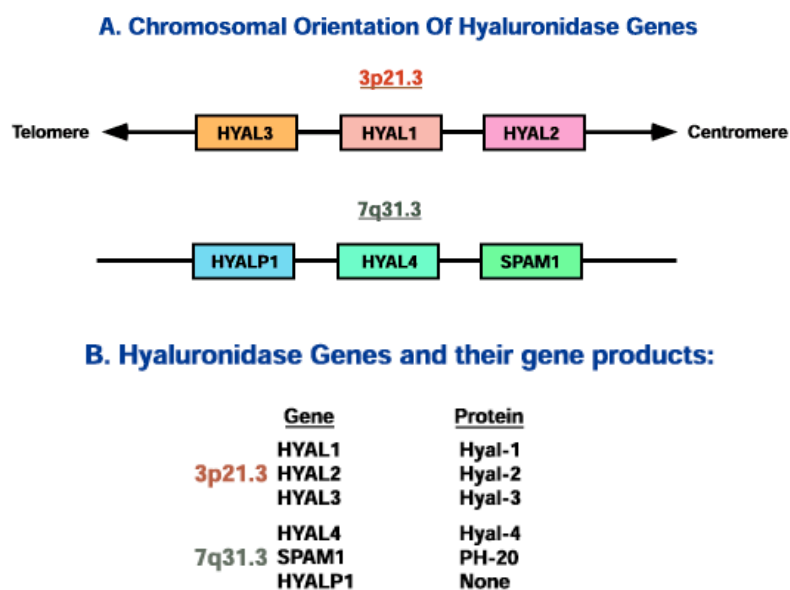


Figure 5. Depicts the chromosomal orientation of the six hyaluronidase genes at their two respective chromosomal sites, and tabulation of their gene products. The relative gene order has been established for the chromosome 7, but their orientation in relation to the centromere and telomere has not yet been determined. This figure is not drawn to scale. Picture was adapted from Glycoforum’s ‘Hyaluronan Today’, of Seikagaku Corp (www.glycoforum.gr.jp/today.html).

PH-20, Hyal-1 and Hyal-2 are well characterized mammalian hyaluronidase. PH-20 is expressed only in the testis and plays important role in mammalian fertilization (more details under PH-20/Sperm adhesion molecule 1). Hyal-1 and Hyal-2 are expressed in the somatic tissues such as liver, kidney, spleen etc., and the expression of these enzymes are extremely low and difficult to purify. Recent development in Hya detection procedure (substrate gel assay) [14] has facilitated the purification of 57 kDa molecular weight Hyal-1 to homogeneity from human plasma [15]. In contrast to plasma, urine contains two hyaluronidases with molecular weight of 57 kDa and 45 kDa. Microsequencing confirmed that both urinary isozymes have N-terminal identical to plasma hyaluronidase. Lower molecular weight isozyme contains a second N-terminal sequence, which was derived from the C-terminal end of the protein. This suggests that 45 kDa isozyme, resulting from endoproteolytic cleavage of the 57 kDa isoform, consists of two polypeptides linked by disulfide bond [16]. In vertebrates, the turnover of HA is controlled by hyaluronidase, which is an endoglycosidase that acts jointly with two lysosomal exoglycosidases, β -glucuronidase and β -N-acetyl glucosaminidase.

Hyal-3 is widely expressed enzyme but no activity was identified by present hyaluronidase assay [17]. In contrast to other hyaluronidases, Hyal-4 appears to have specificity for chondroitin and chondroitin sulfate, with no activity against hyaluronan [4]. In addition, Hyal-2, Hyal-4 and PH-20 are GPI-anchored on the plasma membrane [11].

Biological and medical significance of hyaluronidases:

- ★ The PH-20 protein plays a major role in mammalian fertilization. The male and female guinea pig immunized with PH-20 showed 100% contraception and the effect was long lasting and reversible [18]. This suggest PH-20 can be effectively used as a contraceptive vaccine.
- ★ The level of HA surrounding tumor cells often correlates with tumor aggressiveness and overproduction of HA enhance anchorage-independent cell growth [19-21]. Loss of hyaluronidase activity, permitting accumulation of HA, which might be one of the several steps required by cells during carcinogenesis. In addition, hyaluronidase expression was seen in various metastatic cell lines, which suggest tumor cells use hyaluronidase as "molecular

destroyer" to depolymerize hyaluronic acid in surrounding tissues and facilitate tumor invasion. Hyaluronidase on tumor cells may provide a target for anti-neoplastic drugs [22].

- ★ Testicular enzyme is used as a 'spreading factor', to improve better penetration of chemotherapeutic drug into tumors. Drawback of this approach is hyaluronidase developed symptoms of immediate type 1 allergic reaction [23].

Bibliography

1. Meyer, K. (1971). Hyaluronidases. In *The Enzymes*, 3rd edition, volume V, P.D. Boyer, ed. (New York: Academic press), pp. 307-320.
2. Kreil, G. (1995). Hyaluronidases--a group of neglected enzymes. *Protein Sci* 4, 1666-1669.
3. Laurent, T.C., and Fraser, J.R. (1992). Hyaluronan. *Faseb J* 6, 2397-2404.
4. Henrissat, B. (1991). A classification of glycosyl hydrolases based on amino acid sequence similarities. *Biochem J* 280 (Pt 2), 309-316.
5. Henrissat, B., and Bairoch, A. (1996). Updating the sequence-based classification of glycosyl hydrolases. *Biochem J* 316 (Pt 2), 695-696.
6. Kolarich, D., Leonard, R., Hemmer, W., and Altmann, F. (2005). The N-glycans of yellow jacket venom hyaluronidases and the protein sequence of its major isoform in *Vespa vulgaris*. *FEBS J* 272, 5182-5190.
7. Lu, G., Kochoumian, L., and King, T.P. (1995). Sequence identity and antigenic cross-reactivity of white face hornet venom allergen, also a hyaluronidase, with other proteins. *J Biol Chem* 270, 4457-4465.
8. Gmachl, M., and Kreil, G. (1993). Bee venom hyaluronidase is homologous to a membrane protein of mammalian sperm. *Proc Natl Acad Sci U S A* 90, 3569-3573.
9. Markovic-Housley, Z., Migliorini, G., Soldatova, L., Rizkallah, P.J., Muller, U., and Schirmer, T. (2000). Crystal structure of hyaluronidase, a major allergen of bee venom. *Structure* 8, 1025-1035.
10. Cherr, G.N., Meyers, S.A., Yudin, A.I., VandeVoort, C.A., Myles, D.G., Primakoff, P., and Overstreet, J.W. (1996). The PH-20 protein in cynomolgus macaque spermatozoa: identification of two different forms exhibiting hyaluronidase activity. *Dev Biol* 175, 142-153.
11. Csoka, A.B., Frost, G.I., and Stern, R. (2001). The six hyaluronidase-like genes in the human and mouse genomes. *Matrix Biol* 20, 499-508.
12. King, T.P., and Spangfort, M.D. (2000). Structure and biology of stinging insect venom allergens. *Int Arch Allergy Immunol* 123, 99-106.
13. Soldatova, L.N., Cramer, R., Gmachl, M., Kemeny, D.M., Schmidt, M., Weber, M., and Mueller, U.R. (1998). Superior biologic activity of the recombinant bee venom allergen hyaluronidase expressed in baculovirus-infected insect cells as compared with *Escherichia coli*. *J Allergy Clin Immunol* 101, 691-698.
14. Guntenhoner, M.W., Pogrel, M.A., and Stern, R. (1992). A substrate-gel assay for hyaluronidase activity. *Matrix* 12, 388-396.
15. Frost, G.I., Csoka, A.B., Wong, T., and Stern, R. (1997). Purification, cloning, and expression of human plasma hyaluronidase. *Biochem Biophys Res Commun* 236, 10-15.

16. Csoka, A.B., Frost, G.I., Wong, T., and Stern, R. (1997). Purification and microsequencing of hyaluronidase isozymes from human urine. *FEBS Lett* 417, 307-310.
17. Stern, R. (2003). Devising a pathway for hyaluronan catabolism: are we there yet? *Glycobiology* 13, 105R-115R.
18. Primakoff, P., Lathrop, W., Woolman, L., Cowan, A., and Myles, D. (1988). Fully effective contraception in male and female guinea pigs immunized with the sperm protein PH-20. *Nature* 335, 543-546.
19. Kosaki, R., Watanabe, K., and Yamaguchi, Y. (1999). Overproduction of hyaluronan by expression of the hyaluronan synthase Has2 enhances anchorage-independent growth and tumorigenicity. *Cancer Res* 59, 1141-1145.
20. Liu, N., Gao, F., Han, Z., Xu, X., Underhill, C.B., and Zhang, L. (2001). Hyaluronan synthase 3 overexpression promotes the growth of TSU prostate cancer cells. *Cancer Res* 61, 5207-5214.
21. Zhang, L., Underhill, C.B., and Chen, L. (1995). Hyaluronan on the surface of tumor cells is correlated with metastatic behavior. *Cancer Res* 55, 428-433.
22. Liu, D., Pearlman, E., Diaconu, E., Guo, K., Mori, H., Haqqi, T., Markowitz, S., Willson, J., and Sy, M.S. (1996). Expression of hyaluronidase by tumor cells induces angiogenesis in vivo. *Proc Natl Acad Sci U S A* 93, 7832-7837.
23. Szepfalusi, Z., Nentwich, I., Dobner, M., Pillwein, K., and Urbanek, R. (1997). IgE-mediated allergic reaction to hyaluronidase in paediatric oncological patients. *Eur J Pediatr* 156, 199-203.

The thesis is divided in two parts:

In the first part, I discuss the crystal structure determination of bee venom hyaluronidase in complex with a Fab fragment of an anti-Hya monoclonal IgG antibody (clone 21E11) which is able to compete with human IgE, from the bee venom allergic patient serum pool into Hya binding. Hya is one of the major allergen present in honeybee venom that may induce life threatening allergic reaction in human. Since the allergen-antibody interactions are crucial for triggering of allergic responses, the structures of the antigen/antibody complexes are essential for the identification of Hya epitopes recognized by IgE antibodies. The knowledge of B cell epitope may facilitate the design of new and safer vaccines for allergen immunotherapy in the form of mutated allergens with abolished or reduced IgE binding potency (hypoallergen).

In the second part, I discuss the PH-20 protein, a mammalian hyaluronidase which plays important role in fertilization. Though mammalian hyaluronidases play important role in many biological processes, the study of these enzymes is greatly neglected. In the present study, we were able to purify PH-20 proteins from commercially available testicular extract (Sigma) and from the homogenized bovine testes to highest purity. The aggregation of purified PH-20 was successfully eliminated by the addition of zwitterionic compound, NDSB (non detergent sulfobetaine). Attempt to crystallize the PH-20 protein were not successful but crystallization in the presence of NDSB still remains to be tested.

2.0 Identification of a B-cell epitope of hyaluronidase, a major bee venom allergen, from its crystal structure in complex with a specific Fab (S.Padavattan et al., JMB, v. 368, p. 742-52)

Identification of a B-cell Epitope of Hyaluronidase, a Major Bee Venom Allergen, from its Crystal Structure in Complex with a Specific Fab

Sivaraman Padavattan¹, Tilman Schirmer¹, Margit Schmidt²
Cezmi Akdis³, Rudolf Valenta⁴, Irene Mittermann⁴, Lyudmila Soldatova⁵
Jay Slater⁶, Ulrich Mueller⁷ and Zora Markovic-Housley^{1*}

¹Division of Structural Biology
Biozentrum, University of Basel
CH-4056 Basel, Switzerland

²Department of Biology
East Carolina University
Greenville, NC 27858, USA

³Department of Cellular
Allergology/Immunology
Swiss Institute of Allergy and
Asthma Research, CH-7270
Davos, Switzerland

⁴Christian Doppler Laboratory
of Allergy Research, Division of
Immunopathology, Department
of Pathophysiology, Medical
University of Vienna
A-1090 Vienna, Austria

⁵OPS/ONDQA, Center for
Drug Evaluation and
Research, US Food and Drug
Administration, Silver Spring
MD 20993, USA

⁶Center for Biologics Evaluation
and Research, US Food and
Drug Administration
Bethesda, MD 20892, USA

⁷SpitalBern, CH-3001 Bern
Switzerland

The major allergens of honeybee venom, hyaluronidase (Hyal) and phospholipase A₂, can induce life-threatening IgE-mediated allergic reactions in humans. Although conventional immunotherapy is effective, up to 40% of patients develop allergic side effects including anaphylaxis and thus, there is a need for an improved immunotherapy. A murine monoclonal anti-Hyal IgG1 antibody (mAb 21E11), that competed for Hyal binding with IgEs from sera of bee venom allergic patients, was raised. The fragment of these IgG antibodies which bind to antigen (Fab) was produced and complexed (1:1) with Hyal. The crystal structure determination of Hyal/Fab 21E11 complex (2.6 Å) enabled the identification of the Hyal–IgG interface which provides indirect information on the Hyal–IgE interaction (B-cell epitope). The epitope is composed of a linear array of nine residues (Arg138, His141–Arg148) located at the tip of a helix–turn–helix motive which protrudes away from the globular core and fits tightly into the deep surface pocket formed by the residues from the six complementarity determining regions (CDRs) of the Fab. The epitope is continuous and yet its conformation appears to be essential for Ab recognition, since the synthetic 15-mer peptide comprising the entire epitope (Arg138–Glu152) is neither recognized by mAb 21E11 nor by human IgEs. The structure of the complex provides the basis for the rational design of Hyal derivatives with reduced allergenic activity, which could be used in the development of safer allergen-specific immunotherapy.

© 2007 Elsevier Ltd. All rights reserved.

*Corresponding author

Keywords: hyaluronidase; bee venom allergen; B-cell epitope; hyaluronidase/Fab complex; X-ray structure

Abbreviations used: Hyal (or rApi m 2), hyaluronidase; Ab, antibody; Ag, antigen; IgE, immunoglobulin E; Fab, fragment of IgG which binds to antigen; CDR, complementarity determining region; FWR, frame work region; mAb, monoclonal antibody; MR, molecular replacement; PBS, phosphate-buffered saline; PBST, PBS/0.05% v/v Tween 20; PEG, polyethylene glycol; SIT, specific immunotherapy; SLS, Swiss Light Source.

E-mail address of the corresponding author: zora.housley@unibas.ch

Introduction

Venoms of bees, wasps and fire ants can cause severe IgE-mediated allergic reactions (type I hypersensitivity) including anaphylaxis.^{1–3} It has been estimated that up to 3% of the general population have a history of systemic anaphylactic reactions to insect stings.⁴ Venoms from bee and wasp are different, each containing distinct major allergens: phospholipase A2 and melittin occur only in bee venom, and antigen 5 only in wasp venom, but both venoms contain hyaluronidases (Hyal).³ Clinical studies demonstrated that Hyal and phospholipase A2 are the two major allergens present in bee venom: 71% of patients had specific serum IgE against recombinant Hyal and 78% against recombinant phospholipase A2.⁵ Susceptible individuals respond to bee venom exposure by producing IgE antibodies which bind to the high affinity F_c receptors on basophils in circulation or mast cells in tissues. Following re-exposure, multivalent allergens cross-link F_c -receptor-bound IgE antibodies on the surface of mast cells. This leads to a series of signaling events, which result in mast cell degranulation and the release of histamine, leukotriene and other mediators which are responsible for a variety of allergic symptoms.

Bee venom Hyal is a hydrolytic enzyme that specifically cleaves the hyaluronic acid, a large, linear polymer (hyaluronan) consisting of simple repeats of disaccharide composed of the β -1,4 linked D-glucuronic acid and N-acetyl-glucosamine. Hyaluronan and chondroitin sulfates are the most abundant glycosaminoglycan of vertebrate extracellular matrix, and the relative abundance of these glycoproteins varies with the origin of the connective tissue. Cleavage of hyaluronan by Hyal facilitates the penetration of venom constituents into the body.⁶ Hyaluronan is found in almost all tissues and body fluids and is particularly abundant in the intercellular matrix of skin and the connective tissues of cartilage, synovial fluid and the vitreous humor of the eye. Under physiological conditions, hyaluronan is a large (10^5 to 10^7 kDa), charged and extended polysaccharide which is exceptionally hydrophilic. The ability to bind large amounts of water confers special viscoelastic properties to hyaluronan solutions which are the basis of its structural role as a stabilizer, joint lubricant and shock absorber.^{7,8} Hyaluronan exists in a number of physiological states, associated with themselves, with the extracellular matrix, with the cell surface receptors CD44 and RHAMM⁹ present on the hyaluronan-binding proteins (hyaladherins)^{10–12} forming massive multimolecular aggregates with proteoglycans, such as aggrecan.

Bee venom Hyal is composed of 350 amino acids and has four potential N-glycosylation sites and two disulfide bridges. In fact, only two of the four postulated sites are N-glycosylated, Asn115 and Asn263.^{13–15} Recombinant Hyal has been expressed in prokaryotic (*Escherichia coli*) and eukaryotic

(*Baculovirus*) hosts. Only the *Baculovirus*-expressed enzyme has enzymatic activity and IgE-binding capacity similar to native Hyal.¹⁶ The crystal structure of the recombinant (*Baculovirus*) bee venom Hyal¹³ is the first structural representative of the Hyals belonging to the glycosidase family 56.^{17,18} The overall fold of Hyal resembles a classical (β/α)₈ barrel except that the barrel is formed by seven β strands and is open between β strands 1 and 2. The structure of Hyal in complex with hyaluronic acid-tetrameres enabled to propose an acid–base catalytic mechanism in which Glu113 acts as the proton donor and the N-acetyl group of the substrate as the nucleophile.^{13,19} Recently, the structure of homologous wasp Hyal has been solved showing a fold identical with that of bee venom Hyal.²⁰

Specific immunotherapy (SIT) is the only causal treatment for type I allergies; however, a drawback is the risk of IgE-mediated anaphylactic side effects, which occur in 20%–40% of patients²¹ subjected to SIT based on natural extracts. There is evidence that successful immunotherapy operates on the level of T helper cells, leading to marked changes in cytokine secretion patterns: TH2 cells secreting IL-4, IL-5 and IL-13 diminish strongly and are replaced by IL-10 secreting CD4⁺CD25⁺ regulatory cells (T_{Reg}).^{22,23} Furthermore, it has been shown that immunotherapy induces allergen-specific IgG antibodies which inhibit the binding of allergic patients IgE to the allergen.^{24,25} One way to lower the risk of anaphylaxis during SIT is to use allergens modified in a way which abolishes or reduces its IgE-binding potency (hypoallergen) but retains the allergen T-cell epitopes (linear epitopes) that will induce T-cell tolerance.²³ Other possibilities are to prepare genetically modified allergens or allergen-derived peptides with reduced allergenic activity which induce protective allergen-specific IgG antibodies competing with IgE.²⁶

Since allergen–antibody (Ab) interactions are crucial for the triggering of allergic responses, a promising approach to inhibit this process would be to prevent allergen binding to IgE. Determining the structure of antigen (Ag)/Ab complexes is one way to identify the Hyal epitopes which are recognized by IgE antibodies. The knowledge of the B-cell epitope of the allergen is expected to facilitate the design of a safer SIT in the form of mutated allergens with reduced IgE-binding potency which would be able to bypass the risk of anaphylaxis.

In the present study, a monoclonal murine IgG1 antibody (mAb, clone 21E11) raised against purified recombinant Hyal and able to inhibit IgE binding to Hyal up to 60% in some patients, was chosen to map the B-cell epitope. This is the second study of an allergen–Ab complex, after the Bet v 1–Fab (fragment of IgG which binds to antigen (Fab)) complex structure, although many Ag–Fab complex structures have been reported.^{27–30} It is anticipated that the knowledge of the Hyal epitope may be used to genetically modify the allergenic protein in order to

Table 1. Reactivity of mouse mAbs specific for Api m 2

	Absorbance 21E11	Absorbance 22H7	Absorbance 24F2
Peptide (R138–E152)	0.03	0.03	0.03
Api m 2	0.90	1.11	0.67
HSA	0.03	0.03	0.03

Absorbance values corresponding to the levels of mouse monoclonal IgG1 antibodies (mAbs: 21E11, 22H7, 24F2) specific for Api m 2 and the Api m 2-derived peptide are displayed. Human serum albumin (HSA) was used as negative control.

reduce its IgE-binding potency and to employ it for safer immunotherapy.

Results

Inhibition of IgE binding to Hyal by anti-Hyal monoclonal IgG1 Abs

Hyal (rApi m 2) is recognized by serum IgE from bee venom allergic patients and also by three different mouse monoclonal IgG1 antibodies (clones 21E11, 22H7 and 24F2). In contrast, the Hyal derived 15-mer peptide (Arg138–Glu152) containing nine epitope residues elucidated from the Hyal/Fab complex structure, is not recognized by the mAbs (Table 1). Also sera of bee venom allergic patients do not bind to the isolated peptide (data not shown). The effect of the three mouse mAbs on binding of serum IgE from 10 bee venom allergic patients was tested by an ELISA-inhibition assay (Table 2). A mean inhibition of IgEs binding to Hyal by each of the three mAbs ranged between 18% and 20%. However, this value was as high as 57% for certain patients' sera.

Structure determination of the Hyal/Fab complex

The crystal structure of the complex formed between Hyal and the Fab fragment of the mouse mAb 21E11 has been determined at 2.6 Å resolution

by molecular replacement (MR) (Table 3). MR was performed in three consecutive steps using the structures of apo Hyal (1FCQ), Fab variable domain (1A7Q) and constant domain (15C8) as the search models. This yielded the orientation and location of the three constituents in the asymmetric unit. The final model comprises residues Glu10–Ser333 of Hyal, Asp1–Ile205 of the light chain and Gln1–Val180 of the heavy chain of Fab as well as 63 water molecules. The Fab residues are numbered as described by standard Kabat convention with light and heavy chain identifiers L and H, respectively.^{31,32} In Hyal, the electron density is missing for 9 N-terminal and 17 C-terminal residues (plus the His₆ tail) and loop residues Asp66–Asn70. Likewise, in Fab density is missing for residues L119–L131, L150–L157, L168–L169, L187–L192 and L206 to the C-terminal end of the light chain, and for residues H122–H137, H157–H162 and H181 to the C-terminal end of the heavy chain. Most of these residues belong to the loops of the constant domain and are far away from the Hyal/Fab interface. After conventional refinement, the final model has an *R*-factor of 20.9% (*R*_{free}, 24.7%) at 2.6 Å resolution (Table 3). The residues are well ordered and exhibit good stereochemistry (Table 3). The electron density is of good quality; an example of the final 2*F*_o–*F*_c map is shown in Figure 1.

Overall fold of the Hyal/Fab complex

The structure of the Hyal/Fab complex is shown as a ribbon presentation in Figure 2(a). The Hyal fold is a (β/α)₇ barrel open between strands 1 and 2 and surrounded by 10 α helices.¹³ The overall Ag conformation is not changed significantly upon complex formation. Superposition of the apo Hyal models 1FCQ (1.6 Å resolution) and 1FCU (2.1 Å resolution)¹³ with Hyal of the Hyal/Fab complex gives r.m.s.d. of 0.76 and 0.61 Å (for 312 and 319 C α atoms), respectively, which is comparable with the differences observed between the two unliganded Hyal models (r.m.s.d. of 0.68 Å for 314 C α atoms). In protein Ag/Ab complexes, conformational adjust-

Table 2. Inhibition of IgE binding of bee venom positive sera to purified recombinant Api m 2 by mAbs

Individual	Absorbance mAb control	Absorbance 21E11	% inhibition ^a	Absorbance 22H7	% inhibition	Absorbance 24F2	% inhibition	Absorbance 21E11/22H7/24F2	% inhibition
I	2.57	1.98	23.02	2.28	11.14	1.97	23.26	2.20	14.14
II	1.47	1.15	21.77	0.99	32.56	1.00	31.95	0.98	32.76
III	1.39	1.67	–	1.43	–	1.21	12.83	1.17	15.28
IV	1.18	0.87	26.36	1.01	14.54	1.23	–	0.94	20.41
V	0.61	0.58	5.06	0.58	4.73	0.59	4.08	0.43	29.20
VI	0.54	0.23	56.83	0.25	54.79	0.27	49.82	0.22	60.15
VII	0.32	0.30	6.48	0.25	21.61	0.27	17.91	0.21	36.42
VIII	0.39	0.35	9.51	0.34	13.88	0.34	13.11	0.27	31.36
IX	0.32	0.31	2.79	0.28	11.80	0.28	13.98	0.25	23.91
X	0.22	0.15	32.72	0.16	26.73	0.16	28.57	0.16	26.73
Mean			18.45		19.18		19.55		29.04

^a rApi m 2 bound to ELISA plate was pre-incubated with three individual Api m 2-specific mouse monoclonal IgG1 antibodies (mAbs:21E11, 22H7, 24F2), a mixture of all three mAbs and, for control purposes, with a mouse mAb against Bet v 1 (mAb control). The plates were then incubated with sera of 10 bee venom allergic patients. Api m 2-specific IgE levels were measured. The percentage of inhibition of IgE binding is shown.

Table 3. Crystallographic data for Hyal/Fab complex

Data collection	
Space group	C2
Unit cell dimensions	
a, b, c (Å)	151.6, 70.1, 138.9
α , β , γ (°)	90.0, 123.7, 90.0
X-ray source	SLS-PX
Detector type	MAR CCD
Wavelength (Å)	0.978
Resolution range (Å)	63–2.6 (2.74–2.6) ^a
No. of total observation	101,732 (14,135)
No. of unique observation	32,047 (4437)
Completeness (%)	85.4 (81.8)
Multiplicity	3.2 (3.2)
$I/\sigma(I)$	13.9 (3.6)
R_{sym}^b (%)	8.4 (30)
Refinement	
$R_{\text{factor}}/R_{\text{free}}^c$ (%)	20.9/24.7
Protein atoms	11642
Water molecules	63
Average B -factor (Å ²)	
Hyal	37.5
Fab variable domain	38.0
Fab constant domain	38.2
Solvent	33.8
r.m.s.d. from ideal values	
Bond lengths (Å)	0.009
Bond angles (°)	1.136
r.m.s. ΔB of bonded atoms (Å ²)	
Main chain	1.020
Side-chain	2.257
Ramachandran plot	
Most favored region (%)	88.4
Additionally allowed region (%)	10.3
Generously allowed region (%)	0.5
Disallowed region (%)	0.7

^a Number in parentheses are statistics for the data in the highest resolution shell.

^b $R_{\text{sym}} = \sum \sum |I(h)_i - \langle I(h) \rangle| / \sum \sum I(h)_i$, observed intensity in the i th data set and $\langle I(h) \rangle$, mean intensity of reflection h over all measurements of $I(h)$.

^c R_{factor} is the conventional R -factor and R_{free} is the R -factor calculated with 5% of the data that were not used in refinement.

ment in flexible loops and side-chains of the interacting residues upon complex formation is often observed.²⁹ In Hyal, the largest deviations in the C_{α} position occur in loop residues His141–Asp145, which are part of the epitope (r.m.s.d.=2.6 and 2.1 Å for 1FCQ and 1FCU, respectively), indicating a considerable conformational change of the epitope loop upon Fab binding (Figure 2(b)). However, also the conformation of residues Thr193–Pro197 from the loop which is far from the Ab binding site (r.m.s.d.=2.3 Å) is significantly changed. In the absence of the structure of the free Ab, the extent of possible conformational changes of the residues belonging to the variable domain cannot be evaluated.

The Hyal/Fab interface

The mAb 21E11 recognizes a continuous epitope located at the tip of the helix C–turn–helix D motif of Hyal, which resembles a handle that protrudes away from the globular core of the molecule (Figure 2(a)). The total contact surface area of the complex

interface was estimated to be 1274 Å² (probe radius 1.7 Å, program MS). The epitope is mostly continuous and composed of eight consecutive residues His141–Arg148 (HPFWDDQR) plus Arg138. Hyal structure was submitted to CEP-server for the prediction of conformational epitopes[†].³³ In addition to the predicted conformational epitopes, the server predicted a sequential epitope at position Arg138–Gln151. This prediction is in good agreement with the results from our crystal structure, which showed that 9 of 14 residues predicted by the server are indeed involved in Fab binding. All nine residues belong to the C- and N-terminal ends of helices C and D and the joining turn (Figure 2(c)). Epitope residues fit tightly into the deep pocket formed by the side-chains from all six complementarity determining regions (CDRs) and the light framework region 2 (FWR L2) of the Fab (Figures 2(c) and 3). The interface is formed by 9 Hyal and 17 Fab residues. The total number of polar Hyal/Fab interactions comprises 4 salt bridges and 9 hydrogen bonds while 11 and 39 van der Waals contacts have been found for the cut off values of 3.7 Å and 4.0 Å, respectively (Table 4). Of the nine epitope residues in contact with Fab, two are polar, four are charged and three are hydrophobic. The polar and charged residues are located predominantly at the periphery of the Hyal binding surface, the two hydrophobic residues (Pro142, Phe143) from the turn are buried at the bottom of Hyal/Fab cavity formed by the hydrophobic residues of Fab, whereas Trp144 is only 79% buried (Figures 2(c) and 3). The size of the Fab binding pocket is approximately 14 Å wide and 15 Å deep. The salt bridges are formed between Asp145 and Arg148 from helix D of Hyal and Arg58 and Asp54 from CDR-H2 of Fab, respectively (Figure 3).

Water molecules are often found in the interfaces of Ag–Ab complexes^{34–36} where they are required to improve the fit between the proteins and to neutralize unpaired hydrogen-bonding groups. In the Hyal/Fab complex, three water molecules (21O, 22O and 23O) are completely buried between the two surfaces, filling the cavity and enhancing surface complementarity (Table 5). Three additional water molecules (5O, 20O and 45O) are present at the periphery of the interface where they enable Hyal–water–Fab hydrogen bonding interaction. The shape correlation statistic for Hyal/Fab complex is 0.73 which is slightly higher than the observed mean shape correlation statistic value of 0.64–0.65 for Ag–Ab interface,³⁷ indicating good shape complementarity. Thus, the Hyal/Fab complex structure also confirms the importance of bound water molecules in mediating protein/protein interactions.

The Ab combining site is a pronounced cavity formed by the side-chains of the Fab residues interacting with Hyal: six residues from the light chain CDRs (L1, L2 and L3), nine residues from the

† <http://bioinfo.ernet.in/cep.htm>

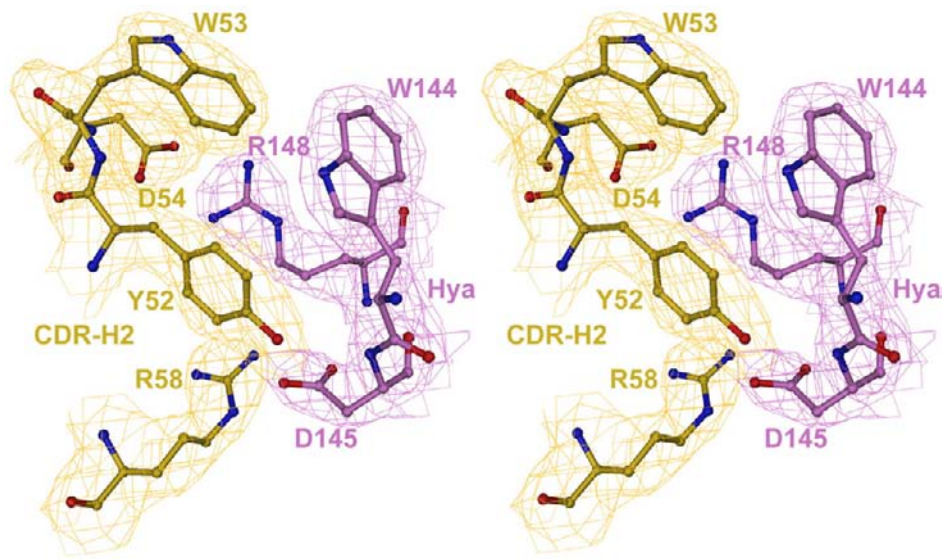


Figure 1. Close-up stereo view of the final SigmaA-weighted $2F_o - F_c$ electron density map⁶⁰ contoured at 1.0σ . Shown is part of the Hyal/Fab interface with Hyal and Fab heavy chain colored magenta and yellow, respectively. All pictures were produced using program DINO [<http://www.dino3d.org/>].

heavy chain CDRs (H1, H2 and H3) and two residues from the FWR L2. Similar to other Ab–Ag complexes,²⁷ the residues from the heavy chain, particularly CDR-H2, make extensive contact with Hyal. In the Hyal/Fab complex, 6 out of 17 Fab residues interacting with Hyal are aromatic, in agreement with a notion that aromatic residues, particularly tyrosines, form most of the contacts with Ag.^{27,38} Residues Tyr32 (L1), Tyr52 (H2) and Tyr95 (H3) are almost completely buried (>90%) within the interface, whereas Tyr49 (FWR L2), Tyr92 (L3) and Trp53 (H2) are partially buried (38–48%). Apart from CDRs, residues Leu46 and Tyr49 from FWR L2 are also involved in apolar interactions with Hyal. The shape of the Ab binding cavity is similar to those observed with haptens which bind in grooves and pockets³⁹ and usually do not cause large conformational changes in Fab. The interaction between residues from CDR-H3 and Hyal is mediated by water and hydrophobic interactions.

Discussion

We have identified the first B-cell epitope of Hyal, a major allergen of bee venom, from the crystal structure of Hyal in complex with the specific Fab fragment of a monoclonal murine anti-Hyal IgG1 Ab. The Hyal epitope is composed of mostly continuous array of nine residues folded as a helix–turn–helix motive, which protrudes away from the globular protein core and fits tightly into the deep pocket formed by the six CDRs of the Fab. A local conformational change of the turn joining two helices is observed upon binding. Although the epitope is continuous, its conformation is important for Ab recognition, since a synthetic peptide (Arg138–Glu152), comprising the entire epitope, is

neither recognized by mAb-IgG 21E11 nor by human IgE from the sera of bee venom allergic patients. This is the second structural study of an allergen–Ab complex after the major birch pollen allergen Bet v 1 in complex with the Fab fragments of a monoclonal murine IgG Ab.⁴⁰ The latter structure revealed a conformational epitope composed of the 16 residues belonging to a rather flat allergen–Ab molecular interface.

The IgE antibodies from allergic patients are polyclonal and bind to several different epitopes of an allergen. We have shown that mAb 21E11 exhibits a varying degree of inhibitory effect on the binding of human IgEs to Hyal, ranging from 3% to 57% depending on the patient. This broad range of inhibition efficacy probably reflects the different IgE repertoire of each patient. The moderate inhibition observed with most of the sera is probably due to the presence of a variety of IgE antibodies which recognize different epitopes. Thus, only a fraction of IgE antibodies will be affected by the presence of mAb 21E11 bound to Hyal. In the case that inhibition is caused by direct competition of IgG and IgE for the same epitope, the Hyal–IgG interaction surface provides indirect information on the interaction of Hyal with IgE. However, allergen-specific IgG antibodies may inhibit the binding of IgE by several alternative mechanisms, such as (i) partial overlap of the IgG and IgE epitopes, (ii) neighboring IgG and IgE epitopes which cannot be occupied simultaneously due to steric hindrance and (iii) perturbation of IgE epitopes by the conformational changes induced by IgG binding. The moderate inhibition (20–30%) is consistent with the overlapping of IgG and IgE epitopes, as well as with mechanisms (i) or (ii). However, an inhibition of 57% would be consistent either with the inhibition of a dominant IgE epitope

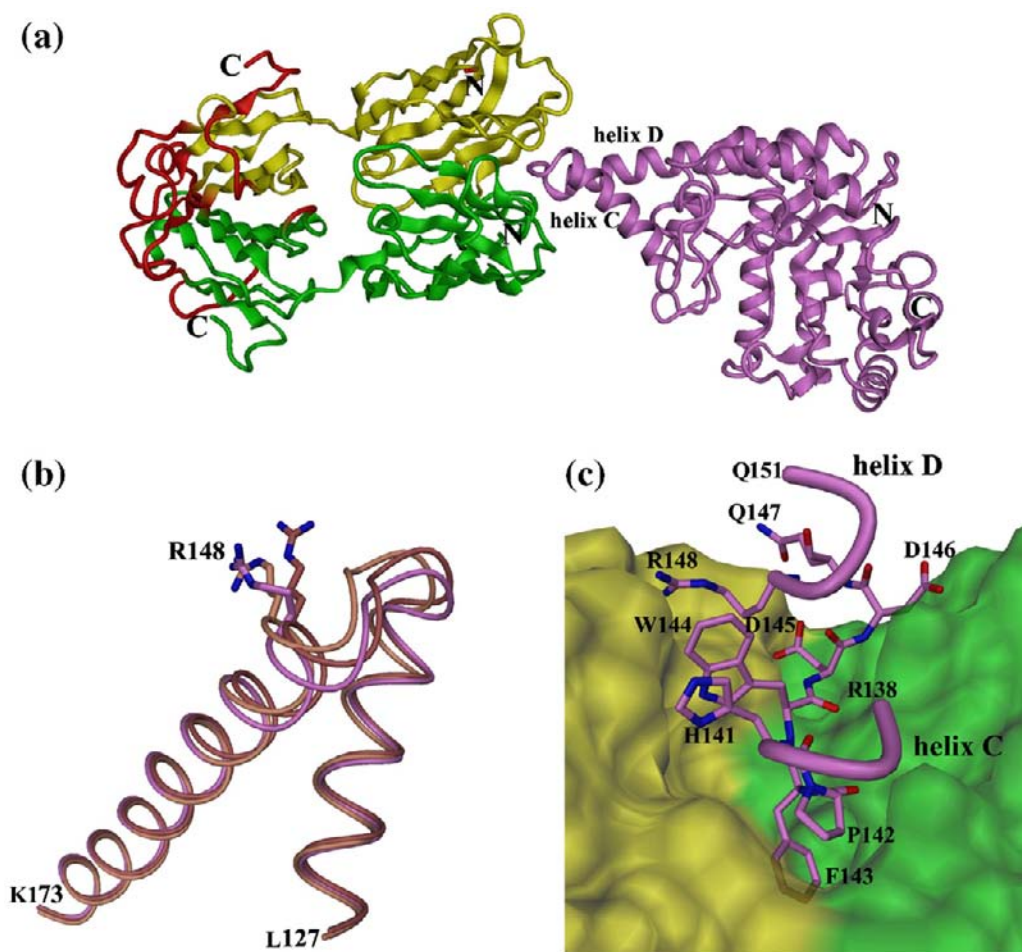


Figure 2. Hyal/Fab complex. (a) Ribbon representation of the Hyal/Fab complex structure. Same color code as in Figure 1; Hyal is shown in magenta and Fab heavy and light chains are colored yellow and green, respectively. For clarity, the residues of the Fab constant and variable domain not defined by electron density are also included and are colored red. The polypeptide chain termini are labeled with N and C. (b) Conformational changes induced in the Hyal epitope upon Hyal/Fab complex formation. Hyal, colored in magenta, is superposed on two models of unliganded Hyal: 1FCQ (light reddish brown) and 1FCU (dark reddish brown). The largest C_{α} atom shifts (more than 2 Å) are seen for Phe143. (c) Close-up view of the Hyal/Fab interface. The Hyal epitope is shown as a full atom representation colored magenta and the molecular surface of the Fab colored yellow and green for the heavy and light chains, respectively. For clarity, residue Arg138 of Hyal that is also involved in the interaction is not shown. For more details, see Table 4.

or with a large conformational change, which would affect a significant part of the molecule and thus cause the simultaneous perturbation of several IgE epitopes. However, the last proposed mechanism is less likely because only a local conformational change is observed.

The Hyal/Fab complex shares a number of general features with other protein–Ab complexes which possess a discontinuous epitope, e.g., all six CDRs interact with the Ag,^{35,41} with the interactions with the heavy chain being most prominent;²⁷ the contacting surfaces are highly complementary and have areas in the range of 600 Å²–900 Å²; the stability of a complex is provided by van der Waals interactions, hydrogen bonds and, to a lesser extent, by salt bridges. Epitopes in most of the protein/antibodies complexes are discontinuous and comprise 14–20 residues.^{35,41,42} In contrast, the Hyal epitope is continuous and composed of only 9 resi-

dues, thus resembling to an Ab–peptide complex.⁴³ However, many conformational epitopes contain a linear stretch of residues which account for most of the interactions with specific antibodies. For example, residues Ile42–Thr52 of the conformational epitope of Bet v 1/Fab complex account for 80% of all Ag–Ab interactions⁴⁰ while residues 101–108 of conformational epitope of extracellular domain of myelin oligodendrocyte glycoprotein account for 65% of the total interaction surface of myelin oligodendrocyte glycoprotein–extracellular domain.⁴⁴ The Hyal/Fab complex contains four salt bridges, between Asp145 and Arg148 of Hyal and Arg58 and Asp54 of Fab CDR-H2, respectively. Similarly, in the lysozyme (likewise Hyal also an $\beta(1,4)$ glycosidase) in complex with Fab fragment of specific Ab HyHEL-5, Arg45 and Arg68 of lysozyme and Glu-H35 and Glu-H50 of Fab fragment form three salt bridges.⁴² Both Hyal and lysozyme

Table 4. Hyal/Fab interaction: direct contacts

	Fab	Hyal	Distance (Å)
<i>Hydrogen bonds</i>			
CDR-L1	Tyr L32 OH	Asp A146 OD1	3.1
CDR-L2	Asn L50 ND2	Arg A138 O	3.1
CDR-L3	His L91 NE2	Pro A142 O	2.9
	Tyr L92 O	Asp A146 N	3.0
	Arg L96 NH2	Phe A143 O	2.7
CDR-H1	Gly H33 O	Trp A144 NE1	3.2
CDR-H2	Tyr H52 OH	Asp A145 N	3.1
	Tyr H52 OH	Asp A145 OD1	2.4
	Arg H58 NH2	Gln A147 OE1	3.0
<i>Salt bridges</i>			
CDR-H2	Arg H58 NE	Asp A145 OD1	2.9
	Arg H58 NH2	Asp A145 OD2	3.2
	Asp H54 OD1	Arg A148 NH1	3.1
	Asp H54 OD2	Arg A148 NH2	3.2
<i>Apolar contacts</i>			
CDR-L1	Tyr L32 CZ	Asp A146 CA	3.6
	Tyr L32 CE1	Asp A146 CB	3.7
FWR2	Tyr L49 CD2	Pro A142 CB	3.5
	Leu L46 CD2	Phe A143 CZ	3.6
CDR-L3	Tyr L92 CE1	Asp A146 CG	3.6
CDR-H1	Gly H33 CA	Trp A144 CZ2	3.7
CDR-H2	Tyr H52 CZ	Arg A148 CG	3.5
	Trp H53 CZ3	Trp A144 CZ2	3.7
	Trp H53 CH2	Trp A144 CZ2	3.5
CDR-H3	Tyr H95 CD1	Phe A143 CG	3.5
	Tyr H95 CD1	Phe A143 CD1	3.6

The cutoff distance for polar contacts is 3.25 Å. The 11 van der Waals interactions are shown for a cutoff value of 3.7 Å; increasing the cutoff value to 4.0 Å results in 39 van der Waals contacts (not shown).

complexes contain three water molecules, located in the cavity formed by V_L and V_H , which mediate hydrogen bonding interactions between the two proteins and their respective antibodies. In Hyal/Fab complex, the CDR-H2 is involved in most of the interactions with Hyal while CDR-H3 makes only few contacts which are similar to those reported in HyHEL-10 Fab-lysozymes complex.⁴¹

Table 5. Hyal/Fab interaction: water-mediated contacts

	Fab	Distance (Å)	Water molecules	Distance (Å)	Hyal
CDR-H3	Gly H97 N	3.1	21O	2.6	His A141 ND1
CDR-H1	Gly H33 O	2.7	21O		
CDR-H2	His H50 NE2	3.1	22O	3.0	Phe A143 O
CDR-L3	Gly L93 O	2.9	23O	2.7	Asp A145 OD1
CDR-L3	Arg L96 NE	3.1	23O		
CDR-L3	Arg L96 NH2	3.2	23O		

The cutoff distance is 3.25 Å.

The shape of the Ag combining site of an Ab is related to the nature of the Ag; deep pockets are observed with haptens, grooves with peptides and flat combining sites with proteins.³⁹ It has been shown that the lengths of the CDRs are directly related to the topography of the Ag combining site such that a longer CDR-H3 loop implies a flat or protruding Ag combining site while a short CDR-H3 loop favors pockets or grooves.⁴⁵ A deep binding cavity is observed in the Hyal/Fab complex which supports this hypothesis and agrees with the short length of CDR-H3 (four residues). In contrast, the epitopes of K^+ channel/Fab complex and lysozyme/HyHEL-10 Fab complex revealed a flat interacting surface, in agreement with a longer CDR-H3 loop consisting of 9 and 11 residues.^{41,46}

The Hyal epitope has a central hydrophobic patch which is surrounded by charge and polar residues. The four salt bridges at the periphery of the Fab binding cavity are probably involved in the initial protein-protein association through long range electrostatic interactions. In the following step, the docking with the formation of specific interactions

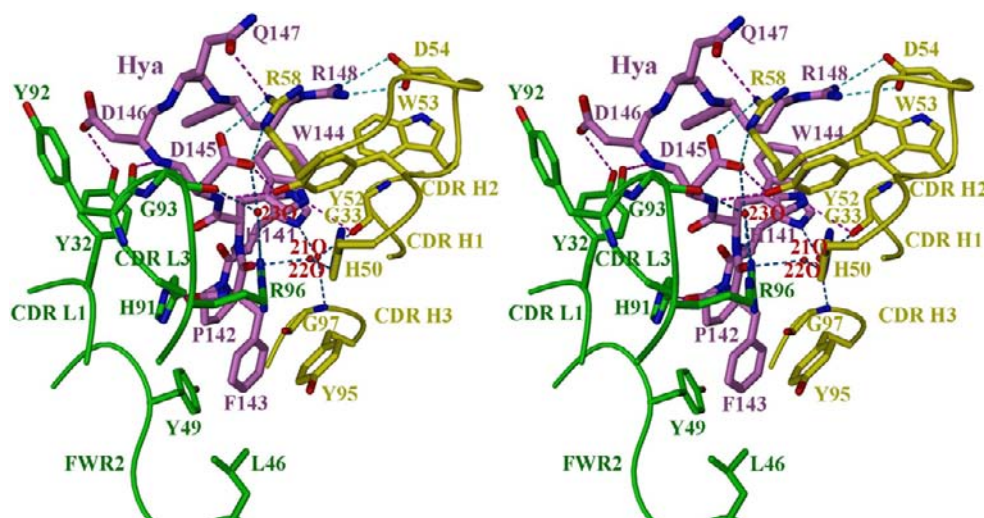


Figure 3. Stereo view of the polar and ionic interactions within the Hyal/Fab complex. Same color code as in Figures 1 and 2. Hydrogen bonds (magenta) and salt bridges (cyan) are shown as dashed lines. Water-mediated interaction is shown in blue. For clarity, residue Arg138 of Hyal is not shown. For more details, see Tables 4 and 5.

takes place. The interaction between the Hyal/Fab surface shows a good shape complementarity which is enhanced by the presence of three water molecules in the interface. Additional water molecules are also observed at the periphery of the binding cavity and are involved in hydrogen bonds which are bridging Hyal with Fab. Similarly, Fv D1.3-HEL and HyHEL-5-lysozyme complexes contain four and seven water molecules which are located in the cavity and mediate the hydrogen bonding interaction.^{34,35}

In more general terms, the structure of each new Ag-Ab complex increases our knowledge and, hence, the probability of identifying any features common for Ag-Ab recognition, which would ultimately help to reveal the characteristics of the allergen and the underlying mechanism, which makes an Ag an allergen. Attempts to predict features responsible for allergenicity, either by the search for common sequence motifs^{47,48} or a common motive on the molecular surface,⁴⁹ have recently been reported. The latter revealed a high occurrence of solvent exposed hydrophobic patches, which is in agreement with a notion that the immune system has evolved to recognize the hydrophobic portion of an immunogenic protein.⁵⁰ Supporting this concept, the Hyal epitope contains a surface-exposed hydrophobic patch formed by loop residues Pro142-Phe143-Trp144 which, upon complex formation, become deeply buried in the interface. Similarly, the crystallographically determined epitope of a major birch pollen allergen Bet v 1 showed that the central part of the conformational epitope consists of a linear stretch of mostly apolar residues (P-loop region: Gly-Asn-Gly-Gly-Pro-Gly-Thr) surrounded on both sides by charged and polar residues.⁴⁰

The Hyals from venoms of honey bee, Api m 2, and wasp, Ves v 2, share 55% sequence identity and have identical fold while the sequence variability is mostly confined to the surface area.²⁰ Of the nine epitope residues of Hyal (Api m 2) only four are conserved in Ves v 2. The central epitope residue Phe143, which fits tightly in the hydrophobic pocket formed by CDR residues of Fab, has been replaced by a polar Thr residue in Ves v 2. Moreover, the charge distribution among the non-conserved surface exposed residues is significantly different and hence, it is unlikely that the identified epitope is responsible for the *in vitro* observed IgE-mediated cross-reactivity between Api m 2 and Ves v 2. Since both enzymes are glycosylated, it is possible that the cross-reactivity can be mediated by carbohydrate moiety, as suggested by Skov *et al.*²⁰

Type I allergy is an IgE-mediated hypersensitivity disease affecting up to 25% of the population of all ages, from infants to the elderly. There is a definite need for an effective treatment of this disease, particularly for bee venom where the allergic reaction to stings can occur suddenly with an occasionally fatal outcome. The antigenicity of Hyal is fully determined by the structure of its epitopes, the areas of the protein surface that are recognized by specific antibodies. The knowledge

of the Hyal epitope allows a structure-based rational modification of the epitope surface aimed at producing allergen variants with low IgE-binding activity but able to induce protective allergen-specific IgG antibodies which compete with IgE (hypoallergens).⁵¹ The hypoallergens are expected to have a significant impact on the development of allergy vaccines with the increased safety and efficacy for allergen-specific immunotherapy.

Experimental Procedures

Protein expression and purification

Recombinant Hyal was produced as a secreted protein by *Baculovirus*-infected insect cells (High Five) and purified by Ni²⁺-chelate chromatography.¹³ The monoclonal hybridoma antibodies, derived from mice immunized with recombinant Hyal, were purified from the supernatants of hybridoma cells rich in specific IgG1 antibodies. To avoid any contamination with bovine IgGs and serum albumin, a serum- and protein-free culture media (TurboDoma) were used for the supernatant production. The IgG1 antibodies purified by Protein G Sepharose affinity chromatography were almost 100% pure, as judged by SDS-PAGE and Coomassie Blue staining (150 kDa under nonreducing conditions). The purified IgG1 antibodies exhibited a high affinity to Hyal and were able to compete with the binding of sera IgEs from bee venom allergic patients.

Amino acid sequence of the complete variable light and heavy chain of mAb 21E11 (murine IgG1, kappa) was deduced from the cDNA sequence obtained by using RT-PCR and the SMART race system (Clontech Laboratories). The PCR products were cloned into TOPO vector (vector with covalently bound topoisomerase I; Invitrogen) and sequenced using M13 forward and reverse primers.

Synthetic peptide

The 15-mer peptide derived from the Hyal/Fab complex (138-RREHPFWDDQRVEQE-152) and covering the entire epitope sequence, was synthesized by Genscript Corporation (Piscataway, NJ, USA)†. The peptide was purified by HPLC and verified by matrix-assisted laser desorption/ionization time-of-flight mass spectroscopy. The peptide was >80% pure and was fully soluble in aqueous solutions.

ELISA

For ELISA experiments, the ELISA plates (Greiner, Kremsmuenster, Austria) were coated overnight, at 4 °C, with rApi m 2 (5 µg/ml dissolved in PBS) or the Api m 2 derived peptide 138-RREHPFWDDQRVEQE-152 (5 µg/ml dissolved in PBS), and for control purposes with human serum albumin (5 µg/ml in PBS) or a control peptide. The plates were washed between each incubation step with PBS containing 0.05% v/v Tween 20 (PBST). Non-specific-binding sites were blocked with PBS/1% w/v bovine serum albumin for 2 h at room temperature. Coated plates

† www.genscript.com

were incubated with sera from bee venom allergic patients (dilution 1:5) or the mouse mAb (dilution 1:1000) in PBS, 0.5% w/v bovine serum albumin, 0.05% v/v Tween 20; both were added in duplicate and incubated overnight at 4 °C. Bound human IgE was detected as described.⁵² Bound mouse mAbs were detected with a monoclonal rat anti-mouse IgG1 Ab (BD Pharmingen, San Diego, CA) followed by the addition of horseradish peroxidase-labeled goat anti-rat IgG antibodies (Amersham Bioscience, Uppsala, Sweden) and visualized by the addition of ABTS solution (60 mM citric acid, 77 mM Na₂HPO₄ × 2H₂O, 1.7 mM ABTS, 3 mM H₂O₂) as a developer.

ELISA inhibition

ELISA plates were coated with 5 µg/ml rApi m 2 overnight at 4 °C. The plates were washed with PBST and after blocking with PBST plus 1% w/v bovine serum albumin, incubated overnight with three mouse monoclonal IgG1 antibodies against Api m 2 (21E11, 22H7, 24F2) or for control purposes, with a mouse mAb against Bet v 1 (diluted 1:100). After washing, the plates were incubated with 1:5 diluted sera from bee venom allergic patients overnight at 4 °C and bound human IgE antibodies were detected as described.⁵²

Production of Fab fragments by papain digestion of IgG

Purified Ab (clone 21E11, 3–6 mg/ml) was dialyzed against 50 mM sodium acetate buffer (pH 5.5) containing 2 mM ethylene diamine tetra-acetic acid. Papain was added (1/100 w/w ratio) in the presence of 10 mM freshly prepared cysteine and digestion was carried out at 37 °C for 6 h. The reaction was stopped by the addition of the specific papain inhibitor E-64 (N-[N-(L-3-*trans*-carboxirane-2-carbonyl)-leucyl]-agmatine) (Roche) in large excess. The digestion mixture was dialyzed against 50 mM sodium acetate buffer (pH 5.5), loaded on a Mono S cation exchange column (Amersham Biosciences) and eluted with a shallow salt gradient 0–150 mM NaCl. The Fab was eluted at 70–80 mM NaCl and its purity was confirmed by SDS-PAGE under both reducing and nonreducing conditions. The Fab yield was about 30% of the starting IgG1 amount. The purified Fab fragments were mixed with Hyal in 1:1.2 molar ratio and incubated at 23 °C for 60 min. The Hyal/Fab complex was separated from excess Hyal by using a Superdex S-75 16/60 gel filtration column (Amersham BioSciences). The protein concentration of the Hyal/Fab complex was calculated from the absorbance measured at 280 nm, assuming an extinction coefficient of 0.7 mg/ml⁻¹ cm⁻¹.

Crystallization and data collection

For the crystallization experiments, the purified Hyal/Fab complex was dialyzed against 5 mM sodium acetate buffer (pH 5.5) and concentrated to 11 mg ml⁻¹. The clusters of thin plate-like crystals were grown by the hanging-drop vapor diffusion method within 4–5 days under the following conditions: the equal volumes (1.5 µl) of the Hyal/Fab complex and precipitant 10% (w/v) polyethylene glycol (PEG) 8000, 0.1 M Ches (2-(*N*-cyclohexylamino)ethanesulfonic acid) (pH 9.5), 0.2 M NaCl (condition 29, Wizard screen kit I) were mixed and equilibrated over the latter solution at 20 °C. The low

crystal reproducibility was overcome by applying a microseeding technique while the substitution of PEG 8000 (10%) by PEG 6000 (11%) resulted in a larger and chunkier, but still clustered plate-like crystals. Prior to data collection, single plates were separated, soaked briefly in the cryoprotective solution (precipitant solution plus 20% PEG 400) and the diffraction data were collected to 2.6 Å resolution at Swiss Light Source (SLS), using a MAR CCD detector ($\lambda = 0.9762$ Å). All measurements were performed at 100 K. The images were indexed and integrated in a monoclinic space group C2 using the program MOSFLM.⁵³ There is one monomer of Hyal/Fab complex per asymmetric unit, resulting in a solvent content of 69% ($V_m = 3.95$ Å³ / Da).⁵⁴

Structure determination and analysis

The structure of the Hyal/Fab complex was determined by the method of MR using the program PHASER.⁵⁵ MR was done in three steps. First, position and orientation of Hyal were obtained using the monoclinic structure of Hyal, 1FCQ¹³ as a search model. Second, the MR was performed separately with variable, *V*, and constant, *C*, domains of various Fab structures, in order to avoid difficulties related to the variable relative orientations of the *V* with respect to the *C* domains of the search models. Out of 30 different models, the *V* domain of 1A7Q gave a good statistic and its position was fixed. Third, out of 18 *C* domain models tested by MR, the PDB code 15C8 gave the best statistics and its position was fixed. Rigid body refinement with five domains (Hyal, *V*_L, *C*_L, *V*_H and *C*_H) with REFMAC⁵⁶ gave an initial *R*/*R*_{free} of 36.0/39.1. Manual adjustment of the model and replacement of the model amino acid sequences with that of 21E11 Fab were performed with program O.⁵⁷ This was followed by restrained maximum-likelihood refinement with REFMAC and addition of water molecules by the program ARP, resulting in the convergence of *R*/*R*_{free} value to 20.9/24.7% at 2.6 Å resolution.⁵⁶ The stereochemistry of the refined structure was validated with program PROCHECK,⁵⁸ which showed that only 0.7% residues are in disallowed regions of a Ramachandran plot (Table 3).

The buried surface area was calculated with program MS⁵⁹ using a probe radius of 1.7 Å. Interactions within the Hyal–Fab interface were assigned with the program CONTACT.⁵⁶

Protein Data Bank accession codes

Coordinates and structure factors have been deposited in the Protein Data Bank with accession codes 2j88 and r2j88sf, respectively.

Acknowledgements

We thank Dr Caroline Peneff for careful reading of the manuscript and valuable discussions. We thank the staff of the synchrotron beam line PX at SLS in Villigen, Switzerland. This project was supported by Swiss National Foundation grant No. 31-67968/02 to Z.M-H and in part by grant F1815 of the Austrian Research Foundation and a research grant from Phadia, Uppsala, Sweden.

References

- King, T. P. & Spangfort, M. D. (2000). Structure and biology of stinging insect venom allergens. *Int. Arch. Allergy Immunol.* **123**, 99–106.
- Müller, U. R. (2002). Recombinant Hymenoptera venom allergens. *Allergy*, **57**, 570–576.
- Hoffman, D. R. (2006). Hymenoptera venom allergens. *Clin. Rev. Allergy Immunol.* **30**, 109–128.
- Roers, A. & Hunzelmann, N. (2005). Immunotherapy of hypersensitivity to hymenoptera venom. *Expert Opin. Biol. Ther.* **5**, 1349–1358.
- Müller, U. R., Cramer, R. & Soldatova, L. (1999). Diagnostik mit rekombinanten/synthetischen Bienengiftallergenen. *Allergologie*, **22**, 551–552.
- Habermann, E. (1972). Bee and wasp venoms. *Science*, **177**, 314–322.
- Laurent, T. C. (1989). *The biology of hyaluronan*. *Ciba Foundation Symp.*, vol. **143**, pp. John Wiley & Sons, New York.
- Laurent, T. C. & Fraser, J. R. E. (1992). Hyaluronan. *FASEB J.* **6**, 2397–2404.
- Turley, E. A., Noble, P. W. & Bourguignon, L. Y. W. (2002). Signaling properties of hyaluronan receptors. *J. Biol. Chem.* **277**, 4589–4592.
- Sherman, L., Sleeman, J., Herrlich, P. & Ponta, H. (1994). Hyaluronate receptors: key players in growth, differentiation, migration and tumor progression. *Curr. Opin. Cell Biol.* **6**, 726–733.
- Knudson, W., Chow, G. & Knudson, C. B. (2002). CD44-mediated uptake and degradation of hyaluronan. *Matrix Biol.* **21**, 15–23.
- Hardingham, T. E. & Muir, H. (1972). The specific interaction of hyaluronic acid with cartilage proteoglycans. *Biochim. Biophys. Acta*, **279**, 401–405.
- Marković-Housley, Z., Miglierini, G., Soldatova, L., Rizkallah, P. J., Müller, U. & Schirmer, T. (2000). Crystal structure of hyaluronidase, a major allergen of bee venom. *Structure*, **8**, 1025–1035.
- Kolarich, D., Leonard, R., Hemmer, W. & Altmann, F. (2005). The N-glycans of yellow jacket venom hyaluronidases and the protein sequence of its major isoform in *Vespa vulgaris*. *FEBS J.* **272**, 5182–5190.
- Soldatova, L.N., Tsai, C., Dobrovolskaia, E., Markovic-Housley, Z. & Slater, J. (2006). Characterization of the N-glycans of recombinant bee venom hyaluronidase (Api m 2) expressed in insect cells. *Asthma Allergy Proc.*, in press.
- Soldatova, L. N., Cramer, R., Gmachl, M., Kemeny, D., Schmidt, M., Weber, M. & Müller, U. R. (1998). Superior biologic activity of the recombinant bee venom allergen hyaluronidase expressed in *Baculovirus*-infected insect cells as compared with *Escherichia coli*. *J. Allergy Clin. Immunol.* **101**, 691–698.
- Henrissat, B. (1991). A classification of glycosyl hydrolases based on amino acid sequence similarities. *Biochem. J.* **280**, 309–316.
- Henrissat, B. & Bairoch, A. (1996). Updating the sequence-based classification of glycohydrolases. *Biochem. J.* **316**, 695–696.
- Marković-Housley, Z. & Schirmer, T. (2002). Structural evidence for substrate assisted catalytic mechanism of bee venom hyaluronidase, a major allergen of bee venom. pp. 19–27, The Royal Society of Chemistry, Cambridge, UK.
- Skov, L. K., Seppel, U., Coen, J. J. F., Crickmore, N., King, T. P., Monsalve, R. *et al.* (2006). Structure of recombinant Ves v 2 at 2.0 Å resolution: structural analysis of an allergenic hyaluronidase from wasp venom. *Acta Crystallogr., D Biol. Crystallogr.* **62**, 595–604.
- Müller, U., Helbling, A. & Berchtold, E. (1992). Immunotherapy with honeybee venom and yellow jacket venom is different regarding efficacy and safety. *J. Allergy Clin. Immunol.* **89**, 529–535.
- Akdis, M., Verhagen, J., Taylor, A., Karamloo, F., Karagiannidis, C., Cramer, R. *et al.* (2004). Immune responses in healthy and allergic individuals are characterized by a fine balance between allergen-specific T regulatory 1 and T helper 2 cells. *J. Exp. Med.* **199**, 1567–1575.
- Jutel, M., Akdis, M., Blaser, K. & Akdis, C. A. (2006). Mechanisms of allergen specific immunotherapy-T-cell tolerance and more. *Allergy*, **61**, 796–807.
- Valenta, R., Ball, T., Focke, M., Linhart, B., Mothes, N., Niederberger, V. *et al.* (2004). Immunotherapy of allergic disease. *Adv. Immunol.* **82**, 105–153.
- Larche, M., Akdis, C. A. & Valenta, R. (2006). Immunological mechanisms of allergen-specific immunotherapy. *Nat. Rev., Immunol.* **6**, 761–771.
- Linhart, B. & Valenta, R. (2005). Molecular design of allergy vaccines. *Curr. Opin. Immunol.* **17**, 646–655.
- Davies, D. R., Padlan, E. A. & Sheriff, S. (1990). Antibody-antigen complexes. *Annu. Rev. Biochem.* **59**, 439–473.
- Poljak, R. J. (1991). Structure of antibodies and their complexes with antigens. *Mol. Immunol.* **28**, 1341–1345.
- Davies, D. R. & Cohen, G. H. (1996). Interactions of protein antigens with antibodies. *Proc. Natl Acad. Sci. USA*, **93**, 7–12.
- Braden, B. C. & Poljak, R. J. (1995). Structural features of the reactions between antibodies and protein antigens. *FASEB J.* **9**, 9–16.
- Kabat, E.A., Wu, T.T., Erry, H.M., Gottesman, K.S. & Foeller, C. (1991). Sequences of proteins of immunological interest. Technical report. U.S. Department of Health and Human Services.
- Martin, A. C. (1996). Accessing the Kabat antibody sequence database by computer. *Proteins: Struct. Funct. Genet.* **25**, 130–133.
- Kulkarni-Kale, U., Bhosle, S. & Kolaskar, A. S. (2005). CEP: a conformational epitope prediction server. *Nucleic Acids Res.* **33**, W168–W171; (Web Server issue).
- Bhat, T. N., Bentley, G. A., Boulot, G., Greene, M., Tello, D., Dall'Acqua, W. *et al.* (1994). Bound water molecules and conformational stabilization help mediate an antigen-antibody association. *Proc. Natl Acad. Sci. USA*, **91**, 1089–1093.
- Cohen, G. H., Silverton, E. W., Padlan, E. A., Dyda, F., Wibbenmeyer, J. A., Willson, R. C. & Davies, D. R. (2005). Water molecules in the antibody-antigen interface of the structure of the Fab HyHEL-5-lysozyme complex at 1.7 Å resolution: comparison with results from isothermal titration calorimetry. *Acta Crystallogr., D Biol. Crystallogr.* **61**, 628–633.
- Yern, X., Fields, B. A., Bhat, T. N., Goldbaum, F. A., Dall'Acqua, W., Schwarz, F. P. *et al.* (1994). Solvent rearrangement in an antigen-antibody interface introduced by site-directed mutagenesis of the antibody combining site. *J. Mol. Biol.* **238**, 496–500.
- Lawrence, M. C. & Colman, P. M. (1993). Shape complementarity at protein/protein interfaces. *J. Mol. Biol.* **234**, 946–950.
- Padlan, E. A. (1990). On the nature of antibody combining sites: unusual structural features that may confer on these sites an enhanced capacity for binding ligands. *Proteins: Struct. Funct. Genet.* **7**, 112–124.

39. MacCallum, R. M., Martin, A. C. & Thornton, J. M. (1996). Antibody-antigen interactions: contact analysis and binding site topography. *J. Mol. Biol.* **262**, 732–745.
40. Mirza, O., Henriksen, A., Ipsen, H., Larsen, J., Wissenbach, M., Spangfort, M. D. & Gajhede, M. (2000). Dominant epitopes and allergic cross-reactivity: complex formation between a Fab fragment of a monoclonal murine IgG antibody and the major allergen from birch pollen Bet v 1. *J. Immunol.* **165**, 331–338.
41. Padlan, E. A., Silverton, E. W., Sheriff, S., Cohen, G. H., Smith-Gill, S. J. & Davies, D. (1989). Structure of an antibody-antigen complex: crystal structure of the HyHEL-10 Fab-lysozyme complex. *Proc. Natl Acad. Sci. USA*, **86**, 5938–5942.
42. Sheriff, S., Silverton, E. W., Padlan, E. A., Cohen, G. H., Smith-Gill, S. J., Finzel, B. C. & Davies, D. R. (1987). Three-dimensional structure of an antibody-antigen complex. *Proc. Natl Acad. Sci. USA*, **84**, 8075–8079.
43. Schulze-Gahmen, U., Rini, J. & Wilson, I. (1993). Detailed analysis of the free and bound conformations of an antibody. X-ray structures of Fab 17/9 and three different Fab-peptide complexes. *J. Mol. Biol.* **234**, 1098–1118.
44. Breithaupt, C., Schubart, A., Zander, H., Skerra, A., Huber, R., Lington, C. & Jacob, U. (2003). Structural insights into the antigenicity of myelin oligodendrocyte glycoprotein. *Proc. Natl Acad. Sci. USA*, **100**, 9446–9451.
45. Collis, A. V. J., Brouwer, A. P. & Martin, A. C. R. (2003). Analysis of the antigen combining site: correlations between length and sequence composition of the hypervariable loops and the nature of the antigen. *J. Mol. Biol.* **325**, 337–354.
46. Jiang, Y., Lee, A., Chen, J., Ruta, V., Cadene, M., Chait, B. T. & MacKinnon, R. (2003). X-ray structure of a voltage-dependent K⁺ channel. *Nature*, **423**, 33–41.
47. Gendel, S. M. (2002). Sequence analysis for assessing potential allergenicity. *Ann. N.Y. Acad. Sci.* **964**, 87–98.
48. Li, K.-B., Issac, P. & Krishnan, A. (2004). Predicting allergenic proteins using wavelet transform. *Bioinformatics*, **20**, 2572–2578.
49. Furmonaviciene, R., Sutton, B. J., Glaser, F., Laughton, C. A., Jones, N., Sewell, H. F. & Shakib, F. (2005). An attempt to define allergen-specific molecular surface features: a bioinformatic approach. *Bioinformatics*, **21**, 4201–4204.
50. Seong, S.-Y. & Matzinger, P. (2004). Hydrophobicity: an ancient damage-associated molecular pattern that initiates innate immune responses. *Nat. Rev., Immunol.* **4**, 469–478.
51. Ferreira, F., Ebner, C., Kramer, B., Casari, G., Briza, P., Kungl, A. J. *et al.* (1998). Modulation of IgE reactivity of allergens by site-directed mutagenesis: potential use of hypoallergenic variants for immunotherapy. *FASEB J.* **12**, 231–242.
52. Denepoux, S., Eibensteiner, P. B., Steinberger, P., Vrtala, S., Visco, V., Weyer, A. *et al.* (2000). Molecular characterization of human IgG monoclonal antibodies specific for the major birch pollen allergen Bet v 1. Anti-allergen IgG can enhance the anaphylactic reaction. *FEBS Letters*, **465**, 39–46.
53. Leslie, A.G.W. (1992). In joint CCP4 and ESF-EACBM newsletter on protein crystallography no. 26. Technical report. SERC Daresbury Laboratory, Warrington, UK.
54. Matthews, B. W. (1968). Solvent content of protein crystals. *J. Mol. Biol.* **33**, 491–497.
55. Storoni, L. C., McCoy, A. J. & Read, R. J. (2004). Likelihood-enhanced fast rotation functions. *Acta Crystallogr., D Biol. Crystallogr.* **60**, 432–438.
56. CCP4 (1994). Collaborative computational project, number 4. *Acta Crystallogr., D Biol. Crystallogr.* **50**, 760–763; (The CCP4 suite: programs for protein crystallography).
57. Jones, T. A., Zou, J., Cowan, S. & Kjeldgaard, M. (1991). Improved methods for building protein models in electron density maps and the location of errors in these models. *Acta Crystallogr., A*, **47**, 110–119.
58. Laskowski, R. A., MacArthur, M. W., Moss, D. S. & Thornton, J. M. (1993). Procheck: a program to check the stereochemical quality of protein structures. *J. Appl. Cryst.* **26**, 283–291.
59. Connolly, M. L. (1993). The molecular surface package. *J. Mol. Graph.* **11**, 139–141.
60. Read, R. J. (1986). SIGMAA-improved Fourier coefficients for maps using phases from partial structures with errors. *Acta Crystallogr., A*, **42**, 140–149.

Edited by I. Wilson

(Received 9 December 2006; received in revised form 22 January 2007; accepted 8 February 2007)

Available online 22 February 2007

2.1 Supplementary information (Hya/Fab complex)

2.1.1 Hya/Fab complex formation, crystallization and diffraction

2.1.1.1 IgG purification

The supernatant containing IgG was dialyzed (Spectra/Pro, membrane cutoff 12-14 kDa) against 20 mM sodium phosphate buffer pH 7.0 and centrifuged at 13000 rpm (Sorval RC-5B, SLA-1500 rotor) for 30 min. The resultant supernatant was applied on a Protein-G affinity column (Amersham Pharmacia) that specifically binds the Fc region of the IgG molecule. The bound IgG was eluted in 1 ml fractions with 100mM glycine buffer pH 2.7 (Figure 1) and immediately neutralized with 200 μ M of 1M Tris buffer pH 9.0.

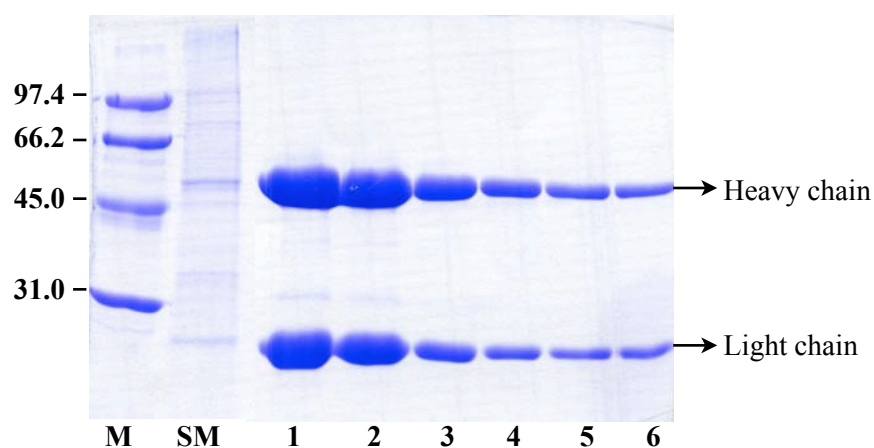


Figure 1. IgG purification. SDS-polyacrylamide gel (12%, reducing condition) analysis of the purified IgG eluted from Protein-G column. M stands for molecular weight markers (kDa), SM for starting material and fraction numbers are indicated at the bottom of the gel.

2.1.1.2 IgG digestion

The purified IgG was dialyzed against 100 mM sodium acetate buffer pH 5.5 containing 2 mM EDTA and was subsequently concentrated to 3-6 mg/ml using a centricon (30 kDa molecular-mass cutoff; Amicon). To the concentrated IgG, freshly prepared cysteine was added to the final concentration of 10 mM and followed by the addition of papain at the ratio of 1/100 (W/W) with respect to IgG concentration. The papain is a cysteine endopeptidase of 23000 Da molecular weight and was used for limited hydrolysis of native immunoglobulin (Ig). Digestion was carried out by incubating sample at 37 °C for 6 hours (Figure 2). The IgG digestion was stopped by addition of 10 fold excess of E64 inhibitor (N-[N-(L-3-trans-carboxyoxirane-2-carbonyl)-L-leucyl]-agmatine, Roche; Molecular weight 357.4 Da) relative to the papain concentration. The E64 stock has been prepared by dissolving the compound in 1:1 ethanol/water mixture to the final concentration of 250 µM.

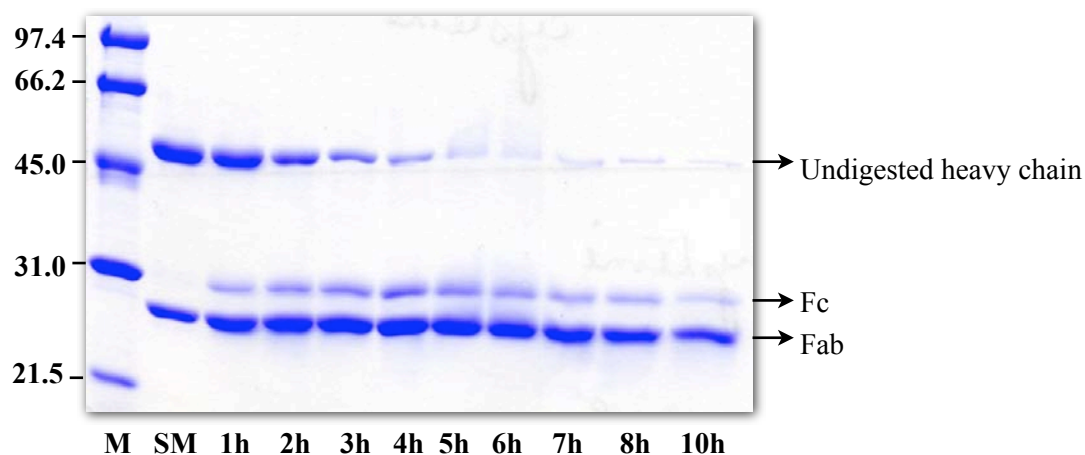


Figure 2. IgG test digestion. Digestion was carried out with papain in the presence of 10 mM cysteine. SDS-polyacrylamide (12%, reducing condition) analysis of the digested sample collected at various time point as indicated at the bottom of the gel. M stands for molecular weight markers (kDa), SM for starting material.

2.1.1.3 Purification of Fab using cation exchange chromatography (Mono-S)

The digested sample was dialyzed against 50 mM sodium acetate buffer pH 5.5 and loaded on a cation exchanger (mono-S) column (Pharmacia) using acta purifier (Amersham Pharmacia). The long shallow salt gradient was carried out between 20 -120 mM NaCl in order to separate Fab isoforms from (Fab)₂ (Figure 3).

2.1.1.4 Complex formation and purification using gel filtration column (Superdex S-75 16/60)

The Fab, eluted as a major peak at 40 mM NaCl was pooled, mixed with hyaluronidase in 1:1.2 molar ratio and incubated at room temperature for 1 hour. The Hya/Fab mixture was concentrated to 4-6 mg/ml using centricon (Amicon) and loaded on a Hiload Superdex S-75 (Amersham Pharmacia) gel filtration column in order to separate Hya/Fab complex from excess Hya (Figure 4).

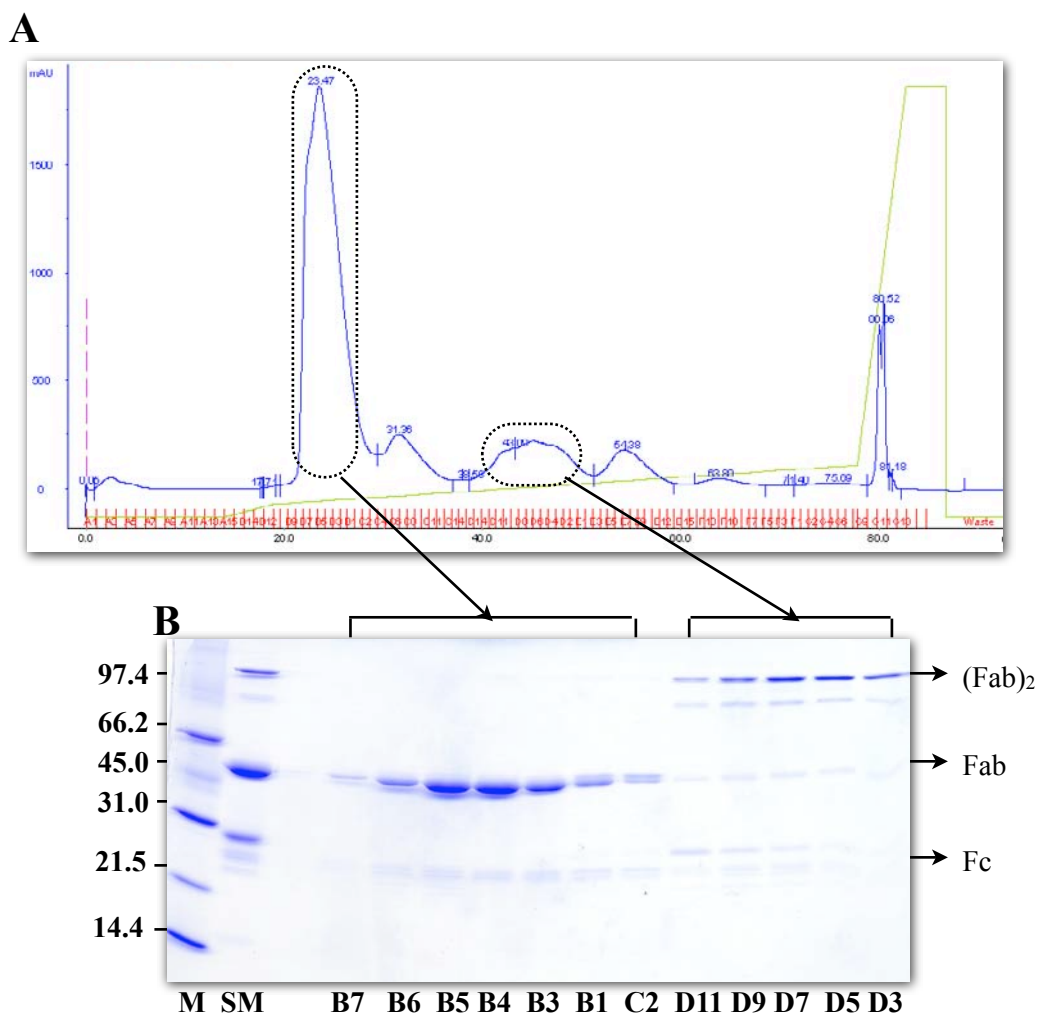


Figure 3. Purification of Fab using cation exchange chromatography (Mono-S column). **A)** Chromatogram of Fab elution profile. **B)** SDS-polyacrylamide (12%, non-reducing condition) analysis of proteins separated on Mono-S column. M stands for molecular weight markers (kDa) and SM for starting material. Fraction numbers are indicated at the bottom of the gel.

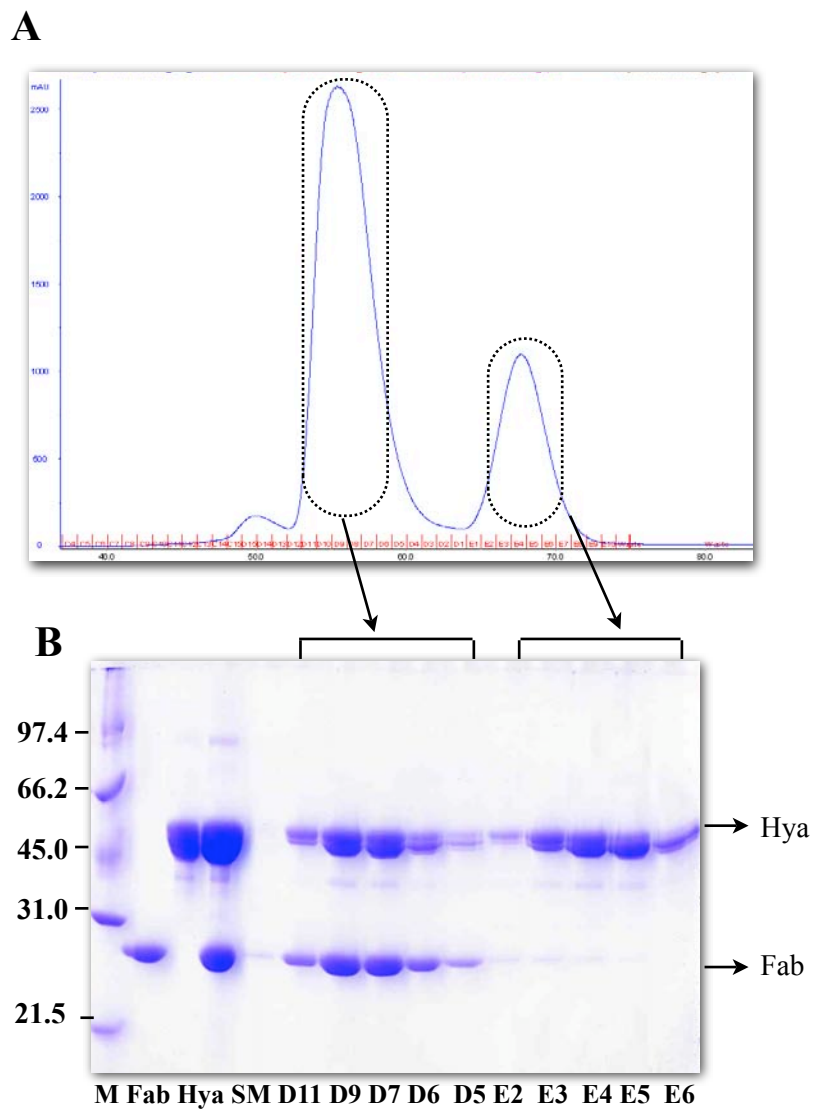


Figure 4. Purification of Hya-Fab complex using Hiload 26/60 Superdex 75 16/60 gel filtration chromatography. **A)** Chromatogram show Hya/Fab complex separated from excess Hya. **B)** SDS-polyacrylamide (12%, reducing condition) analysis of the first peak shows complex whilst the second peak shows an excess of Hya. M stands for molecular weight markers (kDa), SM for starting material and fraction numbers are indicated at the bottom of the gel.

2.1.1.5 Crystallization and diffraction

Hya/Fab - 21E11 complex: The eluted Hya/Fab complex fractions were pooled, dialyzed against 10 mM sodium acetate buffer pH 5.5 and concentrated to 12-14 mg/ml concentration. The crystallization was performed with Hampton and Wizard screening kit I and II using hanging drop vapour diffusion method. The drops were prepared by mixing 1 μ l of protein with 1 μ l of reservoir solution and equilibrated against 500 μ l reservoir solution. The Hya/Fab complex crystals were grown as clustered thin plates in 10 % PEG 8000, 0.1 M CHES pH 9.5 and 0.2 M NaCl (condition 29, Wizard screening kit I) in 4-5 days (Figure 5). The crystals were not reproducible but the microseeding helped to overcome the nucleation problem and subsequently crystals were grown in less than 24 hours. The crystals were cryoprotected with 0.1M TABS pH 9.5, 11.5% PEG 8000 and 20 % PEG 400. Data was collected at Swiss light source (SLS) and Hya/Fab complex crystal diffracted to 2.6 Å (Figure 6).



Figure 5. Hya/Fab-21E11 complex crystals

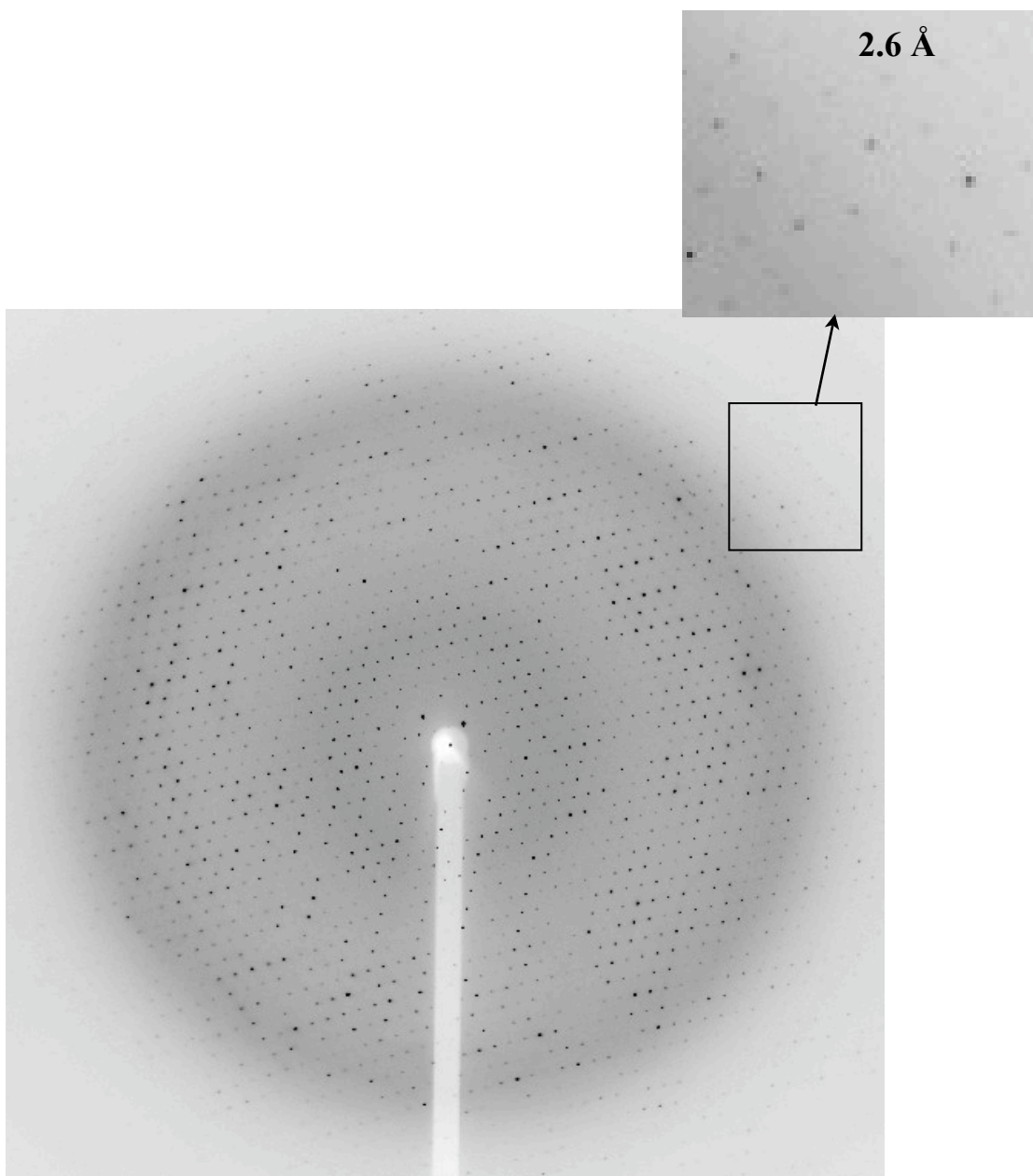


Figure 6. Diffraction pattern of the Hya-Fab complex. The images were recorded on a MAR-CCD image plate detector. The crystal showed isotropic diffraction, with spots diffracting beyond 2.6 Å shown in the inset.

Hya/Fab-22H7 complex: The purified Hya/Fab complex was dialyzed against 10 mM sodium acetate buffer pH 5.4 and concentrated to 12 - 14 mg/ml. The crystallization was performed with commercial screens, that is Hampton and Wizard screening kit I and II using hanging drop vapour diffusion method. The drops were prepared by mixing 1 μ l of protein with 1 μ l reservoir solution and equilibrated against 500 μ l of reservoir solution. The Hya/Fab (22H7.11.12) complex was crystallized in the presence of 9.5% PEG 8000, 0.1 M TABS pH 9.5 and 0.2 M NaCl similar to 21E11.1.6 clone. The microseeding was applied to overcome the nucleation problem. The crystals were grown as thin plates and reached maximum size in 2-3 days (Figure 7).

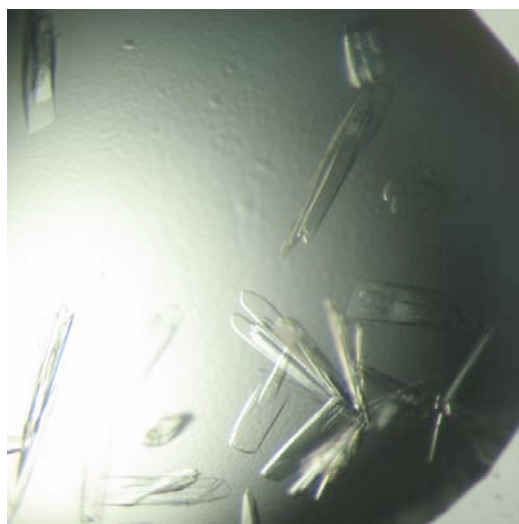


Figure 7. Hya/Fab-22H7 complex crystals

2.1.1.6 Structure solution: Search for useful Fab model for molecular replacement (MR)

The structure of Hya/Fab complex was determined by molecular replacement (MR) using the program PHASER [1]. The orientation and position of the Hya/Fab complex were determined by MR in three consecutive steps. First, Hya was located using PDB code: 1FCQ as a search model. On fixing the Hya position, PHASER gave a Z-score of 13. This was followed by rigid body refinement which gave $R_{\text{factor}}/R_{\text{free}}$ of 41.8/42.5%.

The PDB database consists of more than 500 Fab structures. MR with intact Fab model was not expected to work due to a rather various relative variable (V_L and V_H) and constant domains (C_L and C_H) arrangements. Therefore, the following strategy was applied to locate the correct Fab model from the database. Firstly, mass mapping was carried out with light and heavy chains separately and the sequence of top hits was used for Blast (NCBI BLAST). The Blast with the heavy chain sequence gave the Fab (1S5I and 1ORS) and these Fabs were divided into variable (V_L and V_H) and constant domains (C_L and C_H) whilst the flexible linker region were removed. The MR was carried out in two steps; the position of the variable domain (V_L and V_H) was fixed followed by fixing the constant domain (C_L and C_H). The MR with variable domain of 1S5I and 1ORS gave good Z score of 18 and 20 and the R factor and R_{free} of 39.4/ 42.8% and 39.3/42.0% respectively. The structural neighbor to 1ORS heavy chain was searched using NCBI vast program and the results were sorted based on high redundant and root-mean square deviation (rmsd). For variable domain, four highest hit (marked in pink) gave good statistics, out of which, 1A7Q position was fixed and it gave Z score of 23 and R_{factor} and R_{free} of 37.8/41.6%. In total, 30 different variable domain were used for MR. The variable domain consists of complementary determining regions (CDR) which is involved in antigen binding. The sequence and structure of CDR's varies from one antibody to another. The position of CDR's in 1A7Q were determined by Immunoglobulin (Ig) Blast (NCBI Blast) and the truncation were made in CDR sequence i.e the occupancy of the corresponding amino acid was set to zero, in order to exclude them from the refinement using REFMAC [2]. The truncation in CDR's of 1A7Q, improved the statistics to small extent resulting in the Z score of 24 and $R_{\text{factor}}/R_{\text{free}}$ of 37.7/40.7%.

Search for constant domain models (C_L and C_H) was carried out randomly. Out of 18 constant domain models, 15C8 gave a Z score 20. After five rigid body refinement (Hya, V_L , C_L , V_H and C_H) the $R_{\text{factor}}/R_{\text{free}}$ was 36.0/39.1%. The density for the terminal region of constant domain was not well defined. Thus, Hya, variable and constant domains had been

found representing the full Hya/Fab complex structure. Manual adjustment of the model was performed with program O [3] and was followed by full atom refinement that gave an $R_{\text{factor}}/R_{\text{free}}$ of 26.9/31.2%. Replacement of the model amino acid sequences with that of 21E11 Fab was performed with program O and followed by refinement with REFMAC converged $R_{\text{factor}}/R_{\text{free}}$ to 21.0/24.7% at 2.6 Å.

Molecular replacement (MR) carried out as three step procedure - Phaser

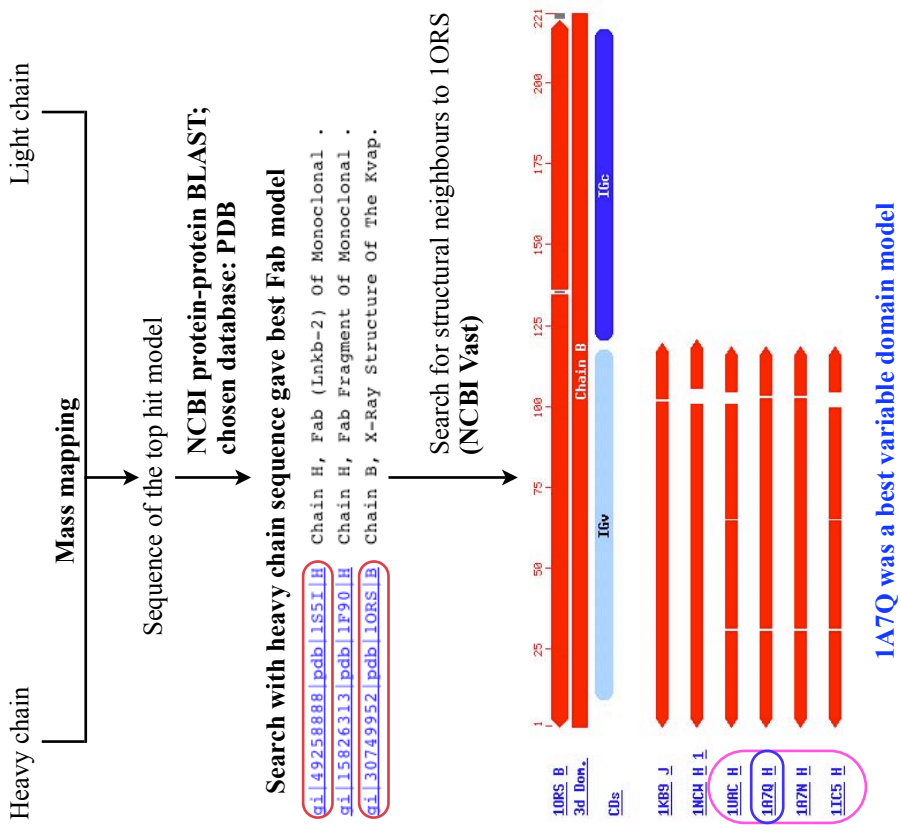
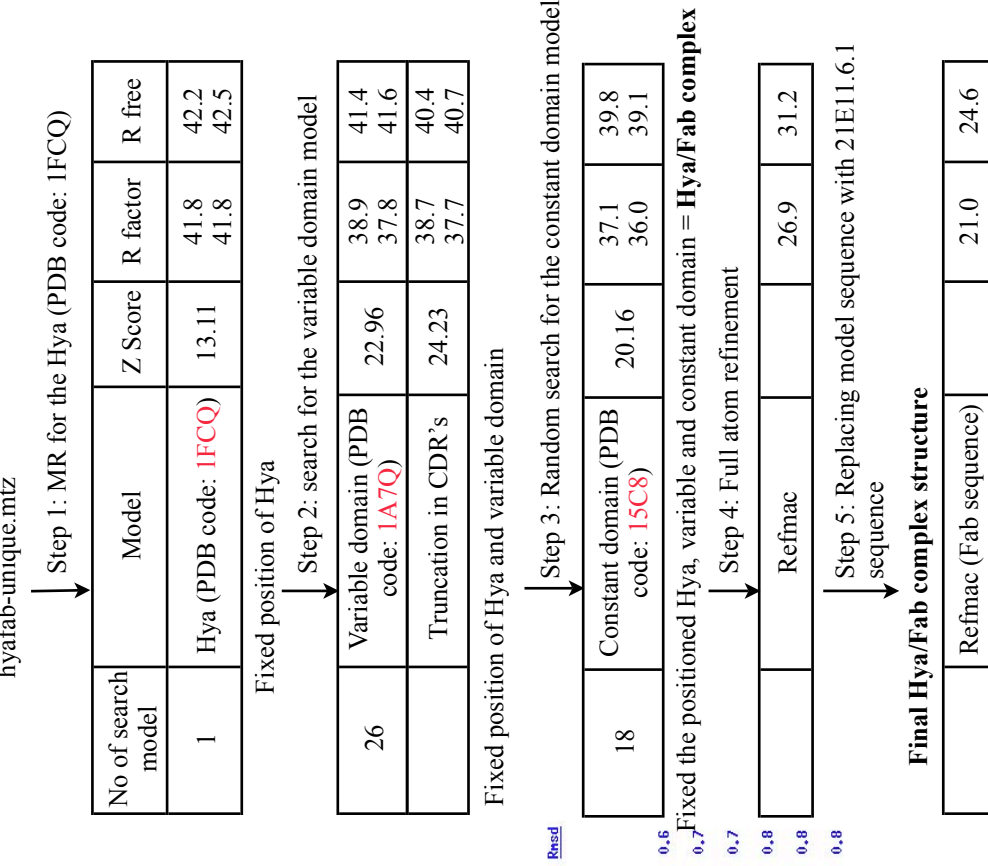


Figure 8. Schematic representation of a search for the Hya/Fab model by molecular replacement (MR). The number of search models, model with PDB code, R_{factor} and R_{free} values, used at various stages of MR are indicated in box. The method used for finding the useful variable domain model is showed on the left.

2.1.1.7 Hya/Fab-21E11 crystal packing

Hya/Fab complex crystallized in C2 (monoclinic) space group, which contains two fold rotation along b-axis and c-centering on ab plane. The C2 space group consists of four asymmetric units. In case of Hya/Fab complex, each asymmetric unit contains one Hya/Fab complex. The crystal contacts are mediated by Hya-Hya and Hya- V_{H} contacts.

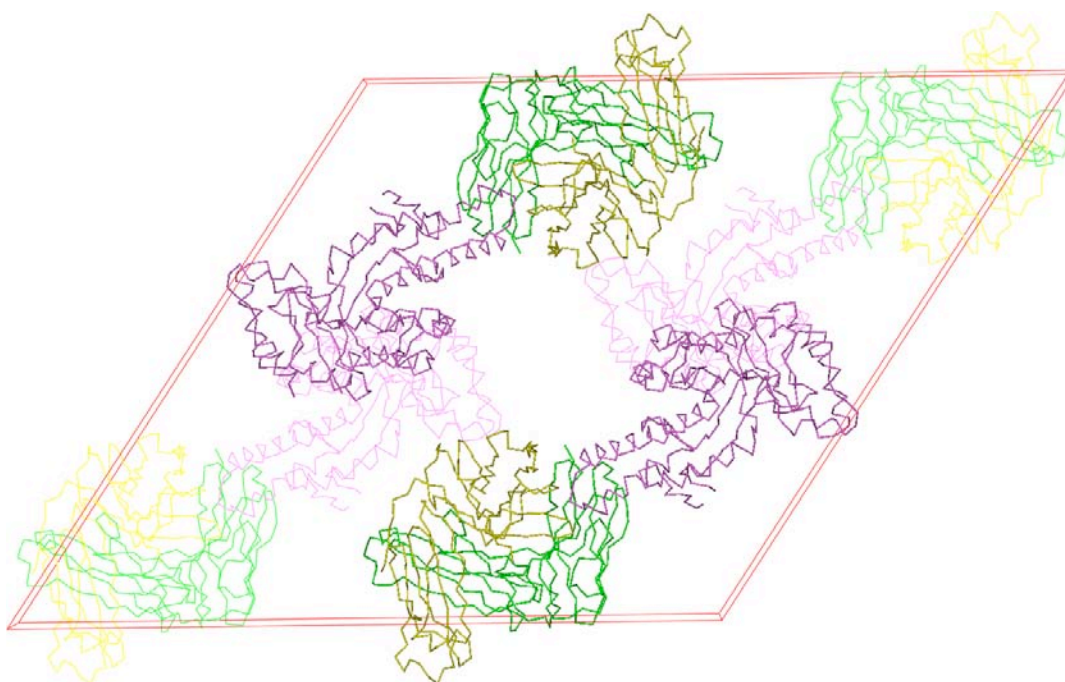


Figure 9. Crystal packing of Hya/Fab-21E11 complex. Magenta represents Hya, yellow heavy chain and green light chain). The picture was produced using the program DINO (A.Philippsen, <http://www.biozentrum.unibas.ch/~xray/dino>).

2.1.2 Mechanism of Type 1 hypersensitivity reaction.

Allergy caused by insect venom is an example of immediate type 1 hypersensitivity reaction. In genetically susceptible individual, some environmental protein antigen, commonly called allergen, can stimulate distinct immune response. They preferentially use particular antigen presenting cells (APC) such as dendritic cells and B cells and stimulate CD4⁺ T cells to differentiate into Th2 effector T cells. The activated Th2-type cells produce cytokines - such as interleukin-4 (IL-4) and IL-13 - which promote switching of B cells to IgE producing plasma cells, whilst IL-5 stimulates eosinophilic survival and activation (Figure 10). In addition to cytokines, various other factors influence the differentiation of CD4⁺ T cells into the Th2 phenotype, such as the genetic background of the individual, the site of antigen contact, allergen dose and conformation, the nature and number of antigen presenting cells, as well as inflammatory mediator (e.g. histamine) [4]. In addition, immune cells recognize allergen epitopes differently: T-cells recognize continuous amino acid sequences (i.e. continuous epitopes), whereas B cells recognize allergens in their intact three dimensional structure (i.e. conformational epitope). The secreted IgE circulates throughout the body and binds to high-affinity Fc receptors FcεRI on the surfaces of circulating basophils and on mast cells in various tissues. This primary response to allergen is known as sensitization.

On second re-exposure, multivalent antigen binds to the cell-associated IgE and cross-links two or more IgE molecules bound to the Fc receptors. This leads to a series of signaling events in the mast cells and basophils, which result in the release of preformed mediators, such as histamine and leukotrienes, stored in the cytoplasmic granules. The clinical and pathologic manifestations are due to the actions of the released mediators. Some of these mediators induce an immediate symptoms of disease, such as rhinitis, conjunctivitis, vascular and smooth muscle reaction and asthma, and others stimulates the influx of leucocytes resulting in the late phase reaction [4-6].

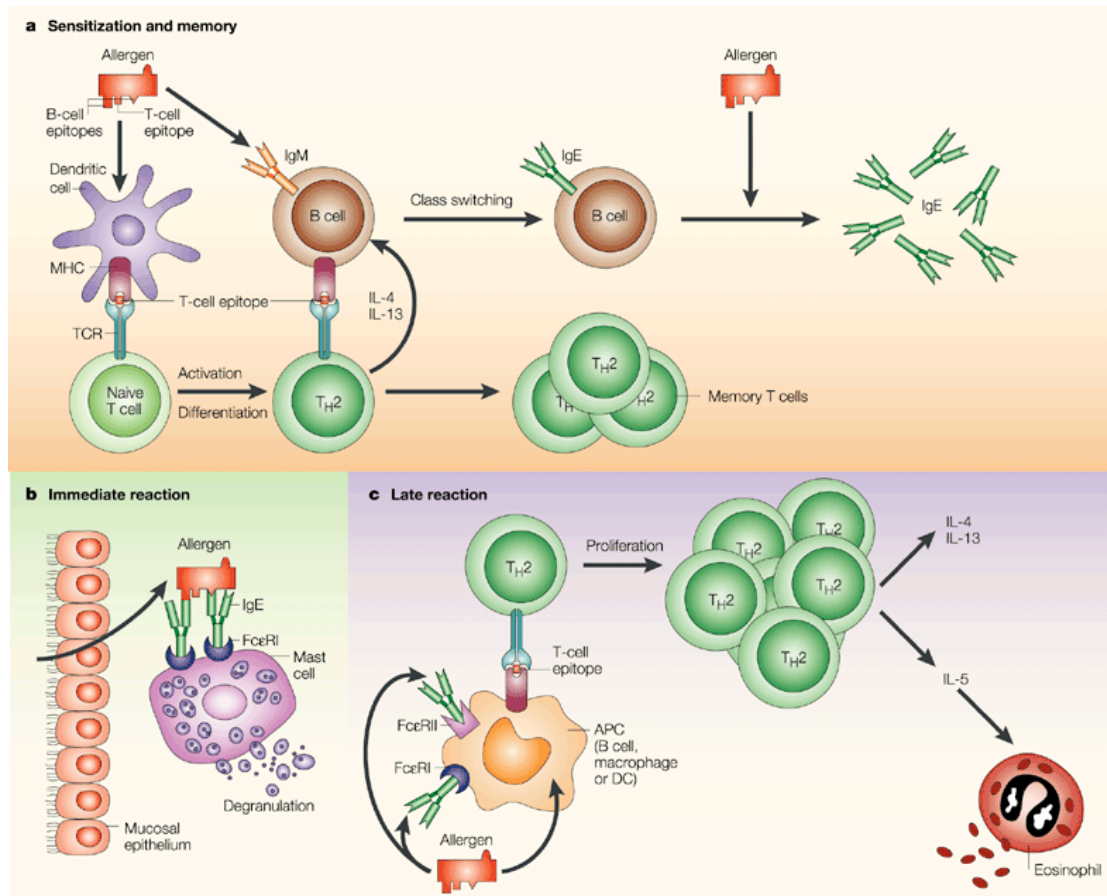


Figure 7. Mechanism of Type 1 allergic reaction. **a)** Sensitization and memory. Initial contact with allergen, might favour allergen uptake by potent antigen presenting cells (APC) and/or immunoglobulin mediated capture by B cells. The activated T helper 2 (Th2) cell produce the cytokines such as interleukin-4 (IL-4) and (IL-13) that favour immunoglobulin-class switching of specific B cells to immunoglobulin E (sensitization). The secreted IgE binds to specific receptors (FcεRI, high affinity receptor; FcεRII, low affinity receptor) on to mast cells, basophils etc. Sensitization leads to the establishment of IgE memory B cells and allergen specific memory T cells. , **B.** Immediate reaction. The cross linking of effector cell bound IgE by allergens leads to the degranulation of cytoplasmic granules which contains biologically active mediators such as histamine, leukotrienes etc. These released mediator are responsible for the immediate symptoms of allergy. **C.** Late reaction. This is caused by the presentation of allergens to T cells, which become activated, proliferate and release proinflammatory cytokines such as IL-4, IL-5 and IL-13. IL-5 induce tissue eosinophilia and the release of inflammatory mediators from eosinophils. This process might be enhanced by the IgE mediated presentation of allergen to T cells This picture has been taken from *Valenta R 2002* [4].

2.1.3 Specific immunotherapy (SIT)

Allergic disease affect more than 30% of the population in industrialized countries, with an increasing prevalence during the last decades. Currently, SIT is performed with natural allergen extracts that are not designed for an individual patient's allergen profile. Besides, they contain various allergenic, as well as non-allergenic components and might even be contaminated with allergen from other sources. In general, successful SIT requires high dose of allergen extract and in most cases, required dose could not be achieved due to the development of severe systemic side effects including anaphylactic reaction [4].

Rapid development in the field of recombinant allergens revealed the molecular nature of many important allergens and facilitated the characterization of their immunological and structural features. This knowledge allowed modifying allergen to contain relevant T-cell epitopes that induce T-cell tolerance and lack antibody-binding sites (hypoallergen) that would otherwise facilitate IgE-mediated allergic responses. The hypoallergenic proteins have diminished or no IgE binding activities thus enabling the administration of high allergen doses with a reduced risks of systemic side effects. Such hypoallergenic allergen derivatives have been generated by modifying the allergen encoding cDNA (e.g. mutation, deletion, oligomerization and production of hybrids) [7].

Most direct method to map IgE binding epitopes is the structure determination of allergen in complex with Fab fragment of IgG antibodies that compete with patient sera IgE antibodies in binding to Hya. The hypoallergenic allergens were generated by destroying the epitope either by introducing mutation or deletion of epitope residues. In case of birch pollen allergen Bet v1, single mutation in the mapped epitope showed 50% reduction in the binding of human polyclonal IgE [8]. The chimeric protein major bee venom allergens (Api 1/2/3), induced 100 to 1000 times less type-1 skin test reactivity in allergic patients. Moreover, treatment in mice with chimeric protein led to significant reduction of specific IgE development towards native allergen, representing a protective vaccine effect *in vivo* [9]. The clinical trial with peptides containing only T-cell epitopes (peptide immunotherapy, PIT) to major cat allergen, Fel d 1 [10] and bee venom major allergen, phospholipase A2 [11] showed beneficial modulation of immune response against whole allergen.

Though numerous clinical studies documented the efficacy of immunotherapy, but the underlying immunological mechanisms remains a matter of controversy. Most likely, several different mechanisms were involved in the observed long term effects of immunotherapy.

Moreover, the importance of blocking antibodies has been questioned because it was not always associated with clinically successful immunotherapy [4].

Bibliography

1. Storoni, L.C., McCoy, A.J., and Read, R.J. (2004). Likelihood-enhanced fast rotation functions. *Acta Crystallogr D Biol Crystallogr* *60*, 432-438.
2. (1994). The CCP4 suite: programs for protein crystallography. *Acta Crystallogr D Biol Crystallogr* *50*, 760-763.
3. Jones, T.A., Zou, J.Y., Cowan, S.W., and Kjeldgaard (1991). Improved methods for building protein models in electron density maps and the location of errors in these models. *Acta Crystallogr A* *47 (Pt 2)*, 110-119.
4. Valenta, R. (2002). The future of antigen-specific immunotherapy of allergy. *Nat Rev Immunol* *2*, 446-453.
5. Akdis, C.A., and Blaser, K. (2001). Bypassing IgE and targeting T cells for specific immunotherapy of allergy. *Trends Immunol* *22*, 175-178.
6. Saini, S.S., and MacGlashan, D. (2002). How IgE upregulates the allergic response. *Curr Opin Immunol* *14*, 694-697.
7. Ferreira, F., Ebner, C., Kramer, B., Casari, G., Briza, P., Kungl, A.J., Grimm, R., Jahn-Schmid, B., Breiteneder, H., Kraft, D., Breitenbach, M., Rheinberger, H.J., and Scheiner, O. (1998). Modulation of IgE reactivity of allergens by site-directed mutagenesis: potential use of hypoallergenic variants for immunotherapy. *Faseb J* *12*, 231-242.
8. Spangfort, M.D., Mirza, O., Ipsen, H., Van Neerven, R.J., Gajhede, M., and Larsen, J.N. (2003). Dominating IgE-binding epitope of Bet v 1, the major allergen of birch pollen, characterized by X-ray crystallography and site-directed mutagenesis. *J Immunol* *171*, 3084-3090.
9. Karamloo, F., Schmid-Grendelmeier, P., Kussebi, F., Akdis, M., Salagianni, M., von Beust, B.R., Reimers, A., Zumkehr, J., Soldatova, L., Housley-Markovic, Z., Muller, U., Kundig, T., Kemeny, D.M., Spangfort, M.D., Blaser, K., and Akdis, C.A. (2005). Prevention of allergy by a recombinant multi-allergen vaccine with reduced IgE binding and preserved T cell epitopes. *Eur J Immunol* *35*, 3268-3276.
10. Pene, J., Desroches, A., Paradis, L., Lebel, B., Farce, M., Nicodemus, C.F., Yssel, H., and Bousquet, J. (1998). Immunotherapy with Fel d 1 peptides decreases IL-4 release by peripheral blood T cells of patients allergic to cats. *J Allergy Clin Immunol* *102*, 571-578.
11. Muller, U., Akdis, C.A., Fricker, M., Akdis, M., Blesken, T., Bettens, F., and Blaser, K. (1998). Successful immunotherapy with T-cell epitope peptides of bee venom phospholipase A2 induces specific T-cell anergy in patients allergic to bee venom. *J Allergy Clin Immunol* *101*, 747-754.

3.0 Purification and biophysical characterization of bovine testes hyaluronidase (PH-20)

3.1 Abstract

PH-20 is well characterized mammalian hyaluronidase, present on the sperm plasma membrane and inner acrosomal membrane *via* GPI-anchor and plays important role in fertilization. It is a bifunctional protein: N-terminal domain carrying hyaluronidase activity involved in cumulus penetration, while the C-terminal is presumably involved in binding of acrosome reacted (AR) sperm to the zona pellucida. In the present study, we were able to purify PH-20 proteins from commercial available bovine testicular extract (Sigma) and from fresh bovine testes to highest purity. PH-20₆₀ purified from commercial source is probably endoproteolytic cleavage product whereas PH-20₆₉ (Sigma) and PH-20₈₀ (bovine testes) are intact protein. The purified PH-20 proteins forms heterogeneous aggregate, most likely by hydrophobic interaction, which was successfully overcome by addition of zwitterionic compound, NDSB (non detergent sulfobetaine).

3.2 PH-20/Sperm adhesion molecule (SPAM1)

PH-20 was first identified as a 'spreading factor' based on the spreading properties exhibited by the extracts from mammalian testes.[1]. Initially, the zona pellucida recognition function of PH-20 was discovered on the guinea pig sperm [2, 3]. Later, when the bee venom hyaluronidase was cloned, a marked cDNA sequence homology with PH-20 was recognized [4], and it is now apparent that PH-20 is the hyaluronidase of mammalian sperm.

PH-20 is a bifunctional protein, composed of the N-terminal domain carrying hyaluronidase activity involved in cumulus penetration [5], while the C-terminal could be involved in binding of acrosome reacted (AR) sperm to zona pellucida [2, 3]. PH-20 is glycosyl phosphatidylinositol (GPI)-anchored on the plasma membrane and inner acrosomal membrane (IAM) of the sperm through C-terminal end [6, 7]. In most mammals, the membrane bound PH-20 proteins are released by treatment with phosphatidylinositol-specific phospholipase C (PI-PLC) [5, 7, 8], whereas 80-kDa protein carrying hyaluronidase activity present on the surface of the bull spermatozoa was not released by PI-PLC treatment [9].

PH-20 proteins from various mammals shares approximately 50-60 % sequence identity. It has number of potential N-glycosylation sites but more interestingly, 12 cysteine residues are highly conserved among PH-20 proteins (Figure 1). PH-20 consists of N- and C-terminal signaling sequence which are removed upon maturation. The length of the N-terminal signaling sequence is about 35 residues based on N-terminal sequencing of the matured protein. Hyaluronidase domain of PH-20 may account for 350 residues based on sequence similarity with bee venom hyaluronidase. The length of the zona pellucida binding domain is approximately 110-130 residues. PH-20 has potential GPI-anchoring site at the C-terminal end in monkey, human and guinea pig, while bovine, mouse and rat PH-20 sequence lack the potential site. The potential active site residues Asp111 and Glu113 have been proposed based on mutagenesis studies on human PH-20 hyaluronidase [10] which was later confirmed by the crystal structure of bee venom hyaluronidase in complex with HA-tetramer which enabled the elucidation of the hyaluronidase catalytic mechanism [11]. Structural features established by disulfide bonds and glycosylation are essential for hyaluronidase activity of PH-20 protein [12]. The predicted isoelectric point of bovine PH-20 protein is 8.56, which is based on the sequence obtained from *Meyer et al., 1997* [13].

mayer et al 1 MRM L R R H H T S S R S F A G S S G T P O A V F T F L L P C C L A L D F R A P P L I S N T S F L W A W N A P V E R C V N R R F Q L P P P
 bovine PH-20 1 M G M F R R H H I S F R S F A G S S G T P O A V F T F L L P C C L A L D F R A P P L I S N T S F L W A W N A P V E R C V N R R F Q L P P P
 human PH-20 1 M G V L R F K H I F F R S F A K S S G V S Q I V F T F L L P C C L L L N F R A P P V I P N V P F L W A W N A P S E E C I G . K F D E P L D
 monkey PH-20 1 M G V L R F K H I F F R S F A K S S G V S Q I V F T F L L P C C L L L N F R A P P I P N V P F L W A W N A P S E E C I G . K F D E P L D
 mouse PH-20 1 M G E L R F K H L F W R S F E S S G G T F Q I V L L F L L P C S L V D Y R A A P I L S N T I F L W I W N V P E R C V G . N V N D P L D
 Rat PH-20 1 M G E L R F K H L F W R S F E S S G G T F Q I V L L F L L P C S L V D Y R A A P I L S N T I F L W I W N V P E R C V G . N V N D P L D
 guinea PH-20 1 M G A F T F K H S F F G S E V F C S G T L Q I V F T F L L P C C L A . D K R A P P L I P N V P L F W I W N A P E R C V G . G T N Q P L D

mayer et al 71 L R L F S V K G S P Q K S A T G Q F T L F Y D R L G Y Y P H I D E K T G K T V F G G I P Q L G N L R S H I E K A K N D I A Y Y I P N D S
 bovine PH-20 71 L R L F S V K G S P Q K S A T G Q F T L F Y D R L G Y Y P H I D E K T G K T V F G G I P Q L G N L R S H I E K A K N D I A Y Y I P N D S
 human PH-20 70 M S L F S F I G S P R I N A T G Q G V T L F Y V D R L G Y Y P I D S I T G V I V N G G P O K I S L Q D H D K A K K D I T F Y M P V D N
 monkey PH-20 70 M S L F T L M G S P R I N A T G Q G V T L F Y V D R L G Y Y P I D L T T G V I V H G G P O K V S L Q D H D K A K K D I T F Y M P V D N
 mouse PH-20 70 L S F F S I L G S P R K T A T G Q P V T L F Y V D R L G Y Y P H I D A N Q . A E H Y G G P Q R G D Y Q A H R K A K K D I E H Y I P D D K
 Rat PH-20 70 L S F F S I L G S P R K T A T G Q P V T L F Y V D R L G Y Y P H I D A N Q . I E H H G G P Q R G D Y Q A H R K A K K D I E H Y I P D D K
 guinea PH-20 69 M S F F S I V G H P R K N I T G O S T L F Y V D R L G Y Y P I D P H I C A I V H G G P O L M N L Q O H R K S R O D I L F Y M P T D S

mayer et al 141 V G L A V I D W E N W R P T W A R N W P K D V Y R D E S V E L V L O K N P Q L S F P S A S K I A R V D F B I A G R S E M Q E T L K L G R L L
 bovine PH-20 141 V G L A V I D W E N W R P T W A R N W P K D V Y R D E S V E L V L O K N P Q L S F P S A S K I A R V D F B I A G R S E M Q E T L K L G R L L
 human PH-20 140 L G M A V I D W E W R P T W A R N W P K D V Y K N R S H E L V Q Q N V Q L S L T E A T E K A K Q E F E K A G K D F L V E T L K L G R L L
 monkey PH-20 140 L G M A V I D W E W R P T W A R N W P K D V Y K N R S H E L V Q Q N V Q L S L P A I D K A K Q E F E K A G K D F L V E T L K L G R L L
 mouse PH-20 139 L G L A I D W E W R P T W I R N W P K D V Y N K S E L V Q S T N P G L S I T A T Q K A I Q Q F E A G R K E M E G T L H L G K F
 Rat PH-20 139 L G L A I D W E W R P T W I R N W P K D V Y N K S E L V Q A A D P A I N I T A T V R A K A Q F E A A K E E M E G T L K L G K H
 guinea PH-20 139 V G L A V I D W E W R P T W I R N W P K D V Y N K S E L V K S C H P Q Y N H S Y A V A V A K R D F E A T G K A E M E T L K L G K S

mayer et al 211 L R P N H L W G Y Y L F P D C Y N H N Y N Q P T Y N G N G P D V E K R R N D D L D W L W K E S T A L F P S V Y L N I R L K S T I Q N A A L Y V
 bovine PH-20 211 L R P N H L W G Y Y L F P D C Y N H N Y N Q P T Y N G N G P D V E K R R N D D L D W L W K E S T A L F P S V Y L N I R L K S T I Q N A A L Y V
 human PH-20 210 L R P N H L W G Y Y L F P D C Y N H H Y K K P G Y N G S G F N V E T R R N D D L S W L W N E S T A L Y P S I Y L N T . Q Q S P V A A T L Y V
 monkey PH-20 210 L R P N H L W G Y Y L F P D C Y N H H Y K K P G Y N G S G F D V E K R R N D D L S W L W N E S T A L Y P S I Y L N T . Q Q S V V V A T L Y V
 mouse PH-20 209 L R P N Q L W G Y Y L F P D C Y N N K F Q D P Y Y D G C P D V E K R R N D L K W L W K A S T G L Y P S V Y L K K D L K S N R Q A T L Y V
 Rat PH-20 209 I R P K H L W G Y Y L F P D C Y N N K F Q V D N Y D G C P D V E K R R N D L D W L W K E S T A L Y P S V Y L K K D L S S R R A T L Y V
 guinea PH-20 209 L R P S L W G Y Y L F P D C Y N T H F I K P N Y D G H C P P I E L Q R N N D L Q W L W N D S T A L Y P S V Y L T S R V R S S N G A L Y V

mayer et al 281 R N R V Q E A I R S K I A S V E S P P F V Y Y R P V F T D G S S T Y L S G G D L V N S V G E V S L G A S G I I M W G S L N L S L S V
 bovine PH-20 281 R N R V Q E A I R S K I A S V E S P P F V Y Y R P V F T D G S S T Y L S G G D L V N S V G E V S L G A S G I I M W G S L N L S L S V
 human PH-20 279 R N R V R E A I R S K I P D A K S P P F V E Y A R I V E T D Q V L K F L S G G D L V Y T F G E V A L G A S G I I W G T L S I M R S V
 monkey PH-20 279 R N R V R E A I R S K I P D A K N P P F V E Y A R L V E T D Q V L K F L S R E E L V S T L G E V A L G A S G I I W G S L S I T R S V
 mouse PH-20 279 R Y R V R E A I R S K V G N A S D P V P I F Y Y I R L V E T D R T S E Y L E D D L V N T I G E V A L G S G I I I W D A M S L A Q R A
 Rat PH-20 279 R Y R V R E A I R S K V S D E S N P P I F Y Y I R L V E T D Q V T T F L E L D D L V N T I G E V A L G S G I I I W D A M S L A Q R S L
 guinea PH-20 279 R N R V R E A I R S K I M D D K N P P I Y Y Y I R L V E T D Q T T F L E L D D L V H S V G E V S L G S G I I W G S L S L T R S L

mayer et al 351 Q S C M N I G T V L N T T L N P Y I I N V T L A A K M C S G V L C H D E G V C F R R H W N S S D Y L H L N P M N F A I Q T G G G K Y T V P
 bovine PH-20 351 Q S C M N I G T V L N T T L N P Y I I N V T L A A K M C S G V L C H D G G V C F R K H W N S S D Y L H L N P M N F A I Q T G G G K Y T V P
 human PH-20 349 K S C L L L D N Y M E T I L N P Y I I N V T L A A K M C S G V L C Q E Q G V C F R K N W N S S D Y L H L N P D N F A I Q L E K G G K F T V R
 monkey PH-20 349 K S C L L L D T Y M E T I L N P Y I I N V T L A A K M C S G V L C Q E Q G V C F R K D W N S S D Y L H L N P D N F A I Q L E K G G K F T V H
 mouse PH-20 349 A G C P T L H K Y M Q T T L N P Y I I N V T L A A K M C S G T L C E K G M C S R R K E S S D V Y L H L N P S H F D M L T E T G K Y E V L
 Rat PH-20 349 A G C P L R Q Y M K T I L N P Y I I N V T L A A K M C S G T L C E K G M C S R K T E S S D A Y L H L D P S S F S I N V T E A G K Y E V L
 guinea PH-20 349 V S C G L E N Y M K G L L E P Y L E N V T L A A K M C S G V L C R K N Q G I C R R D W N I N T Y L H L N A T N F D E L Q N G K E V V H

mayer et al 421 G T V T I E D L K F S D T Y C S C Y A N T H C R K R V D I K N V H S V N V C M A E D T C I D S P V K L Q P S D H S S . S Q K E A S T
 bovine PH-20 421 G T L T I E D L K F S D T Y C S C Y S N L S C K R K A D I K N V H S V D V C M A E D V C I D A F L K P P M E T E . E P Q
 human PH-20 419 G K P T I E D L E F S E K Y C S C Y S T L S C K E K A D V K D I D A V D V C I A D G V C I D A F L K P P M E T E . E P Q
 monkey PH-20 419 G K P I V E D L E F S E K Y C S C Y S T L S C K E K A D V K D I D A V D V C I A D G V C I D A S L K P P V E T E G S P P
 mouse PH-20 419 G N P R V G D L E F S E H K C S C S R M T C E I T S D V K N V Q D V N V C M G D N V C I K A R V E P N P A P Y
 Rat PH-20 419 G K P E V K D L E F S E H K C S C S R M T C E I T S D M R S Q D V N V C M G D N V C I K A T L G P N S A F H
 guinea PH-20 419 G K P S L E D L E F S K N E H C S C Y I N N K C R D R L D H N V R S V N V C T A N N I C I D A V L N E P S L D D D E P P I T D D T S G

mayer et al 489 T F S S I S P S T T I T A T A S P C T P E K H S P E C L K V R C A E R H P Q R H P K G V S K C
 bovine PH-20 489 T F S S I S P S T T I T A T A S P C T P E K H S P E C L K V R C A E R H P Q R H P K G V S K C
 human PH-20 480 I F Y N A S P S T L S A T M F I V S I L F L I I S S V A S L
 monkey PH-20 481 I F Y N I S S S T V S I T M F I V N I L F L I I S S V A S L
 mouse PH-20 477 L L P G K S L L F M T T L G H V L Y H L P Q D I F V F P R K T L V S T P
 Rat PH-20 477 L L P G K G L L L M T T L A H I L H H L P H D I F V F P R M L V S T P
 guinea PH-20 489 N Q D S I S D I T S A P P S S H I L P K D L S W C L F L L S I F S Q H W K Y L L

Figure 1. Multiple sequence alignment of PH-20 proteins. The proteins listed from top to bottom: bovine PH-20 (residues 1-534, sequence obtained from *Mayer et al 1997*), bovine PH-20 fragment (1-474, NCBI accession number Q7YS45), human PH-20 (1-509, P38567), monkey PH-20 (1-510, P38568), mouse PH-20 (1-512, P48794), rat PH-20 (1-512, Q62803) and guinea pig PH-20 (1-529, P23613). Fully conserved residues shown in red box with white character and partially conserved residues shown in red character. Domains are marked as lines with different color on the top of the alignment: orange represent N-terminal signaling sequence, blue represent hyaluronidase domain, pink represent zona pellucida binding domain and green represent C-terminal signaling sequence. Blue arrowheads denote the active site residues Asp111 and Glu113. Green arrowhead represent conserved cysteine residues. Six potential N-glycosylation sites of bovine PH-20 protein are indicated by (★) on the top of the sequence alignment.

Fertilization is a complex process; which results in the fusion of sperm and egg. An ovulated mammalian egg is enclosed by two layers, an outer layer consists of cumulus cells embedded in extracellular matrix rich in hyaluronic acid and an thick inner layer which is zona pellucida. For fertilization to occur, sperm must penetrate both layers in steps requiring sperm motility, sperm surface enzymes, and probably secreted acrosomal enzymes [14-16] (Figure 2). Since cumulus cells are embedded in the extracellular matrix abundant in hyaluronan, a GPI-anchored sperm hyaluronidase, PH-20, thus enables the penetration of acrosome intact (AI) sperm through cumulus mass [4, 5, 17]. In addition to hyaluronan hydrolyze, PH-20 protein is believed to be involved in the binding of acrosome reacted (AR) sperm to zona pellucida [2, 3]. Then acrosome reacted spermatozoa deprived of membrane penetrate through the zona pellucida and reach the egg's plasma membrane, where binding and fusion of the gametes take place. In support of this proposal, the immunization of guinea pigs with PH-20 results in 100% contraception of both male and female, the effect being long-lasting and reversible [18].

Mammals consists of two PH-20 variants, the lower molecular weight isozyme is believed to be produced by endoproteolytic cleavage of the larger protein during the acrosomal reaction. PH-20 has variable pH optima: high molecular weight isozyme has broad range with the highest activity at neutral pH (pH 7.0) [7, 9], whereas lower molecular weight isozyme exhibits hyaluronidase activity only at acidic pH (pH 4.0) [7]. Amino acid sequencing of lower molecular weight bovine testis PH-20 protein lacks the signal peptide at the amino terminus and 56 amino acids at the carboxyl end in comparison to mature protein. This strongly suggests

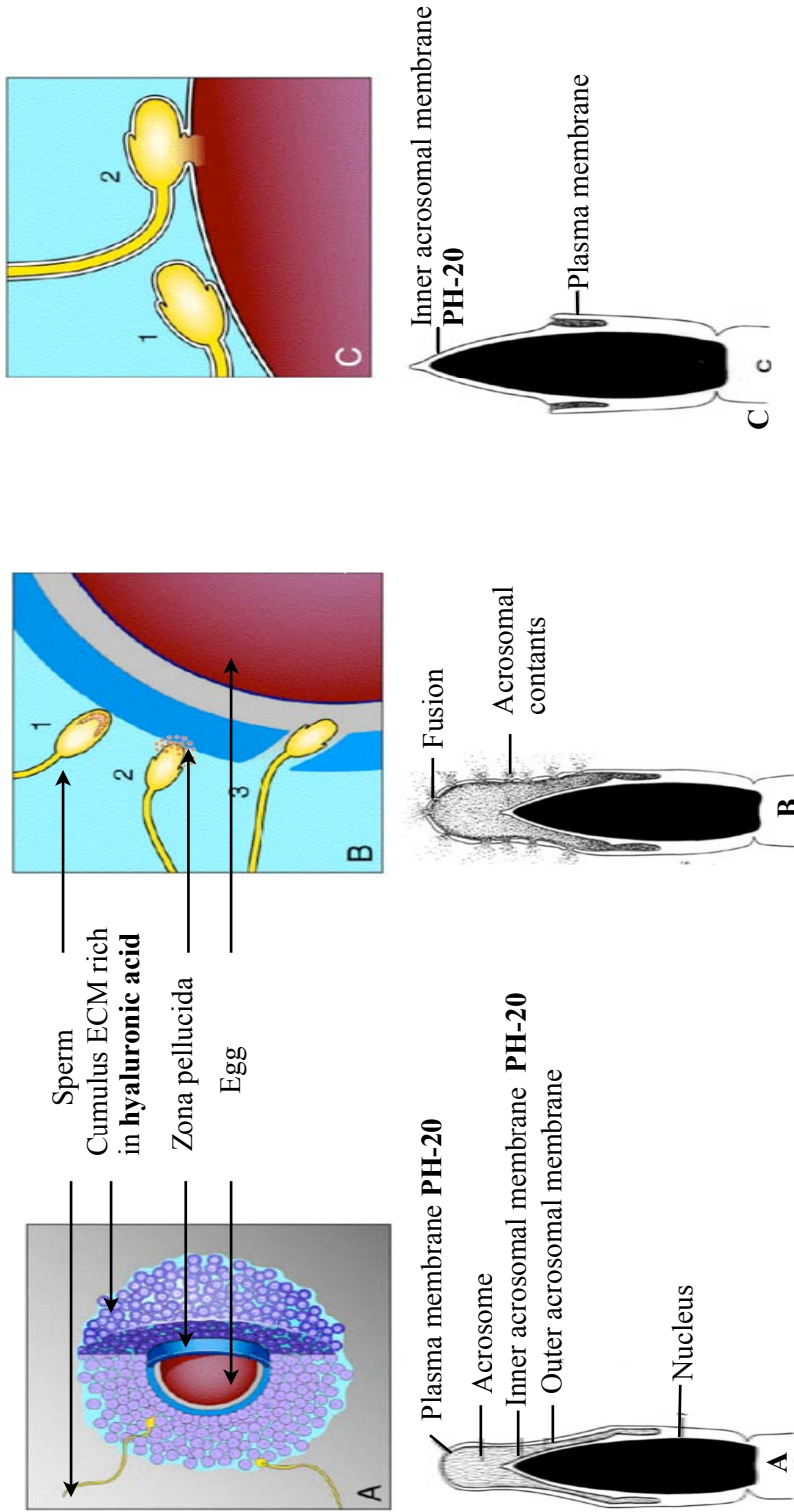


Figure 2. Schematic diagram of mammalian fertilization: **A**) Sperm penetration of cumulus cells (purple) to reach zona pellucida (navy blue) in top and the acrosome intact sperm head is shown in bottom; **B**) Ovary depicted with cumulus cells removed; sperm 1 binds to the zona pellucida (navy blue); sperm 2 undergoes exocytosis, releasing acrosomal contents (orange-red); sperm 3 penetrate the zona pellucida and begins entry into perivitelline space (gray) shown in top and the fusion between outer acrosomal membrane and plasma membrane is shown in bottom. **C**) Sperm 1 binds to the egg plasma membrane by the side of its head, in a central region (equatorial region); sperm 2 fuses with the egg plasma membrane in top and the acrosomal reacted sperm is shown in bottom. These figures were adapted from Primakoff et al., 2002 and Wassarman.P 1999 [15, 16].

that the lower molecular weight form is generated by proteolysis, probable by the action of acrosomal enzymes [13].

In addition to fertilization, mammalian hyaluronidases plays important role in many biological process but the study of these enzymes are greatly neglected. In the present study, we purified PH-20 protein from bovine testicular extract (Sigma) and bovine testes to homogeneity and characterized them.

3.3 Material and methods

3.3.1 Substrate gel assay

Hyaluronic acid substrate gel electrophoresis was performed according to the protocol described by *Guntenhoener et al., 1992* [19]. The protein was subjected to electrophoresis under non-reducing condition on 12% (w/v) SDS-PAGE gel copolymerized with 0.17 mg/ml of hyaluronic acid. The gel was incubated in the TBS buffer (20 mM Tris-HCl, pH 7.5 150 mM NaCl) containing 3% (v/v) TritonX-100 for 3 hours at room temperature on a rocking platform to remove SDS and then in 100 mM sodium acetate buffer pH 4.0, for 14 to 16 hours at 37°C. To visualize digestion of hyaluronic acid, gels were stained with 0.5% (w/v) alcian blue in 3% (v/v) acetic acid for 2 hours at room temperature and destained in 7% (v/v) acetic acid. The presence of activity in the gel was revealed by a lack of coloration of a digested area against the blue background characteristic for undigested hyaluronic acid.

3.3.2 Protein Electrophoresis and Immunoblotting

Protein samples were solubilized in sample buffer (62.5 mM Tris-HCl pH 6.8, 10% glycerol, 2% (w/v) SDS, 0.01% (w/v) bromophenol blue with or without 100 mM DTT) and heated at 99°C for 3 min and separated on 12% SDS-PAGE [20].

The immunoblotting was done according to standard protocol (Molecular cloning, Sambrook et al., 2nd edition). After electrophoresis, the protein was transferred onto a nitrocellulose membrane (BA85, Schleicher & Schuell, Dassel, Germany) using Bio-Rad PROTEAN 2 Electrophoresis / Mini Trans-Blot Module. The transfer was carried out in the presence of blotting buffer (20 mM Tris buffer pH 8.3, 150 mM glycine and 20% methanol) at 100V, 4°C for 1 hour. The transferred membrane was blocked with TTBS buffer (20 mM Tris pH 7.4, 150 mM NaCl, 0.1% (v/v) Tween 20) containing 5% (w/v) dry skim milk to prevent non-specific binding. The membrane was incubated with TTBS buffer (with 5% (w/v) dry skim milk) containing primary antibody, ram PH-20 polyclonal antibody (Babraham bioscience technologies) at dilution 1:2500 for 1 hour in room temperature. Subsequently, the membrane was washed with TTBS for three times at the interval of 10 minutes and then incubated with TTBS (with 5% (w/v) dry skim milk) containing secondary antibody, anti-mouse IgG antibody-peroxidase conjugate (Sigma) at 1:5000 dilution for 1 hour at room temperature. Again, the membrane was extensively washed in TTBS as described before and incubated in ECL Western blotting detection reagents according to manufacturers protocol (Amersham Biosciences). The blot was

subsequently exposed to KodakX-OMAT XAR-5 radiography film for 15 sec to 15 min until the positive bands were visualized by enhanced chemiluminescence.

3.3.3 Cloning and expression of human PH-20

Cloning and expression of PH-20 fragment (1-332) containing a C-terminal 6xHis tag was carried out by Dr. Margit Schmidt, Department of Biology, East Carolina University. Human PH-20 gene comprising amino acids Leu1 to Ile332 was ligated into the Pichia expression vector pPICZ α A (Invitrogen) and transformed into TOP 10 *E. coli* cells (Invitrogen). The plasmid was purified and transformed into *Pichia pastoris* strains X33 and KMH71H using 10 μ g plasmid. From each strain ten single colonies were isolated, cultured in complex liquid media and expression was induced by the addition of methanol. The harvested culture supernatant and the cell extract from positive clones were analyzed for expression in our laboratory by SDS gel electrophoresis, anti-His antibodies and substrate gel assay.

3.3.4 Protein purification from crude extract (type IV-S: From bovine testes, Sigma)

The PH-20 was purified according to the modified procedure described elsewhere [9, 13, 21, 22]. Lyophilized crude extract (type IV-S: From bovine testes, Sigma) was dissolved in 20 mM sodium phosphate buffer pH 7.0 and purification was carried out as a six step procedure. As a first step the ammonium sulfate was added slowly to reach 45% saturation by constant stirring using magnetic bead (Heidolph MR 3001) for 4 to 6 hours at 4°C. This was followed by centrifugation at 13000 rpm for 30 min at 4°C (Sorval RC-5B) and the precipitant was removed. To the supernatant ammonium sulfate was added to reach 70% saturation by constant stirring for 4 to 6 hours followed by centrifugation of mixture at 13000 rpm for 30 min at 4°C. The precipitate obtained between 45-70% saturated ammonium sulfate was rich in PH-20 (monitored by Western blot analysis and substrate gel as described earlier), dissolved in 20 mM sodium phosphate pH 6.0 and dialyzed (Spectra/Pro, membrane cutoff 12 - 14 kDa) against the same buffer. The insoluble precipitate formed during the dialysis was removed by centrifugation at 13000 rpm for 30 min and resultant supernatant was loaded on a Resource Q anion exchanger column (Amersham Pharmacia) using acta purifier (Amersham Pharmacia). PH-20 elutes in flow through (monitored by substrate gel) whereas many contaminant proteins bound to Resource Q resin were eluted with 20 mM sodium phosphate pH 6.0 containing 1 M NaCl. The flowthrough was dialyzed against 20 mM sodium phosphate pH 7.0 and applied onto

Protein-G affinity column (Amersham Pharmacia) to separate immunoglobulins. The PH-20 found in flowthrough was concentrated using centricon (Amicon Ultra, membrane cutoff 30000 kDa) and applied on a Mono-S cation exchanger column (Pharmacia). The PH-20 was bound to the Mono-S column and eluted with 20 mM sodium phosphate buffer pH 7.0 containing 1 M NaCl as step gradient. The fractions containing PH-20 (identified by substrate gel and mass mapping), were concentrated and applied to Hiload 26/60 Superdex G-75 (Amersham Pharmacia) gel filtration column. Protein concentration of purified PH-20 was determined by absorption spectroscopy (Hewlett Packard 8453, HP845X UV-Visible system, Switzerland) at 280 nm using extinction coefficient of 89435 (lower species) and 90430 (higher species) $M^{-1} cm^{-1}$ calculated from the amino acid sequence obtained from Mayer *et al.*, 1997. The extinction coefficient was calculated using ProtParam (<http://www.expasy.org/tools/protparam.html>) from Ex-pasy server.

3.3.5 Protein purification from bovine testes

Fresh bovine testes were obtained from regional slaughterhouse and stored at $-80^{\circ}C$. When needed, frozen testes were thawed overnight at $4^{\circ}C$. Outerlayer of the testis was removed, the inner layer cut into small pieces and homogenized using buffer (20 mM sodium phosphate pH 7.0) containing protease inhibitor (1 mM EDTA, 10 μ M Leupeptin, 1 mM PMSF) at $4^{\circ}C$. Homogenized sample was centrifuged at 8000 rpm for 30 min at $4^{\circ}C$ and pellet was removed. To the supernatant ammonium sulfate was added slowly to reach 40 % saturation by constant stirring for 4 to 6 hours in the cold room. The sample was then centrifuged at 8000 rpm for 30 min and pellet was removed. To the resultant supernatant ammonium sulfate was added slowly to reach 70 % saturation by constant stirring for 4 to 6 hours followed by centrifugation at 8000 rpm for 30 min. The pellet obtained from 40 - 70 % saturation was dissolved and dialyzed against 20 mM sodium phosphate buffer pH 6.0.

To handle large volume in each step of purification, ion exchange column was packed manually with Q sepharoseTM fast flow (Amersham Biosciences) and SP sepharoseTM fast flow (Amersham Bioscience) beads separately. Dialyzed sample was applied on the anion exchanger (Sephacrose-Q), PH-20 elutes in flowthrough whereas most contaminant were bound to the column. The collected flowthrough was dialyzed against 20 mM sodium phosphate pH 7.0 and applied on a Protein-G column, which bound the immunoglobulins whereas PH-20 eluted in flowthrough. The collected supernatant was applied on a cation exchanger (Sephacrose-S) and bound proteins were batch eluted with 20 mM sodium phosphate pH 7.0 containing 30, 120,

200, 1000 mM NaCl. The fractions containing PH-20 (monitored by substrate gel and mass mapping) were pooled and applied onto Hiloal 26/60 Superdex G-75 (Amersham Pharmacia) gel filtration column. The concentration of the higher species of PH-20 protein was determined by absorption spectroscopy (Hewlett Packard 8453, HP845X UV-Visible system, Switzerland) at 280 nm using extinction coefficient of 90430 M⁻¹ cm⁻¹ calculated from the amino acid sequence.

3.3.6 Analytical ultracentrifugation

The sedimentation equilibrium (SE) and sedimentation velocity (SV) were performed on a Beckman optima XL-A analytical ultracentrifuge (Beckman Instruments) equipped with 4 and 12 mm Epon double sector cells. The experiments were carried out in the presence and absence of NaCl and with the presence of dimethylammonium sulfonate (Zwitterionic compound). Sedimentation velocity runs were carried out at two different speeds 44000 and 52000 rpm at 20°C and the sedimentation coefficients were corrected to standard condition (water, 20 °C). Sedimentation equilibrium measurements were carried out at 20 °C at rotor speeds from 5000 to 7000 rpm using 12-mm double sector cells filled with 0.1 ml solution. Molecular masses were evaluated in sedimentation equilibrium experiments from $\ln A$ versus r^2 plots, where A represents the absorbance and r is the distance from the rotor center. A partial specific volume of 0.73 cm³/g was assumed in all calculations. The molecular masses were calculated using the Segal computer program (www.biozentrum.unibas.ch/auc). All the analytical ultracentrifugation experiments were performed by Ariel Lustig, Biozentrum, University of Basel.

3.3.7 Mass spectral analysis

The mass spectrometry experiments were performed by the group of Dr. Paul Jenoe, Biozentrum, University of Basel as described [23, 24]. Liquid chromatography (LC) / Mass spectrometric (MS) analysis of the protein and its digest was carried out on 100 μm i.d.(inner diameter) capillary column packed with C₁₈ Monitor-Spherical silica (5-μm particle size, Column Engineering Inc., Ontario, CA). The bound peptide were eluted with 0.05% trifluoroacetic acid to 60% acetonitrile containing 0.05% trifluoroacetic acid at the flow rate of 1-2 μl/min. The outlet of the column was directed to a microspray needle, which was pulled from 100 μm i.d.(inner diameter) × 280 μm o.d. (outer diameter) fused silica capillaries (LC Packings) on a model P-2000 quartz micropipette puller (Sutter Instruments Co.). The needle was placed into an XYZ micropositioner, and the voltage was applied directly to the sample stream through the capillary union. Spray voltages were usually between 1100 and 1400 V. Mass determina-

tions were carried out on a TSQ7000 triple quadrupole mass spectrometer (Finnigan, San José, CA). All measurements were carried out in the positive ion mode. Precursor ion scanning was between 200 and 2000 Da for 3 s at unit resolution. For operation in the MS/MS mode, the resolution of Q1 was set to transmit a mass window of 4 Da and the resolution of Q3 was adjusted to 1.5 Da. Scanning was between 50 and 2250 Da in 3.5 s. Argon was used as a collision gas at a pressure of 3.5 mTorr.

3.3.8 Mass fingerprinting

The protein bands corresponding to PH-20 were cutout of the SDS/PAGE gel and incubated with trypsin (sequencing grade, Promega) at 37°C for 2 h. Trypsined fragments were desalted on C18 ZipTips (Millipore) and eluted with 1.5 µl 80% acetonitrile, 0.1% TFA, containing 1 µl/ml α -cyano-4-hydroxycinnamic acid (Aldrich). About 300 nl of the elute was deposited onto anchor spots of a Scout 400 µm/36 sample support (Bruker Daltonik, Germany) and the droplet was left to dry at room temperature. Mass spectra were recorded on a Bruker Scout 26 Reflex III instrument (Bruker Daltonik). The instrument was calibrated with angiotensin II, substance P, bombesin, and adrenocorticotrophic hormone. Peptides were analyzed in reflector mode using delayed ion extraction with a total acceleration voltage of 23 kV. The molecular weights of the each ejected peptide fragment were measured and searched in the sequence library using the programme MASCOT.

3.3.9 Crystallization attempts

Two different molecular weight species purified from Sigma crude extract were dialyzed against 5mM sodium acetate pH 4.0, concentrated using centricon to 4.3 mg/ml (lower species) and 8.3 mg/ml (higher species), respectively. PH-20 purified from bovine testes (higher species) was dialyzed against 20 mM HEPES pH 7.0 and concentrated to 10 mg/ml. Crystallization was performed with concentrated protein solutions using Hampton screen kits I and II by hanging drop vapour diffusion method. The drops were prepared by mixing 1 µl of protein with 1 µl of reservoir solution and equilibrated against 500 µl of reservoir solution.

3.3 Results

3.3.1 Expression of recombinant human PH-20 protein

The attempts to clone and express the N-terminal hyaluronidase domain of PH-20 (residue Leu1-Ile312) in *Pichia pastoris* were not successful. Unfortunately, PH-20 protein expression was neither detected in the supernatant nor in the cell extract. Cloning and expression of the same PH-20 fragment in *Baculovirus* was also not successful (data not shown). All these experiments were performed by Dr. M. Schmidt.

3.3.2 Purification of PH-20 protein from Sigma crude extract

Since the human PH-20 protein could not be expressed successfully in *Baculovirus* and *Pichia pastoris* expression systems, an attempt was made to purify PH-20 from commercial bovine testicular crude extract (type IV-S, Sigma).

The PH-20 purification comprised of six steps (see PH-20 purification scheme, Figure 3). In each step of purification, PH-20 protein was monitored by one or more of the following methods: 1) substrate gel electrophoresis assay, 2) Western blot analysis using a polyclonal ram anti PH-20 antibody, and 3) MALDI mass mapping of tryptic fragments.

Lyophilized crude extract (Sigma) was dissolved and fractionated by ammonium sulfate precipitation. The resultant fractions were analyzed by SDS/PAGE and Western blot (Figure 4). The hyaluronidase rich pellet obtained with 45-70% saturated ammonium sulfate precipitation (Figure 4B).

The PH-20 rich precipitant was dissolved and dialyzed against 20 mM sodium phosphate buffer pH 6.0. The sample was loaded on an anion exchanger (Resource Q) where PH-20 eluted in the flowthrough while some major contaminants remained bound to the column (Figure 5B). The substrate gel of the flowthrough sample showed strong hyaluronidase activity corresponding to two different molecular weight proteins, whereas the elution sample showed less activity (Figure 5C).

The flowthrough from Resource Q column, in addition to PH-20 contained immunoglobulin as one major contaminant as determined by MALDI mass mapping. The sample was dialyzed against 20 mM sodium phosphate pH 7.0 and applied onto a Protein-G affinity column. PH-20 eluted in flowthrough as confirmed by the substrate gel and the immunoglobulin remained bound to the column (Figure 6).

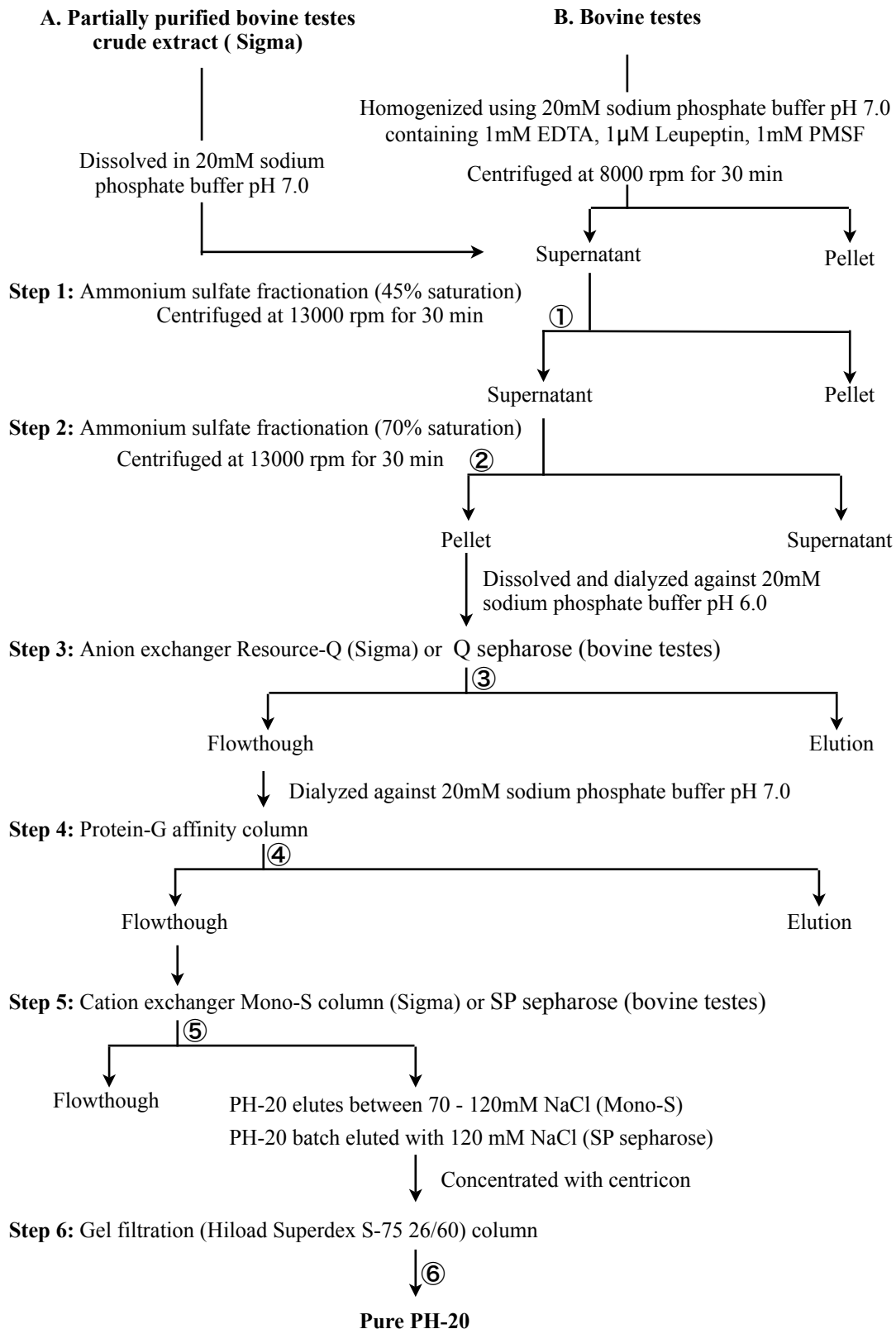


Figure 3. PH-20 purification scheme. **A)** From partially purified bovine testes crude extract (Sigma). **B)** From fresh bovine testes.

The flowthrough from the Protein-G column was applied onto a cation exchanger (Mono-S) column. It was found that PH-20 bound to the column and eluted between 70-120 mM NaCl (Figure 7). At this stage of the purification, the majority of the contaminant proteins were removed and PH-20 migrated in SDS-PAGE as two different molecular weight proteins with the molecular weight of approximately 60 kDa (PH-20₆₀) and 69 kDa (PH-20₆₉) (Figure 7 B). The MALDI mass mapping of two different molecular weight protein bands, cutout from the lane D3 matched to bovine testicular hyaluronidase (AAP55713) (shown in figure 12).

The fractions containing PH-20 were pooled, concentrated and subjected to gel filtration chromatography (Hiload Superdex S-75 26/60). Two different molecular weight PH-20 proteins were partially resolved and several lower molecular weight contaminants were separated by this purification procedure (Figure 8 A). The yield of PH-20₆₉ and PH-20₆₀ protein was approximately 3.0 mg/1g and 2.5 mg/1g of crude extract, respectively. Two purified PH-20 variants were dialyzed and concentrated to 4.3 mg/ml (PH-20₆₀) and 8.3 mg/ml (PH-20₆₉) respectively. Crystallization trials were performed with Hampton screening kits I and II. Despite the high purity and extensive screening neither of the two proteins could be crystallized.

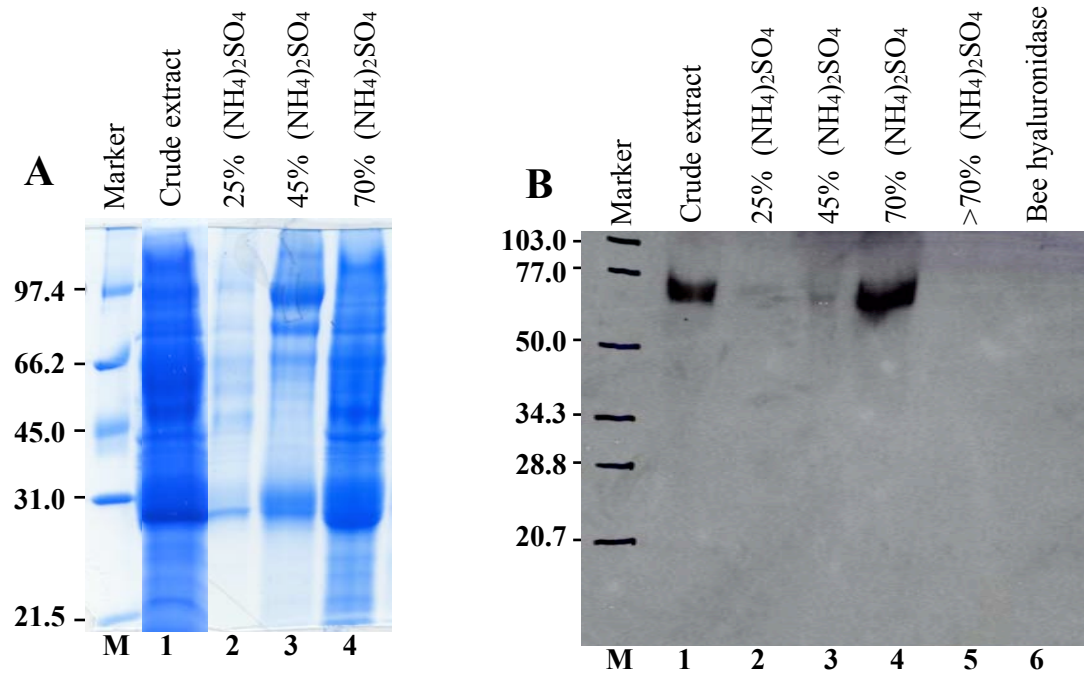


Figure 4. Ammonium sulfate fractionation of bovine crude extract (Sigma). **A)** 12% SDS-polyacrylamide gel of crude extract fractions. **B)** Western blot analysis of fractionated crude extract using ram PH-20 polyclonal antibody. Both SDS-polyacrylamide gel and Western blot analyses were carried out under non-reducing condition. The molecular weight marker are indicated by M.

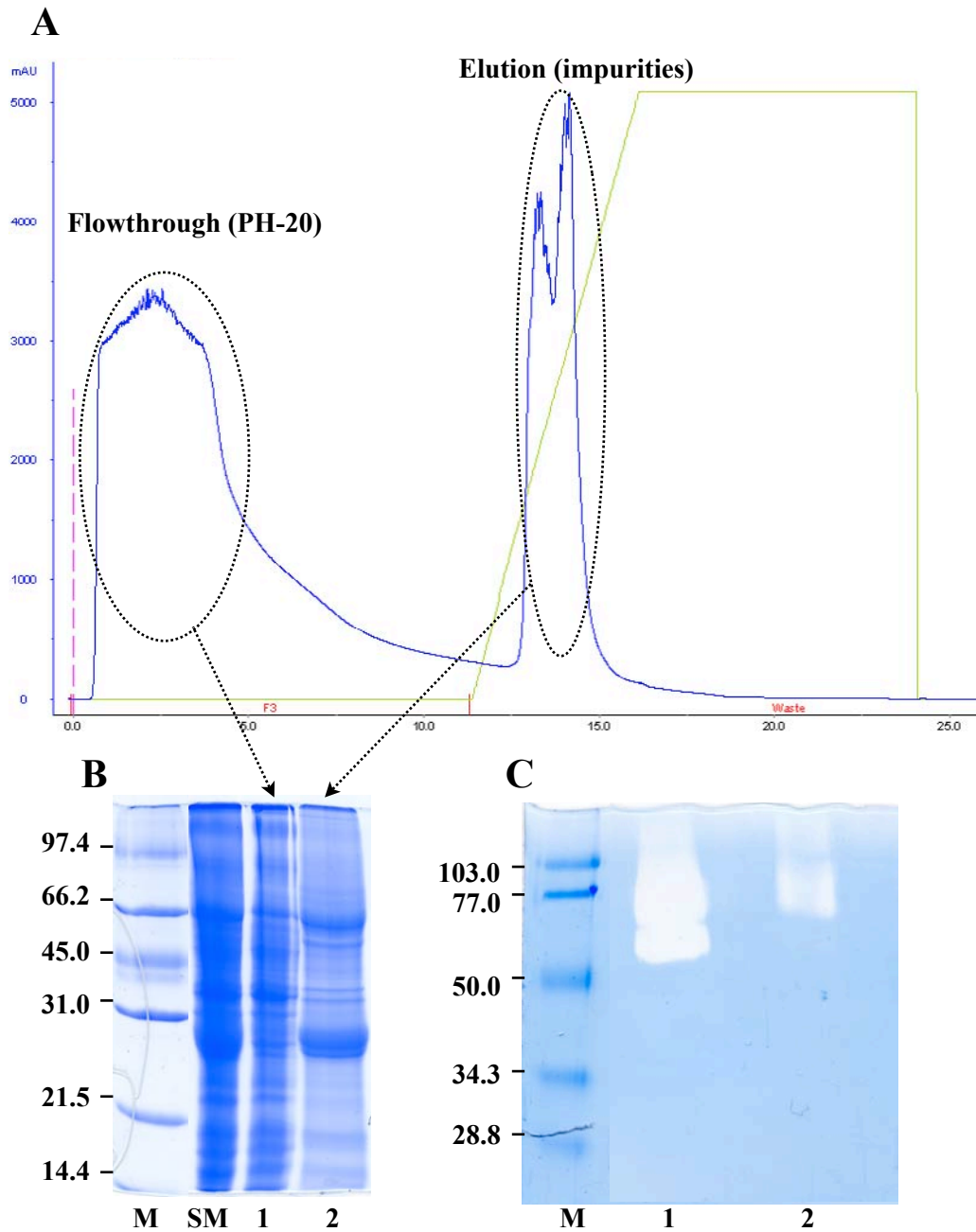


Figure 5. Purification of PH-20 using anion exchange chromatography (Resource-Q column). **A)** Chromatogram of PH-20 elution profile with NaCl gradient. **B)** SDS-polyacrylamide (12%, non-reducing condition) analysis of the peak fractions. **C)** Hyaluronidase acid substrate SDS-PAGE (12%, non-reducing condition) at pH 4.0. Lane1: flowthrough; lane 2: elution fraction. M stands for molecular weight markers (kDa) and SM for starting material.

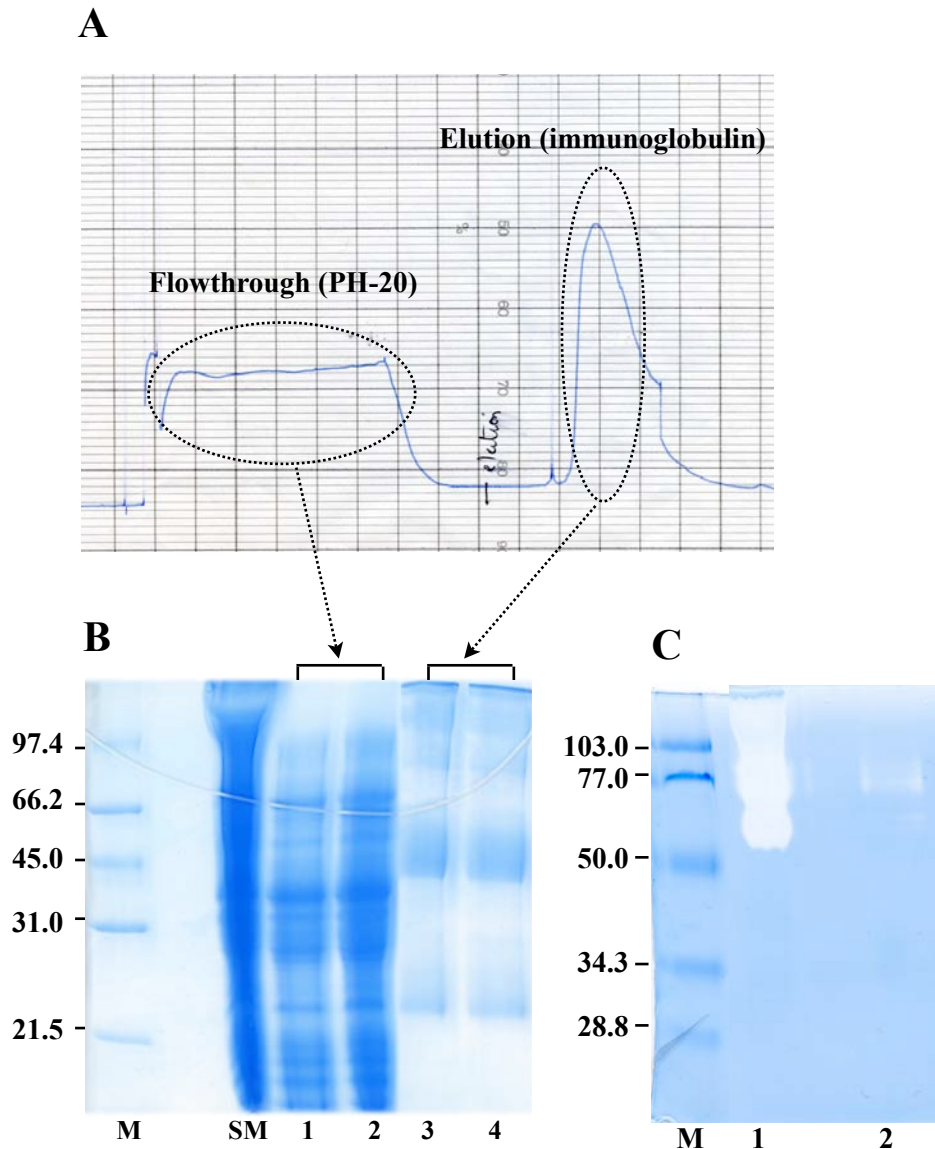


Figure 6. Separation of immunoglobulin contaminant by Protein-G column. **A)** Chromatogram of PH-20 elution profile on Protein-G column. **B)** SDS-polyacrylamide (12%, non-reducing condition) analysis of peak fractions, lane 1 - 2: flowthrough fraction; lane 3 - 4: elution fraction using 100 mM glycine pH 3.0. **C)** Hyaluronic acid substrate SDS-PAGE (12%, non-reducing condition) at pH 4.0, lane1: flowthrough; lane2: elution fraction. M strands for molecular weight markers (kDa) and SM for starting material.

Flowthrough

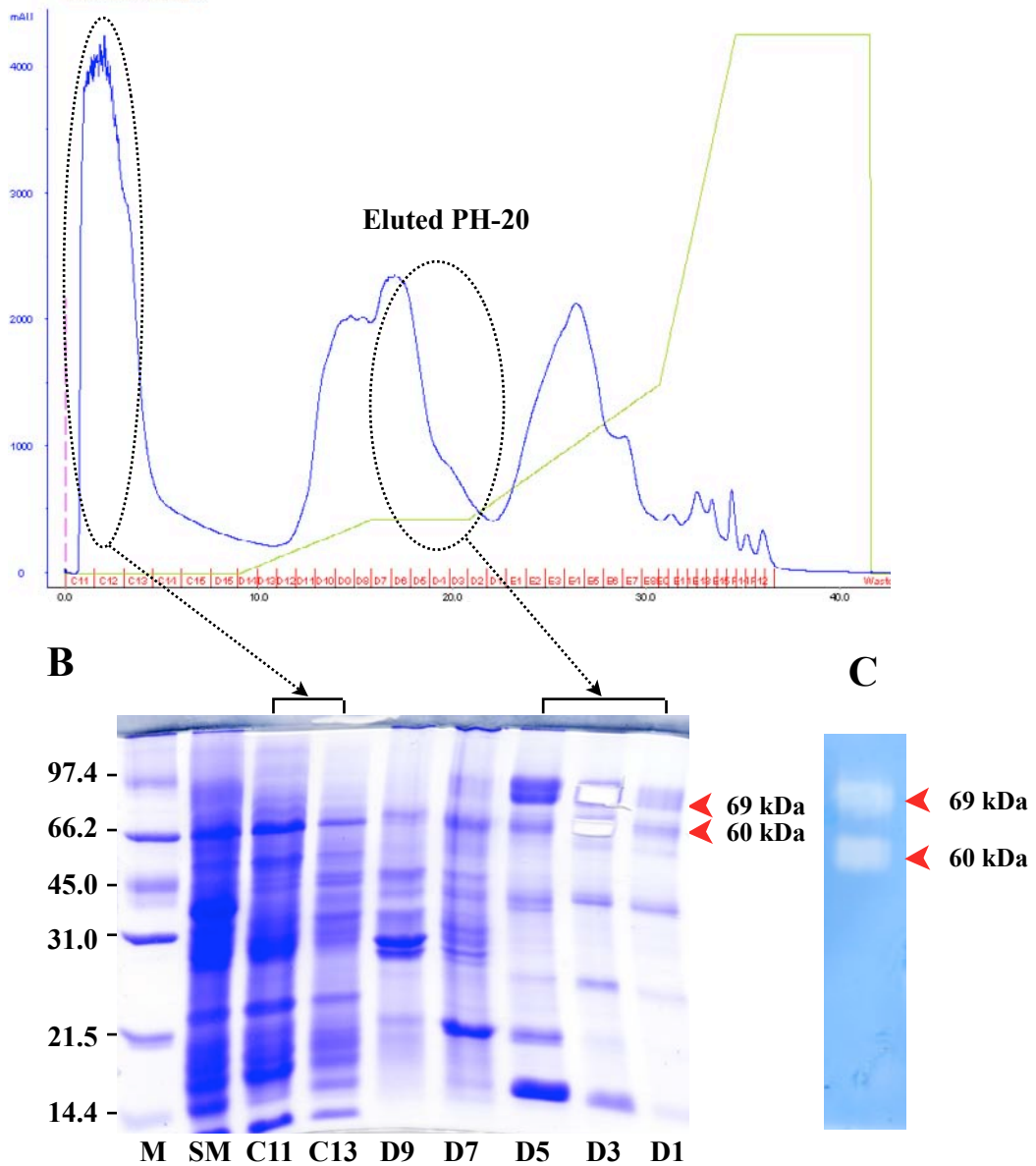


Figure 7. Purification of PH-20 protein using cation exchange chromatography (Mono-S column) **A**) Chromatogram of PH-20 elution profile with NaCl gradient. **B**) SDS-polyacrylamide (12%, non-reducing condition) analysis of proteins separated on Mono-S column. **C**) Hyaluronic acid substrate SDS-PAGE (12%, non-reducing condition) at pH 4.0. M stands for molecular weight markers (kDa) and SM for starting material. Fraction numbers (A1 to B11) are indicated at the bottom of the gel.

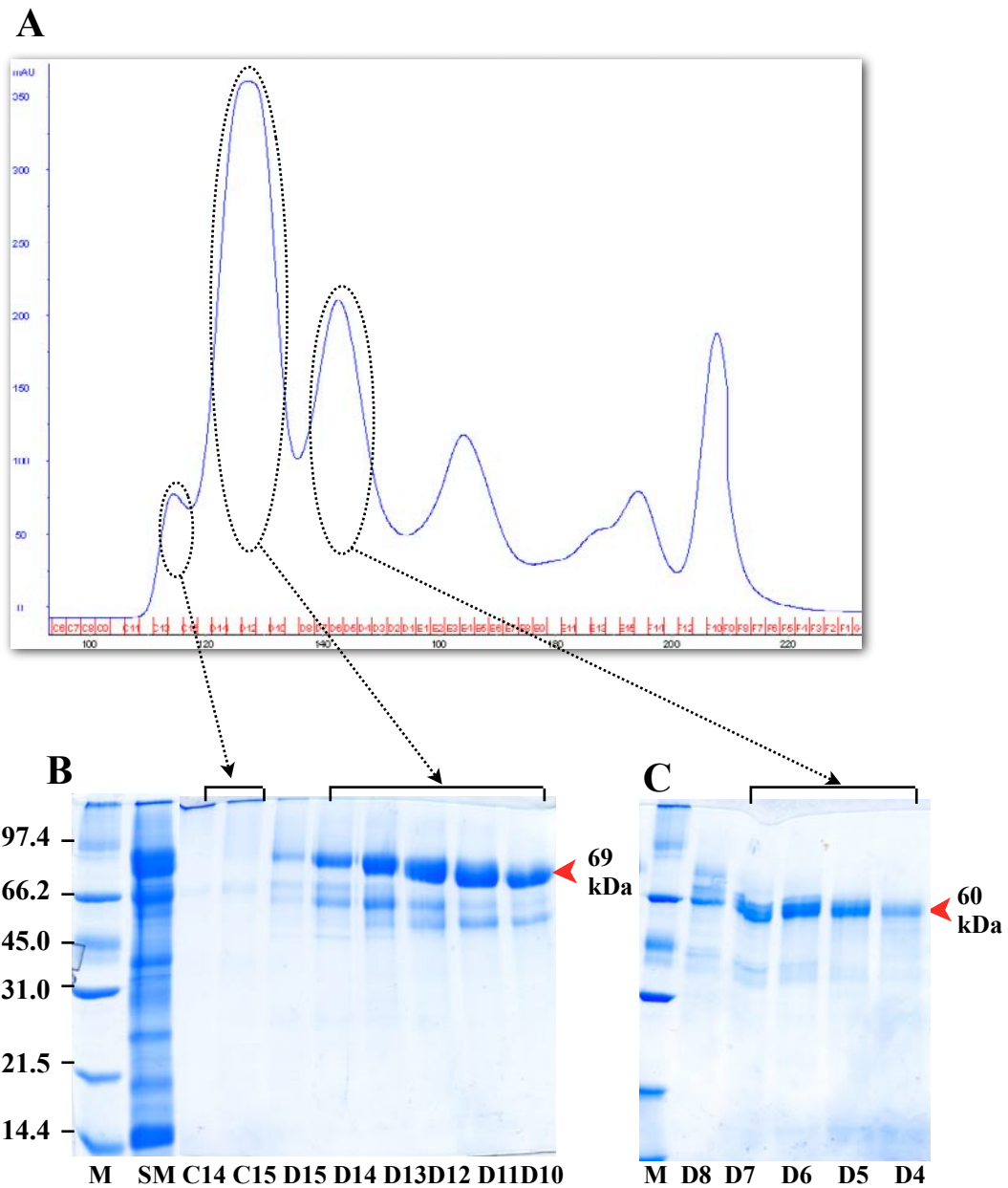


Figure 8. Purification of PH-20 using gel filtration chromatography (Hiload Superdex -75 26/60 gelfiltration column). **A)** Chromatogram of PH-20 elution profile. **B)** SDS-polyacrylamide analysis of the first peak shoulder shows aggregates while the main peak shows PH-20₆₉ protein. **C)** SDS-polyacrylamide analysis of second peak shows pure PH-20₆₀ protein. Protein sample were solubilized under non-reducing condition. M stands for molecular weight markers (kDa) and SM for starting material. Fraction numbers (C14 to D4) are indicated at the bottom of the gel.

3.3.3 Purification of PH-20 from bovine testes

Purification of PH-20 protein from commercial crude extract of bovine testes has been discontinued due to the high cost of the extract and very low yield of pure protein. Instead, purification of PH-20 protein from bovine testes supplied by a local slaughterhouse was pursued.

The frozen bovine testes were thawed and homogenized using buffer containing protease inhibitors. The homogenized sample was centrifuged and the resultant supernatant and pellet were checked for hyaluronidase activity (Figure 9). Substrate gel showed maximum activity for the supernatant whereas the pellet showed negligible activity. The purification procedure was similar to that used for the purification of Sigma crude extract (Figure 3. PH-20 purification scheme), except for the ion exchange columns which were packed manually in order to handle the large volumes.

A protein with an apparent molecular weight of about 80 kDa (PH-20₈₀) with hyaluronidase activity was purified from fresh bovine testes (Figure 10 B) and identified as bovine PH-20 protein by MALDI mass mapping (Figure 12). The yield was approximately 1-1.5 mg/1 kg of fresh bovine testes and could not be improved despite numerous trials. In contrast to commercial crude extract, the relative amount of PH-20₆₆ protein obtained from fresh bovine testes was negligible and was not purified to homogeneity (Figure 10 C). Purified PH-20₈₀ protein was dialyzed and concentrated to 10 mg/ml and crystallization trials were performed with Hampton screening kits I and II. Crystallization was not successful and precipitation was seen in most of the conditions tested which suggested protein aggregation.

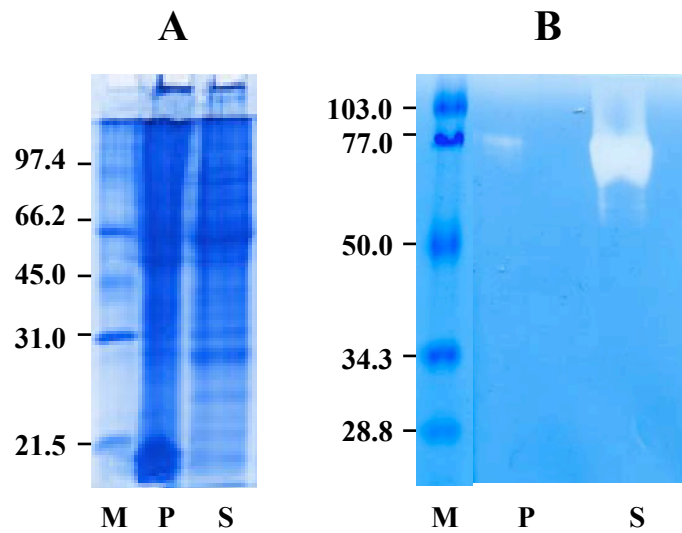


Figure 9. Homogenization of bovine testes. **A)** SDS-polyacrylamide (12% gel) analysis. **B)** Hyaluronic acid substrate SDS-PAGE (12% gel) at pH 4.0. Lane P and S stands for pellet and supernatant collected after centrifugation at 8000 rpm for 30 minutes, respectively. Protein sample were solubilized under non-reducing condition. M stands for molecular weight markers (kDa).

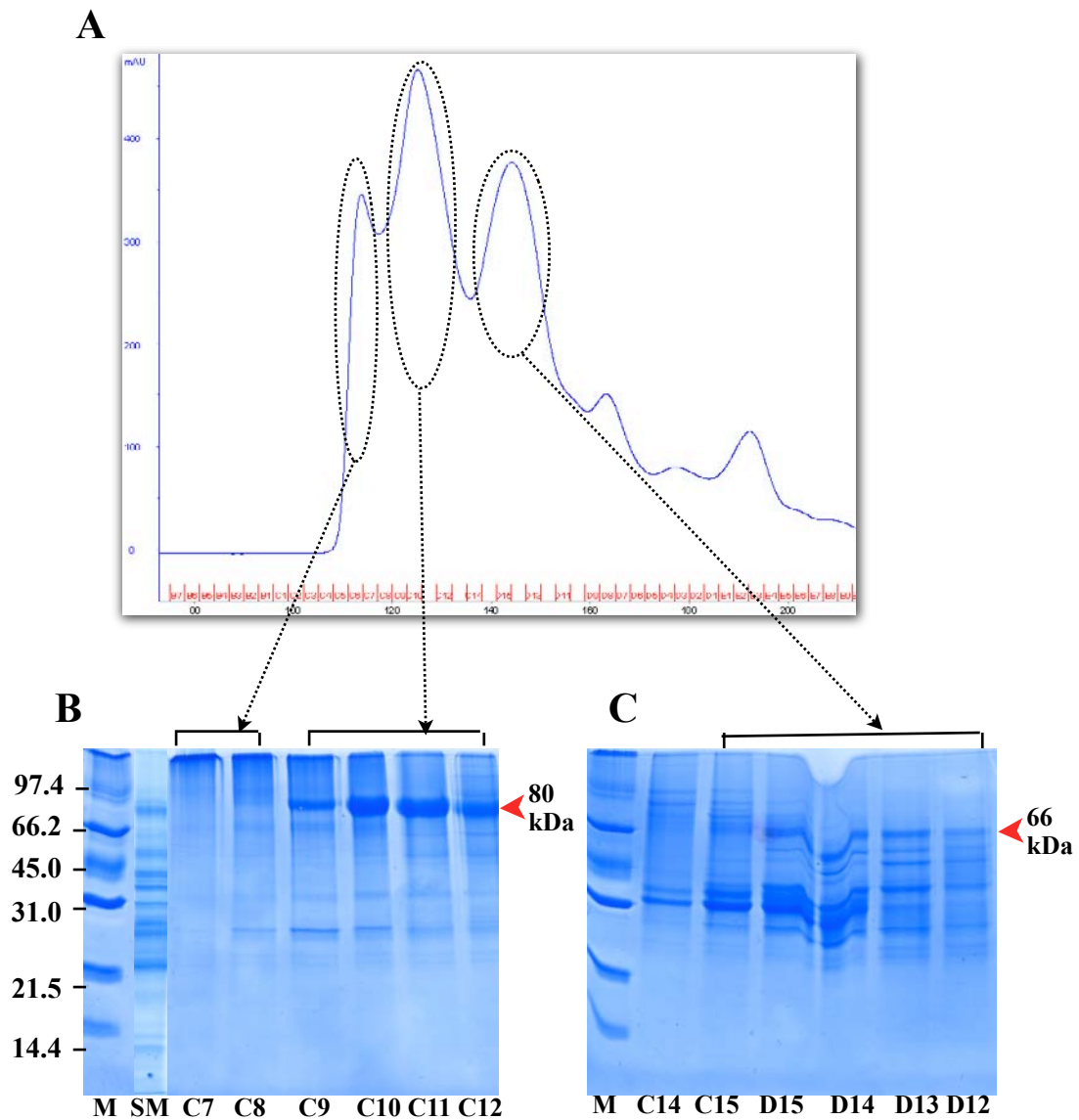


Figure 10. Purification of PH-20 using gel filtration chromatography (Hiload Superdex-75 26/60 column) **A)** Chromatogram of PH-20 elution profile. **B)** SDS-polyacrylamide analysis of the first peak shoulder shows aggregates while the main peak shows PH-20₈₀ protein. **C)** SDS-polyacrylamide analysis of second peak shows PH-20₆₆ protein with contaminant. Protein sample were solubilized under non-reducing condition. Molecular weights marker (M; kDa), starting material (SM) and fraction numbers (C7 to D12) are indicated at the bottom of the gel.

3.2.4 Endoproteolytic cleavage of PH-20 protein

Purified PH-20 proteins from both commercial source (PH-20₆₀ and PH-20₆₉) and from fresh bovine testes (PH-20₈₀) were analyzed for endoproteolytic cleavage. For this the proteins were reduced by DTT and analyzed on SDS gels (Figure. 11). The PH-20₆₀ protein (Sigma) run as two bands with apparent molecular weight of 35 and 30 kDa (Figure. 11 B, Lane 1). In contrast, PH-20₆₉ protein from commercial source and PH-20₈₀ protein from fresh bovine testes run as single band under reducing condition. This suggests that PH-20₆₀ protein is endoproteolytically cleaved and a disulfide bridge holds the two polypeptides.

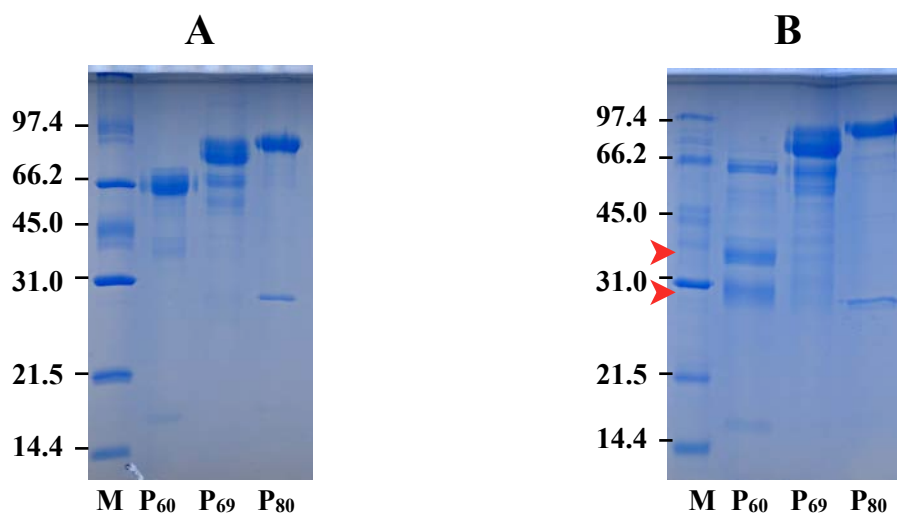


Figure 11. Purified PH-20 from two different source (Sigma crude extract and bovine testes). **(A)** non-reducing condition **(B)**. reducing condition (12% SDS-polyacrylamide gel). Lane 1 and lane 2 corresponds to PH-20₆₀ and PH-20₆₉ proteins purified from Sigma crude extract. Lane 3: PH-20₈₀ purified from bovine testes. Molecular weights marker (M) are indicated at the bottom of the gel. Arrows indicate reduced PH-20₆₀ protein fragments

3.3.5 Mass spectrometry

Mascot search results of tryptic fragment of the PH-20₆₀ and PH-20₆₉ proteins purified from commercial crude extract (Sigma) and PH-20₈₀ from fresh bovine testes matched to the hyaluronidase domain of bovine PH-20 sequence (NCBI accession number: AAP55713) (Figure 12). This strongly suggests that these proteins have identical N-termini. LC-MS method was used to determine the molecular weight of purified PH-20 proteins. The PH-20 proteins purified from commercial crude extract (Sigma) have a molecular weight of 60334 Da and 68780 Da, respectively. Whereas PH-20 protein purified from fresh bovine testes has a MW of 80350 Da (Figure 13). The molecular weight estimates are based on broad peaks and therefore is not accurate. This may be due to posttranslational modification and may account for approximately 5% error.

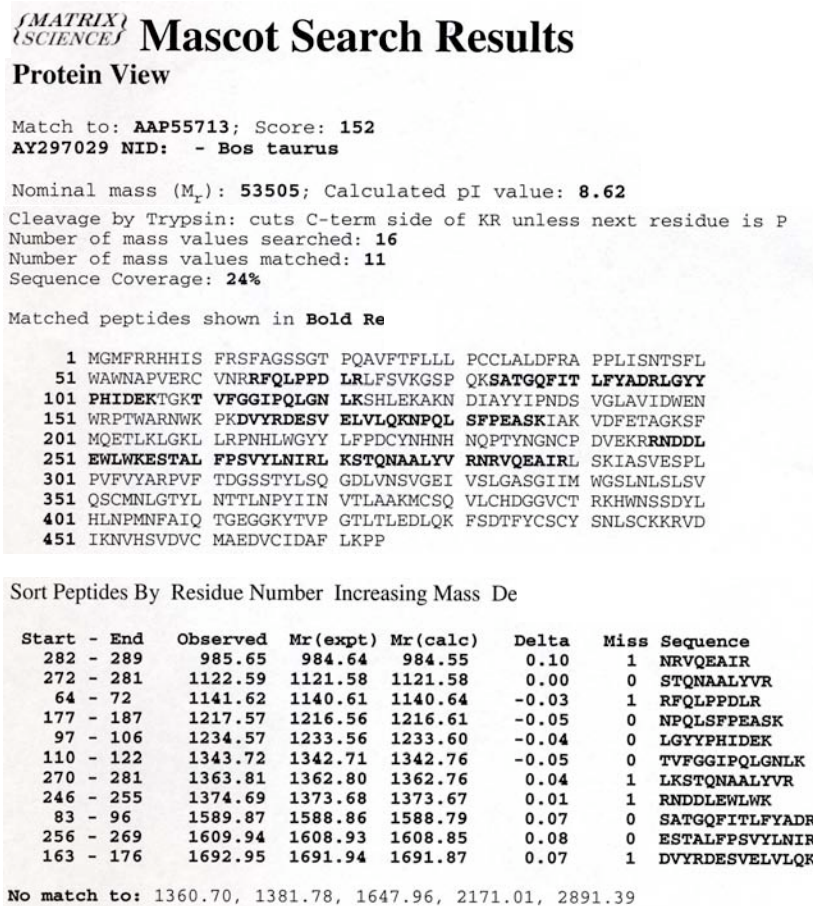


Figure 12. Mascot Search Results for PH-20₆₀ protein (commercial source). Tryptic fragments matched to the N-terminal region of AAP55713 sequence (deposited in the NCBI) and are shown in bold (top) and peptides were sorted based on increasing mass (bottom).

3.3.6 PH-20 aggregation

To test for homogeneity, sedimentation equilibrium (SE) and sedimentation velocity (SV) experiments were performed with PH-20₈₀ protein purified from fresh bovine testes in the presence and absence of 100 mM NaCl. The result revealed extensive protein aggregation in the presence of 100 mM NaCl whereas aggregation was less extensive in the absence of NaCl. The PH-20₆₀ protein purified from commercial testicular extract gave similar results (Figure 14C). Changing the pH from 7.0 to 5.4 had no effect on the heterogeneity of the protein solution (data not shown). Many additives were tested with the aim to eliminate the protein aggregation. Success was achieved with non detergent sulfobetains (NDSB), which are zwitterionic, powerful non denaturing protein solubilizing agents used in protein extraction, solubilization and crystallization [25, 26]. On addition of dimethylethylammonium propane sulfonate (NDSB-195), at a final concentration of 250 mM, aggregation was abolished for PH-20₈₀ (Figure 14E) and PH-20₆₀ (data not shown). Whereas in the presence of 100 mM NDSB-195, PH-20₈₀ showed diminished, but not abolished heterogeneity (data not shown).

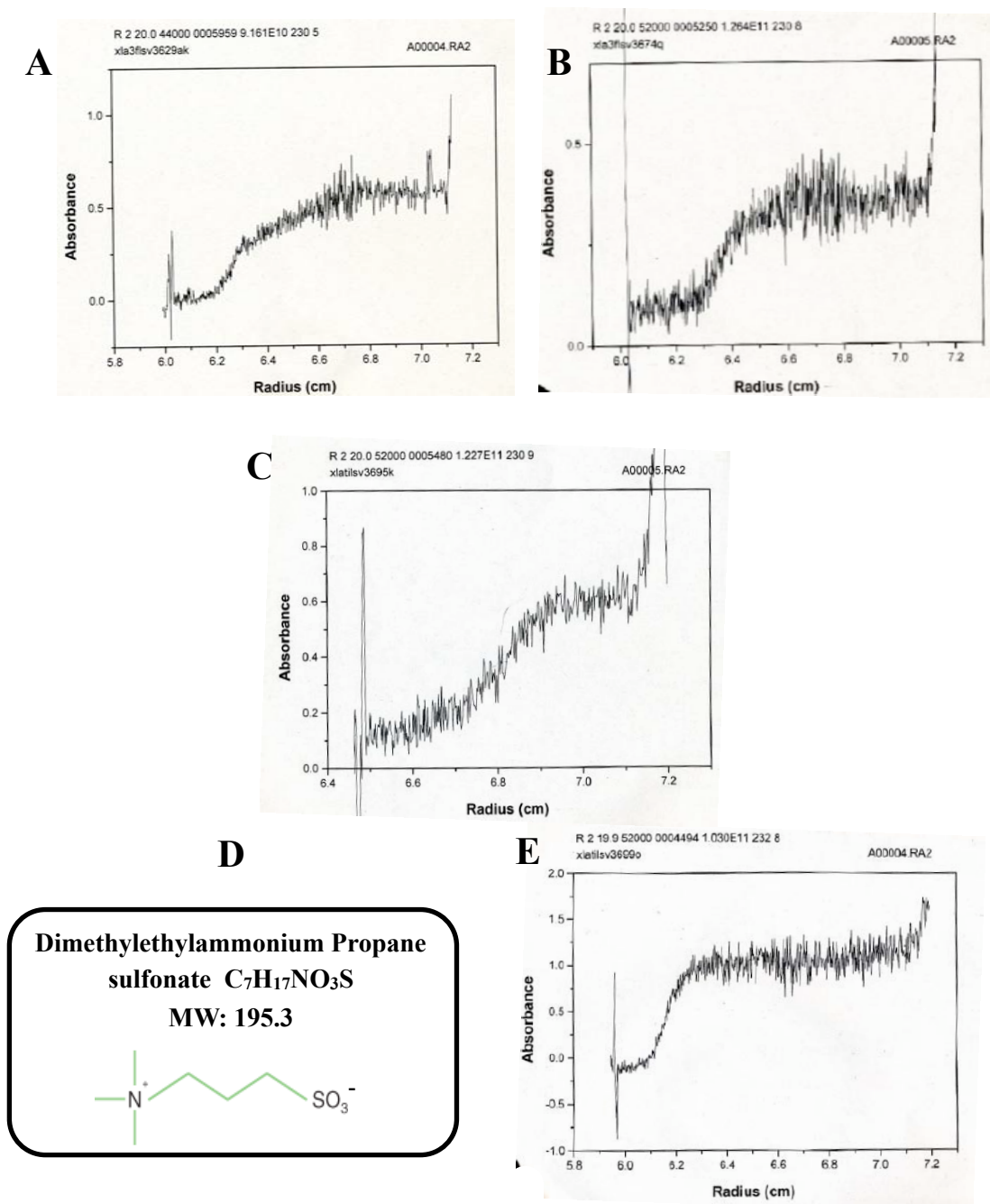


Figure 14. Sedimentation equilibrium (SE) experiment with purified PH-20 proteins. **A**) PH-20₈₀ (fresh bovine testes) in the presence of NaCl. **B**) PH-20₈₀ protein in the absence of NaCl. **C**) PH-20₆₀ protein (Sigma) in the absence of NaCl. **D**) Non Detergent sulfobetaines (NDSB). The molecular structure of this compound adapted from Hampton catalog. **E**) PH-20₈₀ protein in the presence of 250 mM NDSB-195 compound.

In addition to the above mentioned heterogeneous aggregates, protein aggregates with hyaluronidase activity eluted in the shoulder of the first peak during gel filtration chromatography was analyzed (Figure 9 and 11). Under reducing condition, the aggregates were dissociated into many different protein bands (Figure 15 B). By mass mapping, some of these dissociated proteins were identified as bovine testicular hyaluronidase (NCBI accession number: AAP55713), H⁺-exporting ATPase (NCBI accession number: A23671) and 3-hydroxyacyl-CoA (NCBI accession number: AA19510). The latter two proteins have free cysteine, which suggest they are involved in disulfide bonding to PH-20 isoform.

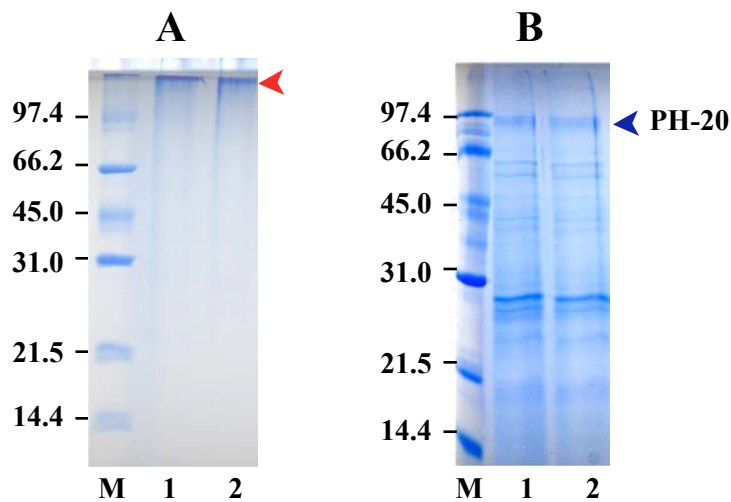


Figure 15. Analysis of aggregates (indicated by red arrow) on 12% SDS-polyacrylamide gel. **A)** non-reducing condition. **B)** reducing condition. Lane 1: sample is boiled; lane 2: sample is not boiled before loading into the gel. Molecular weights marker (M; kDa) are indicated at the bottom of the gel.

3.4 Discussion

3.4.1 PH-20 purification

We were able to purify two PH-20 variants with hyaluronidase activity from the commercially available bovine testicular extract (Sigma). Though, PH-20 protein purification from commercial source (Sigma) has been previously reported [13, 21], we isolated them to highest purity using modified protocol. Purified PH-20 variants have molecular weight of 60 kDa (PH-20₆₀) and 69 kDa (PH-20₆₉) respectively, as determined by LS/MS analysis and these values are comparable to those reported [13]. Due to high cost and low yield of PH-20 proteins from commercial source, purification from bovine testes supplied by a local slaughterhouse was pursued.

Although the 80 kDa band of bovine PH-20 was reported earlier [9], we were the first to purify the 80 kDa protein (PH-20₈₀) with hyaluronidase activity from fresh bovine testes to highest purity. Homogenization of fresh bovine testes resulted in an effective release of membrane bound PH-20 protein into the supernatant, which suggest PH-20 protein is freed either by action of released acrosomal enzymes or by mechanically affecting the stability of the plasma membrane. The yield of PH-20₈₀ protein was very low which might be due to the many purification steps employed. Unlike the commercial source (Sigma), the PH-20₆₅ fragment was presented only in negligible amount.

The MALDI mass mapping of the protein bands correspond to PH-20 variants from Sigma crude extract (PH-20₆₀ and PH-20₆₉) and from fresh bovine testes (PH-20₈₀ and PH-20₆₅), showed peptides matched to that of N-terminal region of bovine testicular hyaluronidase PH-20 protein (NCBI accession number: AAP55713). It remains to be shown whether the glycosylation and / or proteolytic cleavage can account for the difference in observed molecular weights of PH-20 proteins isolated from commercial source and fresh bovine testes.

3.4.2 Endoproteolytic cleavage of PH-20

In guinea pig and macaque sperm, lower molecular weight PH-20 form is transformed into two lower weight fragments under reducing condition, indicative of endoproteolytic cleavage of the protein into two disulfide-linked fragments [3, 7]. Our data suggested that a similar alteration on bovine PH-20 protein, under reducing PH-20₆₀ transformed into lower molecular weight fragment of 35 kDa and 30 kDa, respectively, whereas PH-20₆₉ and PH-20₈₀

protein are intact (Figure 17). Apart from PH-20 proteins, similarly modification occurs in Hyal-1 protein [27]. It was reported that bovine PH-20₆₀ comprises of 443 amino acids, in comparison to the PH-20 polypeptide deduced from cloned cDNA from the same source, it lacks the signaling peptide (35 residues) and 56 residues from carboxyl end [13]. This strongly suggests that PH-20₆₀ is probably proteolytically processed product of the larger isozyme PH-20₆₉. Structural features established by disulfide bridges, as well as glycosylation are essential for the hyaluronidase activity of macaque sperm PH-20 protein [12]. Similarly, the reduction of purified bovine PH-20 results in loss of hyaluronidase activity (data not shown).

3.4.3 PH-20 crystallization and aggregation

Based on amino acid sequence obtained from *Mayar et al., 1997* [13], the calculated molecular weight of two PH-20 variants are 56208.9 kDa and 50240.2 kDa respectively, much lower than estimated molecular weight by LS/MS analyses. The difference account for approximately 18 % for PH-20 purified from Sigma crude extract and 29 % for PH-20 from bovine testes, which suggest the purified PH-20 proteins are heavily glycosylated. This could be a one major reason for unsuccessful crystallization trials of purified PH-20 proteins. Moreover, crystallization of PH-20₈₀ protein showed precipitation in most of the conditions screened, which is indicative of protein aggregation.

Analytical ultracentrifugation studies showed that purified PH-20 is extensively aggregated both in the presence or absence of NaCl. The problem was successfully overcome by the addition of dimethylethylammonium propane sulfonate (NDSB-195), at the final concentration of 250 mM. It was hypothesized that the short hydrophobic group on sulfobetaines interacts with the hydrophobic regions of the protein and prevents their aggregation [25, 26]. This strongly suggests that purified PH-20 aggregates in solution by hydrophobic interactions, which are weakened by addition of NDSB. In addition to hydrophobic interaction, some PH-20 isoform, forms aggregation involving disulfide bridge in agreement with previous report [12].

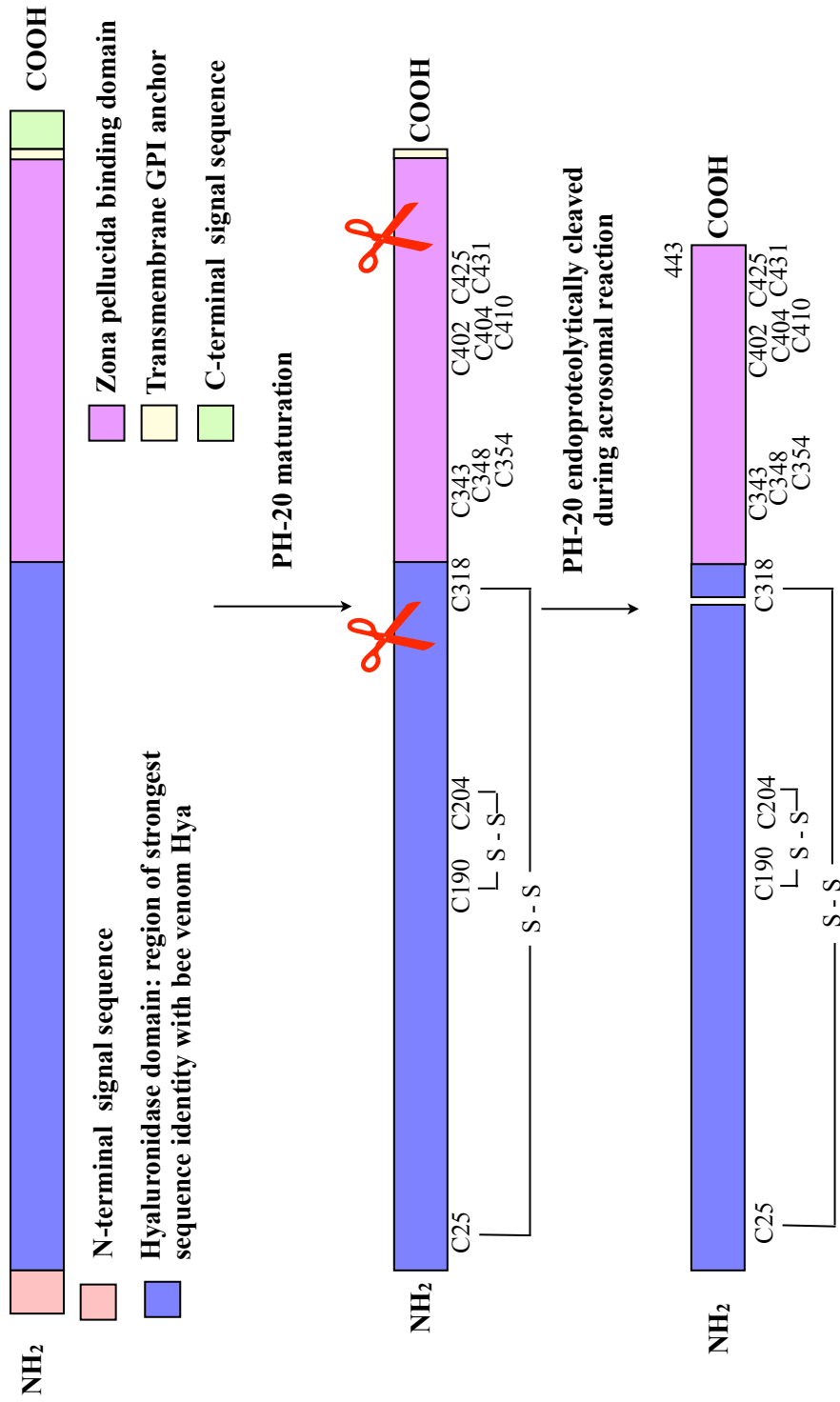


Figure 17. Schematic representation of the putative endoproteolytic processing of bovine PH-20 protein. Upper figure represents unprocessed PH-20 protein containing both N- and C-terminal signaling sequence. Middle figure represents matured PH-20 protein with N- and C-terminal signaling sequence removed. Bottom figure represent endoproteolytically cleaved PH-20 protein, which lacks the signaling sequence and 56 residues from carboxyl end. Relative polypeptide lengths are not drawn to scale.

3.5 Conclusion

Though cloning and expression of the hyaluronidase domain of human PH-20 failed (M.Schmidt, unpublished data), we were successful in purifying PH-20 proteins from both commercial source (Sigma) and bovine testes to the highest purity except for the lower molecular weight PH-20 (PH-20₆₅) from latter source. The MALDI mass mapping of PH-20 variants from both sources matched to the N-terminal part of bovine testicular hyaluronidase (NCBI accession number: AAP55713). PH-20₆₀ from the commercial source (Sigma) was endoproteolytically cleaved and linked by disulfide bridge, while PH-20₆₉ and PH-20₈₀ were intact. Reduction of disulfide bridges resulted in inactive enzyme (not shown), suggesting that structural integrity established by disulfide linkage are essential for enzymatic activity. The aggregation of purified PH-20 protein was successfully overcome by addition of zwitterionic compound, 250 mM of NDSB-195 (non detergent sulfobetaine; MW 195), which is indicative of hydrophobic interaction. In addition to hydrophobic interaction, some PH-20 isoforms form aggregation with other protein by disulfide linkage. Crystallization of PH-20 protein was not achieved but crystallization in the presence of NDSB still remains to be tested. In addition, cloning and expression of various length of hyaluronidase domain should be explored.

Bibliography

1. Meyer, K. (1971). Hyaluronidases. The enzymes, 3rd ed, *vol V*, pp 307-320.
2. Primakoff, P., Hyatt, H., and Myles, D.G. (1985). A role for the migrating sperm surface antigen PH-20 in guinea pig sperm binding to the egg zona pellucida. *J Cell Biol* *101*, 2239-2244.
3. Hunnicutt, G.R., Primakoff, P., and Myles, D.G. (1996). Sperm surface protein PH-20 is bifunctional: one activity is a hyaluronidase and a second, distinct activity is required in secondary sperm-zona binding. *Biol Reprod* *55*, 80-86.
4. Gmachl, M., and Kreil, G. (1993). Bee venom hyaluronidase is homologous to a membrane protein of mammalian sperm. *Proc Natl Acad Sci U S A* *90*, 3569-3573.
5. Lin, Y., Mahan, K., Lathrop, W.F., Myles, D.G., and Primakoff, P. (1994). A hyaluronidase activity of the sperm plasma membrane protein PH-20 enables sperm to penetrate the cumulus cell layer surrounding the egg. *J Cell Biol* *125*, 1157-1163.
6. Overstreet, J.W., Lin, Y., Yudin, A.I., Meyers, S.A., Primakoff, P., Myles, D.G., Katz, D.F., and Vandevoort, C.A. (1995). Location of the PH-20 protein on acrosome-intact and acrosome-reacted spermatozoa of cynomolgus macaques. *Biol Reprod* *52*, 105-114.
7. Cherr, G.N., Meyers, S.A., Yudin, A.I., VandeVoort, C.A., Myles, D.G., Primakoff, P., and Overstreet, J.W. (1996). The PH-20 protein in cynomolgus macaque spermatozoa: identification of two different forms exhibiting hyaluronidase activity. *Dev Biol* *175*, 142-153.
8. Thaler, C.D., and Cardullo, R.A. (1995). Biochemical characterization of a glycosylphosphatidylinositol-linked hyaluronidase on mouse sperm. *Biochemistry* *34*, 7788-7795.
9. Lalancette, C., Dorval, V., Leblanc, V., and Leclerc, P. (2001). Characterization of an 80-kilodalton bull sperm protein identified as PH-20. *Biol Reprod* *65*, 628-636.
10. Arming, S., Strobl, B., Wechselberger, C., and Kreil, G. (1997). In vitro mutagenesis of PH-20 hyaluronidase from human sperm. *Eur J Biochem* *247*, 810-814.
11. Markovic-Housley, Z., Miglierini, G., Soldatova, L., Rizkallah, P.J., Muller, U., and Schirmer, T. (2000). Crystal structure of hyaluronidase, a major allergen of bee venom. *Structure* *8*, 1025-1035.
12. Li, M.W., Yudin, A.I., Robertson, K.R., Cherr, G.N., and Overstreet, J.W. (2002). Importance of glycosylation and disulfide bonds in hyaluronidase activity of macaque sperm surface PH-20. *J Androl* *23*, 211-219.
13. Meyer, M.F., Kreil, G., and Aschauer, H. (1997). The soluble hyaluronidase from bull testes is a fragment of the membrane-bound PH-20 enzyme. *FEBS Lett* *413*, 385-388.

14. Cherr, G.N., Yudin, A.I., and Overstreet, J.W. (2001). The dual functions of GPI-anchored PH-20: hyaluronidase and intracellular signaling. *Matrix Biol* 20, 515-525.
15. Primakoff, P., and Myles, D.G. (2002). Penetration, adhesion, and fusion in mammalian sperm-egg interaction. *Science* 296, 2183-2185.
16. Wassarman, P.M. (1999). Mammalian fertilization: molecular aspects of gamete adhesion, exocytosis, and fusion. *Cell* 96, 175-183.
17. Kim, E., Baba, D., Kimura, M., Yamashita, M., Kashiwabara, S., and Baba, T. (2005). Identification of a hyaluronidase, Hyal5, involved in penetration of mouse sperm through cumulus mass. *Proc Natl Acad Sci U S A* 102, 18028-18033.
18. Primakoff, P., Lathrop, W., Woolman, L., Cowan, A., and Myles, D. (1988). Fully effective contraception in male and female guinea pigs immunized with the sperm protein PH-20. *Nature* 335, 543-546.
19. Guntenhoner, M.W., Pogrel, M.A., and Stern, R. (1992). A substrate-gel assay for hyaluronidase activity. *Matrix* 12, 388-396.
20. Laemmli, U.K. (1970). Cleavage of structural proteins during the assembly of the head of bacteriophage T4. *Nature* 227, 680-685.
21. Borders, C.L., Jr., and Raftery, M.A. (1968). Purification and partial characterization of testicular hyaluronidase. *J Biol Chem* 243, 3756-3762.
22. Yang, C.H., and Srivastava, P.N. (1975). Purification and properties of hyaluronidase from bull sperm. *J Biol Chem* 250, 79-83.
23. Radimerski, T., Mini, T., Schneider, U., Wettenhall, R.E., Thomas, G., and Jenö, P. (2000). Identification of insulin-induced sites of ribosomal protein S6 phosphorylation in *Drosophila melanogaster*. *Biochemistry* 39, 5766-5774.
24. Bonenfant, D., Schmelzle, T., Jacinto, E., Crespo, J.L., Mini, T., Hall, M.N., and Jenö, P. (2003). Quantitation of changes in protein phosphorylation: a simple method based on stable isotope labeling and mass spectrometry. *Proc Natl Acad Sci U S A* 100, 880-885.
25. Blisnick, T., Morales-Betoulle, M.E., Vuillard, L., Rabilloud, T., and Braun Breton, C. (1998). Non-detergent sulphobetaines enhance the recovery of membrane and/or cytoskeleton-associated proteins and active proteases from erythrocytes infected by *Plasmodium falciparum*. *Eur J Biochem* 252, 537-541.
26. Benetti, P.H., Kim, S.I., Chaillot, D., Canonge, M., Chardot, T., and Meunier, J.C. (1998). Expression and characterization of the recombinant catalytic subunit of casein kinase II from the yeast *Yarrowia lipolytica* in *Escherichia coli*. *Protein Expr Purif* 13, 283-290.
27. Csoka, A.B., Frost, G.I., Wong, T., and Stern, R. (1997). Purification and microsequencing of hyaluronidase isozymes from human urine. *FEBS Lett* 417, 307-310.

Appendix

Curriculum Vitae

Sivaraman Padavattan

ADDRESS	Division of Structural Biology, Biozentrum, University of Basel, Klingelbergstrasse 50-70, CH-4056, Switzerland
TELEPHONE	+41 61 267 2092
EMAIL	s.padavattan@unibas.ch
NATIONALITY	Indian
EDUCATION	
2003 - Present	PhD in Biophysics, Prof. Tilman Schirmer's Group, Biozentrum, University of Basel, Switzerland “Crystal structure determination of hyaluronidase, a major bee venom allergen in complex with an IgG Fab fragment and the purification and biophysical characterization of bovine testes hyaluronidase”
1999 - 2001	MSc Microbiology, Bharathidasan University, Trichy, INDIA
1995 -1998	BSc Microbiology, Madras University, Chennai, INDIA
PUBLICATION	Padavattan, S., T. Schirmer, M. Schmidt, C. Akdis, R. Valenta, I. Mittermann, L. Soldatova, J. Slater, U. Mueller, and Z. Markovic-Housley, 2007b, Identification of a B-cell Epitope of Hyaluronidase, a Major Bee Venom Allergen, from its Crystal Structure in Complex with a Specific Fab: J Mol Biol, v. 368, p. 742-52.

RELEVANT EXPERIENCE

- 2005 Oral presentation in the '19th Regio meeting on Biocrystallography', Les Feignes, La Bresse, France.
Presented poster in the 'Murnau conference on Structural Biology of Molecular recognition', Murnau, Germany.
Presented poster in the 'Biozentrum conference', University of Basel, Switzerland.
- 2004 Participated in the 'EMBO Conference on Structures in Biology', EMBL, Heidelberg, Germany
Participated in the '18th Regional Meeting on the X-ray Crystallography of Biomacromolecules', Switzerland.
- 2003 Participated in the '17th Regional Meeting on the X-ray Crystallography of Biomacromolecules', Germany.
- 2001 Participated in the 'International symposium on Crystallography and Bioinformatics in Structural biology', Indian Institute of Science, India.
Participated in the 'Asian crystallography association meeting', Indian Institute of Science, India.

LANGUAGES English and Tamil

REFERENCE

Dr. Zora Markovic-Housley, Division of Structural Biology, Biozentrum, University of Basel, Klingelbergstrasse 50-70, CH-4056 Basel, Switzerland.

Phone: +41 61 267 2088

Email: zora.housley@unibas.ch

Prof. Tilman Schirmer, Division of Structural Biology, Biozentrum, University of Basel, Klingelbergstrasse 50-70, CH-4056 Basel, Switzerland.

Phone: +41 61 267 2089

Email: tilman.schirmer@unibas.ch

